

DOCTORAL THESIS

**STRATEGIES FOR OCULAR
ADMINISTRATION OF ANTIVIRAL AND
ANTIOXIDANT AGENTS**

Ángela Varela García

INTERNATIONAL DOCTORAL SCHOOL
DOCTORAL PROGRAM IN DRUG RESEARCH AND DEVELOPMENT

SANTIAGO DE COMPOSTELA

2020



TESIS DOCTORAL
ESTRATEGIAS PARA LA
ADMINISTRACIÓN OCULAR DE
FÁRMACOS ANTIVIRALES Y
ANTIOXIDANTES

Ángela Varela García

ESCUELA DE DOCTORADO INTERNACIONAL
PROGRAMA DE DOCTORADO EN INVESTIGACIÓN Y DESARROLLO DE
MEDICAMENTOS

SANTIAGO DE COMPOSTELA
2020



AUTHORIZATION OF THE THESIS SUPERVISORS

Strategies for ocular administration of antiviral and antioxidant agents

Prof. Carmen Alvarez Lorenzo

Prof. Angel Concheiro Nine

REPORT:

*That the present Thesis, corresponds to the work carried out by Miss **Ángela Varela García**, under our supervision, and that we authorize its presentation considering it gathers the necessary requirements of article 34 of the USC Doctoral Studies Regulation, and that as supervisors of this Thesis, it does not incur in the abstention causes established by the law 40/2015*

At Santiago de Compostela, on June 8th 2020

Prof. Carmen Alvarez Lorenzo

Prof. Angel Concheiro Nine



AUTORIZACIÓN DEL DIRECTOR / TUTOR DE LA TESIS

Estrategias para la administración ocular de fármacos antivirales y antioxidantes

Prof. Carmen Alvarez Lorenzo

Prof. Angel Concheiro Nine

INFORMAN:

*Que la presente Tesis, se corresponde con el trabajo realizado por Dña. **Ángela Varela García**, bajo nuestra supervisión y autorizamos su presentación, considerando que reúne los requisitos exigidos en la Regulación de Estudios de Doctorado de la USC, y que como directores de ésta no incurre en las causas de abstención establecidas en la Ley 40/2015.*

En Santiago de Compostela, a 8 de Junio de 2020

Prof. Carmen Alvarez Lorenzo

Prof. Angel Concheiro Nine



PhD CANDIDATE STATEMENT

Strategies for ocular administration of antiviral and antioxidant agents

Miss Ángela Varela García

I submit my Doctoral Thesis, following the procedure according to the Regulation, stating that:

- 1) This Thesis gathers the results corresponding to my work.
- 2) When necessary, explicit mention is given to the collaborations the work may have had.
- 3) The present document is the final version submitted for its defense and coincides with the document sent in electronic format.
- 4) I confirm that the Thesis does not incur in any plagiarism of any other authors or documents submitted by me for obtaining other degrees.

At Santiago de Compostela, on June 8th 2020

Sgd. Ángela Varela García



DECLARACIÓN DE LA AUTORA DE LA TESIS
Estrategias para la administración ocular de fármacos
antivirales y antioxidantes

Dña. Ángela Varela García

Presento mi Tesis Doctoral, siguiendo el procedimiento adecuado a la Regulación, y declaro que:

- 1) La Tesis abarca los resultados de la elaboración de mi trabajo.
- 2) De ser el caso, en la Tesis se hace referencia a las colaboraciones que tuvo este trabajo.
- 3) La Tesis es la versión definitiva presentada para su defensa y coincide con la versión enviada en formato electrónico.
- 4) Confirmo que la Tesis no incurre en ningún tipo de plagio de otros autores ni de trabajos presentados por mí para la obtención de otros títulos.

En Santiago de Compostela, a 8 de Junio de 2020

Fdo. Ángela Varela García



A mis padres





*“No temas a las dificultades: lo
mejor surge de ellas”*
Rita Levi-Montalcini



AGRADECIMIENTOS

Cuando una etapa tan importante de tu vida llega a su fin, es inevitable echar la vista atrás para hacer balance de todo lo positivo que ha ocurrido e influido en tu crecimiento personal y profesional. Son muchas las personas que han aportado algo durante este largo trayecto, las cuales formarán parte de esta historia para siempre. Por ello, me gustaría agradecer a todos los que de una forma u otra han estado presentes en ella.

A mis directores de tesis, los profesores *Carmen Alvarez Lorenzo* y *Angel Concheiro Nine*. Estaré eternamente agradecida por haberme dejado formar parte de vuestro equipo. Me habéis enseñado que, con esfuerzo y perseverancia, todo se puede conseguir. Gracias por todo lo aprendido.

A los profesores del Departamento de Farmacología, Farmacia y Tecnología Farmacéutica, *José Luis Gómez Amoza*, *Carlos García González*, *Mariana Landín Pérez*, *Loli Torres López*, *Carmen Remuñán López*, y, en especial, a *Francisco Otero Espinar*, siempre dispuestos a prestar ayuda en todo lo necesario.

A los profesores *Aisling Ní Annaidh*, de School of Mechanical and Materials Engineering de la UCD de Dublín, y *Lorenzo Pastrana*, del International Iberian Nanotechnology Laboratory de Braga, por haberme dado la oportunidad de seguir formándome y de ampliar mis conocimientos desde otro punto de vista.

A los ya doctores, *Ale, Sonia, Patri, Isa y Luis*, por darme la bienvenida a esta familia y por ayudar a resolver siempre las dudas de una novata. En especial a *Fer*, que pasó de ser mentor a amigo, por haber pasado tantas horas explicándome y ayudándome, por todas las risas y cabreos, y por el apoyo constante.

A mis colegas de máster, *Laura, Lucía, Ana y Diego*, por haber compartido tantos momentos, por esas charlas infinitas que nunca son suficiente y por todo el apoyo mutuo.

Al “Team Fran”, *Victoria, Andrea Conde, Xurxo, Rubén, Guille, Iria, Carlos y Andrea Luaces*, por esa locura contagiosa que, sin duda, hace que el día a día sea mucho más que agradable.

A mis compañeros de batalla. A *María*, porque estoy convencida de que sin ti nada sería igual, porque tu generosidad no tiene límites y por haber forjado esta bonita amistad que será para siempre. A *Xián*, por todas las conversaciones, risas y llantos compartidos. A los vecinos de arriba, *Clara, Viti, Rebeca y Ana*, por ser tan buenos compañeros y por haber pasado juntos tantos buenos momentos, así como a *Lorena* y a *Helena*. A las incorporaciones más recientes, *Ana Filipa, Iago, Axel y Patri* porque aunque llevemos poco tiempo juntos, el compañerismo y el buen ambiente que tenemos es en parte gracias a vosotros. A los que ya se han ido, *Mirian y Mariano*, por haber estado siempre dispuestos a ayudar sin dudarlo. Y a los que estuvieron de paso, pero dejaron huella, a *Anna Paula, Catia y Adrián*, porque en poco tiempo habéis pasado a formar parte de esta gran familia y, en

especial, a *Claudia*, por todos los buenos momentos compartidos y por esta amistad que nos une.

A *Andrea*, por haber sido una compañera de trabajo excepcional, por todos los buenos momentos pasados y por todos los que vendrán.

A *Sole*. Resulta complicado expresar en pocas palabras lo agradecida que estoy por todo lo que haces. Jefa, compañera, mentora y amiga, siempre dispuesta a ayudar en todo. Ha sido un placer y un privilegio haber podido compartir esta etapa de mi vida contigo.

A todos mis amigos y a mi familia, en especial a *Rocío y Vanesa*, mis “hermanas” mayores; también a *Diana, Cores y Sofía*, por estar siempre ahí. A *Marcos*, mi compañero de vida, cuya paciencia infinita y apoyo incondicional hacen que pueda mantenerme siempre a flote. Por último, a las personas más importantes de mi vida, *Pilar y Ricardo*, mis padres, ejemplos máximos de superación y valentía, que me han sabido enseñar lo más valioso de la vida, nunca rendirse y no temer a las dificultades. No hay palabras suficientes para agradecer todo el apoyo recibido en cada momento, sin el cual nunca llegaría a ser la persona que hoy en día soy.

A todos, de corazón, mil gracias.



Index

Resumen	3
1. Introduction.....	19
1.1.Ocular anatomy.....	22
1.2.Eye-defense mechanisms	26
1.2.1. Lacrimal film.....	27
1.2.2. Corneal barrier	28
1.2.3. Non-corneal barriers.....	29
1.2.4. Blood ocular barriers.....	30
1.3.Ocular drug administration	31
1.4.Cornea diseases	34
1.4.1. Ocular trauma.....	35
1.4.2. Degenerative disorders.....	36
1.4.3. Inflammatory diseases.....	38
1.4.4. Infectious diseases.....	39
1.4.5. Prevention and treatment of corneal lesions: antioxidant agents	39
1.5.Ocular viral infections	41
1.5.1. Treatment of ocular viral infections.....	44
1.6.Micelles and contact lenses as platforms for ocular delivery	46
1.6.1. Polymeric micelles.....	46
1.6.2. Contact lenses.....	50
1.7.References.....	58
2. Aims.....	73
3. Polymeric micelles for acyclovir ocular delivery: formulation and cornea and sclera permeability	81
3.1.Introduction.....	81

3.2. Materials and methods	86
3.2.1. Materials	86
3.2.2. Micelles preparation and characterization	87
3.2.3. Rheological behavior	87
3.2.4. Acyclovir solubilization	88
3.2.5. Micelle stability against dilution	89
3.2.6. Corneal and sclera permeability assay	90
3.3. Results and Discussion	91
3.3.1. Micelles preparation and characterization	91
3.3.2. Rheological behavior	93
3.3.3. Acyclovir solubilization	94
3.3.4. Micelle stability against dilution	99
3.3.5. Cornea and sclera permeability assay	100
3.4. Concluding remarks	105
3.5. References	106
4. Imprinted hydrogels for acyclovir and valacyclovir ocular administration	115
4.1. Introduction	115
4.2. Materials and methods	121
4.2.1. Materials	121
4.2.2. Computational modeling	122
4.2.3. Synthesis of imprinted hydrogels	122
4.2.4. Drug removal	124
4.2.5. Direct drug release test from boiled hydrogels	125
4.2.6. Drug loading and release from conditioned hydrogels	126
4.2.7. Degree of swelling	127
4.2.8. Light transmittance	128
4.2.9. Mechanical properties	128

4.2.10. HET-CAM test.....	129
4.2.11. Bovine corneal and scleral permeability test.....	129
4.3.Results and Discussion.....	131
4.3.1. Computational modeling	131
4.3.2. Synthesis of hydrogels and drug removal	133
4.3.3. Direct drug release test from boiled hydrogels	134
4.3.4. Drug loading in washed hydrogels.....	136
4.3.5. Drug release	138
4.3.6. Hydrogel characterization	140
4.3.7. HET-CAM test.....	142
4.3.8. Bovine corneal and scleral permeability test.....	143
4.4.Concluding remarks	146
4.5.References.....	147
5. Cytosine-functionalized bioinspired hydrogels for ocular delivery of antioxidant transferulic acid	155
5.1.Introduction.....	155
5.2.Materials and methods	161
5.2.1. Materials.....	161
5.2.2. Hydrogel synthesis	162
5.2.3. Functionalization with cytosine	163
5.2.4. Hydrogels characterization.....	164
5.2.5. TA loading	166
5.2.6. TA release	166
5.2.7. HET-CAM test.....	167
5.2.8. Cytocompatibility assay	167
5.2.9. Antioxidant activity.....	168
5.2.10. Cornea and sclera penetration and accumulation.....	169
5.3.Results and discussion	171

5.3.1. Hydrogels synthesis and cytosine grafting	171
5.3.2. Swelling, light transmission and mechanical properties.....	175
5.3.3. TA loading.....	177
5.3.4. TA release.....	180
5.3.5. Biocompatibility	182
5.3.6. Antioxidant activity	183
5.3.7. Cornea and sclera penetration.....	185
5.4. Concluding remarks.....	189
5.5. References	190
6. Conclusions	201
7. Patent.....	207
8. Abbreviations.....	239



Resumen





Resumen

Las enfermedades oculares afectan a más del 17% de la población mundial. Encontrar el tratamiento adecuado resulta difícil en muchas ocasiones, ya que los síntomas no se manifiestan de manera temprana, y los signos de la enfermedad solo pueden ser identificados si se hacen revisiones periódicas. Además, muchas veces la patología no es exclusiva del ojo, sino que se deriva de otra enfermedad en una zona distinta del organismo. A nivel mundial, las principales causas de discapacidad visual son: errores refractivos no corregidos, cataratas, degeneración macular asociada a la edad, glaucoma, retinopatía diabética, opacidad corneal y tracoma. Según la Organización Mundial de la Salud (OMS), existen diferencias en la prevalencia de cada enfermedad dependiendo del país y de la edad.

Encontrar un tratamiento efectivo a nivel ocular constituye un desafío, ya que son muchos los factores a considerar para conseguir que el fármaco alcance su diana. El ojo cuenta con mecanismos de defensa específicos, como los reflejos mecánicos (parpadeo o lagrimeo), el drenaje nasolacrimal, los componentes y la dinámica de la película lacrimal y las distintas barreras anatómicas (corneales, no

corneales y sanguíneas). Además, según la zona del ojo que esté afectada (segmento anterior o segmento posterior), la administración plantea más o menos dificultades. La vía sistémica (oral, intramuscular o intravenosa) apenas se utiliza, ya que se necesitan dosis altas de fármaco para que se alcancen niveles eficaces en las estructuras oculares, con lo que los riesgos de efectos secundarios son muy elevados.

La administración tópica en forma de colirios es la más común entre los métodos clásicos para suministrar fármacos al ojo. Se trata de un procedimiento de administración no invasivo, indoloro, con un aceptable grado de cumplimiento de la pauta posológica, que permite conseguir un efecto inmediato. Su principal desventaja es que la biodisponibilidad ocular de los fármacos administrados es inferior al 5%, debido a las barreras antes mencionadas. Esto obliga a efectuar instilaciones repetidas de disoluciones concentradas a intervalos de tiempo cortos, con las consiguientes molestias para el paciente y el incremento del riesgo de que aparezcan efectos secundarios a nivel sistémico, ya que parte de la dosis instilada puede acceder al torrente circulatorio a través de la conjuntiva, mucosa nasal o tracto gastrointestinal. Las formas semisólidas permiten prolongar el tiempo de permanencia en la superficie ocular, pero su desarrollo encierra también dificultades relacionadas con la estabilidad de los componentes y el mantenimiento de las propiedades reológicas durante la esterilización. Además, las formas semisólidas tienen el

inconveniente adicional de que producen sensación de cuerpo extraño y visión borrosa.

La administración de fármacos en inyecciones intraoculares permite abordar el tratamiento de patologías que afectan al segmento posterior. Es más eficaz que la utilización de una vía sistémica, pero resulta altamente desagradable para el paciente e implica riesgo de daños en los tejidos oculares e infecciones.

La búsqueda de nuevas estrategias para la administración ocular de fármacos que permitan incrementar la biodisponibilidad ocular, combinando una cesión sostenida eficiente y minimizando el dolor y las molestias del paciente, resulta un desafío.

Una posible estrategia de formulación consiste en incorporar el fármaco a micelas poliméricas que se forman a partir de copolímeros anfifílicos. La autoasociación espontánea de los copolímeros da lugar a agregados de tamaño nanométrico (5-100 nm) que presentan un núcleo interno hidrófobo, capaz de alojar fármacos liposolubles, y una cubierta externa hidrófila, que proporciona una interfase muy adecuada con medios externos acuosos como los biológicos. La encapsulación de un fármaco en una micela polimérica minimiza su contacto con el medio externo y permite incrementar de una manera muy significativa su solubilidad aparente. La estructura de la micela, su composición (naturaleza del copolímero, peso molecular y balance hidrofilia-lipofilia), y las interacciones que se establecen con el fármaco encapsulado determinan, junto con el procedimiento de

preparación de las micelas, tanto su eficacia de encapsulación como la velocidad de cesión del fármaco. Las nanomicelas poliméricas están atrayendo una creciente atención como formas de administración tópica ocular por sus prestaciones multifunción: (i) facilitan el contacto del fármaco con la superficie del epitelio corneal y, al aumentar la solubilidad aparente del fármaco, originan gradientes de concentración mayores que promueven el paso a través de la córnea hacia las estructuras del segmento anterior; (ii) las nanomicelas pueden penetrar a través del entramado poroso de la esclera, abriendo la posibilidad de acceder de forma no invasiva a estructuras del segmento posterior; y (iii) algunos copolímeros son inhibidores de las bombas de eflujo presentes en la superficie ocular, lo que debe facilitar la acumulación intracelular de los fármacos.

La búsqueda de sistemas sólidos que actúen como plataformas de cesión sostenida en la superficie ocular durante tiempos prolongados y que, a diferencia de los insertos clásicos, resulten más confortables para el paciente y no se ubiquen en contacto con la conjuntiva (principal zona de absorción sistémica), ha llevado a plantear el uso de las lentes de contacto (LC) como vehículos de administración de fármacos oftálmicos. Las LC pueden ceder el fármaco al fluido lacrimal post-lente, es decir, el comprendido entre la cara interna de la LC y la superficie ocular. La presencia de la LC ralentiza la dinámica de renovación del fluido, lo que permite que se alcancen concentraciones elevadas del fármaco en la superficie corneal.

Además, durante el tiempo que dura el parpadeo, la cara externa de la LC se seca, con lo que se minimiza la cesión hacia el fluido lacrimal que baña externamente la LC y, por lo tanto, también las pérdidas no productivas. Las LC medicadas podrían actuar como lentes neutras, sin alterar la visión del paciente, o como lentes graduadas, para abordar simultáneamente la corrección de un problema óptico. A pesar de las ventajas potenciales que encierran las LC medicadas, su diseño ha de enfrentarse a la baja afinidad que presentan la mayoría de los componentes que se usan en su preparación por los fármacos oftálmicos, lo que determina que incorporen cantidades insuficientes de fármaco y que lo cedan de manera prácticamente inmediata al entrar en contacto con la superficie ocular.

El objetivo general de la Tesis Doctoral fue diseñar micelas poliméricas y LC útiles para la administración tópica ocular de fármacos. Específicamente, el trabajo se centró en los antivirales aciclovir y valaciclovir, y el antioxidante ácido transferúlico, todos ellos con baja solubilidad y prestaciones terapéuticas que podrían verse considerablemente mejoradas si se consiguen niveles sostenidos en las estructuras oculares. De acuerdo con estos objetivos, el trabajo se desarrolló en las siguientes etapas:

- 1) Preparación de micelas poliméricas para la administración de aciclovir. Este agente antiviral es el de primera elección para el tratamiento del herpes ocular, causado por el virus del herpes simple. Este virus puede afectar a todas las capas de la córnea, causando

visión borrosa, enrojecimiento o lagrimeo. La queratitis por herpes simple (infección e inflamación de la córnea) es la principal causa de ceguera por infección a nivel mundial. El aciclovir penetra en las células infectadas y compite con los nucleósidos naturales para incorporarse al ADN y poder actuar como terminador de cadena. Después de anclarse, da lugar a un mecanismo de inactivación suicida, puesto que el ADN terminado se une a la polimerasa del ADN viral y la inhibe de manera irreversible, impidiendo la replicación del virus. El tratamiento tópico clásico requiere un periodo de aplicación prolongado y da lugar a efectos secundarios graves. La administración oral se caracteriza por presentar una biodisponibilidad inferior al 20%, por lo que son necesarias dosis muy altas durante tiempos prolongados.

La hipótesis de esta primera etapa de la Tesis fue que la encapsulación de aciclovir en nanomicelas poliméricas debe aumentar la solubilidad del fármaco y promover su acumulación en córnea y esclera y el acceso a estructuras más profundas. Para llevar a cabo el trabajo, primero se hizo un barrido de las prestaciones de los copolímeros Soluplus y Solutol. Se prepararon dispersiones de cada copolímero cubriendo un amplio intervalo de concentraciones (1, 4, 8, 12, 16 y 20% p/p) en agua y tampón fosfato (PBS) pH 7.4, y se evaluó su tamaño, potencial Z y comportamiento reológico.

Las propiedades viscoelásticas se caracterizaron a partir de medidas de los módulos de almacenamiento (G') y de pérdida (G'') de

las dispersiones de Soluplus y Solutol al 12% y al 20%, en función de la temperatura (15-40 °C). Las dispersiones de Solutol mostraron un comportamiento viscoso. En cambio, las dispersiones de Soluplus mostraron incrementos muy marcados en G' y G'' a temperaturas próximas a la corporal. La capacidad de las nanomicelas para solubilizar aciclovir se evaluó en agua, PBS pH 7.4 y fluido lacrimal artificial (FLS) pH 7.5. Se calcularon parámetros de solubilidad como la capacidad de solubilización molar, el coeficiente de reparto micela-agua y la energía de solubilización libre de Gibbs. Únicamente las micelas de Soluplus dieron lugar a incrementos relevantes de la solubilidad de aciclovir, mostrando una elevada capacidad de encapsulación y estabilidad frente a la dilución.

Finalmente, se llevaron a cabo ensayos de permeabilidad a través de córnea y esclera bovinas en células de difusión. En comparación con el aciclovir libre en disolución, la encapsulación en micelas de Soluplus dio lugar a marcados aumentos en la cantidad de fármaco acumulada en ambos tejidos, así como en la cantidad que pasa al compartimento receptor. En suma, las micelas de Soluplus presentaron propiedades fisicoquímicas adecuadas para la administración ocular de aciclovir, mejorando la penetración del fármaco a través de córnea y esclera.

2) Diseño de hidrogeles imprinted para fármacos antivirales. Con el fin de prolongar la permanencia del fármaco en la superficie ocular más allá de lo que permiten las formulaciones en nanomicelas, el

objetivo de la segunda etapa de la Tesis fue diseñar hidrogeles válidos para LC blandas con afinidad por aciclovir y valaciclovir. Entre los procedimientos propuestos para dotar a los hidrogeles de afinidad por moléculas específicas, destaca la creación de receptores artificiales utilizando la técnica de moldeado molecular (*molecular imprinting*). Esta técnica requiere incorporar la sustancia de interés a la mezcla de monómeros para que estos se reordenen en función de su afinidad, y el reordenamiento se haga permanente durante la polimerización. La remoción de las moléculas molde genera cavidades con el tamaño y los grupos químicos más adecuados para alojar de nuevo la sustancia de interés.

La selección del ácido metacrílico (MAA) como monómero funcional se hizo teniendo en cuenta que, además de ser un monómero habitual en la preparación de LC, en un estudio preliminar por modelización computacional mostró capacidad para interaccionar tanto con el anillo de aciclovir y valaciclovir como con el grupo amino de la cadena lateral valaciclovir.

Se sintetizaron hidrogeles mezclando HEMA con MAA como monómero funcional, y se añadió aciclovir o valaciclovir en distintas proporciones. Tras la polimerización, se confirmó la extracción del fármaco durante los lavados mediante espectrofotometría UV. Con algunos hidrogeles se llevó a cabo un estudio de cesión directa del fármaco (sin lavado previo), para determinar la capacidad de control de la cesión del fármaco incorporado durante la polimerización. Una

vez lavados los hidrogeles, se estudió su capacidad de reincorporación de aciclovir o valaciclovir, por inmersión en disoluciones acuosas de cada fármaco. Se comprobó que los discos presentaban mayor afinidad por valaciclovir. A continuación, se llevó a cabo un estudio de cesión con ambos fármacos en FLS, lo que confirmó que los hidrogeles impresos y cargados con valaciclovir presentaban perfiles de cesión más adecuados, con una liberación sostenida durante 10 h que da lugar a niveles terapéuticos. Los hidrogeles se caracterizaron en términos de hinchamiento, transmitancia y propiedades mecánicas, obteniéndose valores similares a los que son comunes para las LC hidrófilas. También se sometieron a un ensayo de irritación en membrana corioalantoidea de huevo (HET-CAM), no observándose hemorragia, lisis ni coagulación. Finalmente, con los hidrogeles con mejores propiedades de carga y cesión de valaciclovir se llevaron a cabo ensayos de permeabilidad en córnea y esclera bovinas. De la misma forma que en el caso de la disolución acuosa de valaciclovir, el fármaco cedido por los hidrogeles fue capaz de acumularse en la cornea y de penetrar a través de la esclera. Los resultados obtenidos indican que los hidrogeles preparados con MAA como monómero funcional e impresos con valaciclovir son buenos candidatos para la administración tópica ocular de este fármaco.

3) Diseño de hidrogeles bioinspirados funcionalizados con citosina para la administración ocular de ácido transferúlico. El ácido transferúlico es uno de los antioxidantes naturales más potentes y

puede eliminar especies reactivas de oxígeno (ROS) y de nitrógeno (RNS), así como regular los sistemas citoprotectores. A nivel ocular, es útil en el tratamiento de lesiones corneales y puede suprimir la producción de amiloide a nivel del cristalino. El principal inconveniente es que su biodisponibilidad oral es inferior al 20%, por lo que resulta conveniente diseñar formulaciones que permitan su administración tópica ocular. La creación de receptores artificiales utilizando la técnica de moldeado molecular (*molecular imprinting*) no es aplicable cuando la molécula de interés es un antioxidante, ya que se degradaría durante la polimerización y, además, haría que ésta fuese incompleta. Por lo tanto, el desarrollo de hidrogeles con afinidad por antioxidantes requiere la identificación de grupos funcionales que puedan actuar como receptores, sin necesidad de llevar a cabo la polimerización en presencia de la molécula de interés. Muchos fármacos basan su mecanismo de acción en su capacidad para interaccionar con las bases púricas (adenina y guanina) o pirimidínicas (timina, citosina y uracilo), que constituyen el ADN y el ARN. Esta etapa de la Tesis se planteó partiendo de la hipótesis de que la incorporación de una base pirimidínica, como la citosina, a la estructura de un hidrogel debe dotarlo de afinidad por las moléculas con estructura complementaria en términos de capacidad para establecer puentes de hidrógeno e interacciones hidrofóbicas π - π . La utilización de bases nitrogenadas como grupos funcionales no ha sido ensayada previamente, por lo que para su incorporación a los

hidrogeles se puso a punto un procedimiento de anclaje post-polimerización.

Para llevar a cabo el estudio, los hidrogeles se prepararon mezclando HEMA con glicidilmetacrilato (GMA) y etilenglicolfenileter metacrilato (EGPEM) en distintas proporciones. El GMA se utilizó como puente para inmovilizar citosina en los hidrogeles, mientras que el EGPEM se incorporó para evaluar la posibilidad de reforzar la interacción entre el ácido transferúlico y la citosina formando complejos de Rebek. Los hidrogeles se prepararon con un espesor de 0.45 mm y la funcionalización con citosina se llevó a cabo por inmersión en una disolución de citosina en agua:dioxano (1:1 vol/vol), a 80 °C durante 24 h. Tras el lavado, la presencia de citosina se confirmó visualmente bajo luz ultravioleta, puesto que es una molécula altamente fluorescente, y también mediante espectroscopía FTIR-ATR y análisis elemental.

Los hidrogeles se caracterizaron en cuanto a grado de hinchamiento, transmitancia y propiedades mecánicas, obteniéndose valores situados dentro de los intervalos admitidos para LC hidrofílicas.

La incorporación de ácido transferúlico se llevó a cabo sumergiendo discos de hidrogel en una disolución acuosa del fármaco. Los hidrogeles funcionalizados con citosina dieron lugar a una mayor incorporación de agente antioxidante, hasta 2.5 veces superior y, por lo tanto, a coeficientes de reparto entramado/agua ($K_{N/W}$) más

elevados que los hidrogeles sin funcionalizar. Los ensayos de cesión *in vitro*, que se llevaron a cabo en FLS, revelaron que los hidrogeles con mayor $K_{N/W}$ dan lugar a perfiles de cesión más sostenidos. A continuación, los hidrogeles se sometieron a un ensayo de compatibilidad con membrana corioalantoidea de huevos fecundados (ensayo HET-CAM), que es un método alternativo al ensayo *in vivo* en animales para evaluar el riesgo de irritación ocular. También se evaluó la compatibilidad de los hidrogeles con células epiteliales de la córnea humana (HCEC) mediante la prueba WST-1. Ambos ensayos confirmaron que los hidrogeles son altamente biocompatibles.

Los hidrogeles con mejores propiedades de carga y cesión de ácido transferúlico se ensayaron en cuanto a actividad antioxidante, mediante el test ORAC. Los resultados obtenidos indicaron que la incorporación del ácido transferúlico a los hidrogeles no deteriora su actividad antioxidante.

Finalmente, se llevó a cabo un estudio de permeabilidad a través de córnea y esclera. Al igual que el ácido transferúlico libre en disolución, el que se cedió a partir de los hidrogeles mostró una elevada tendencia a acumularse en córnea y esclera, y también a pasar al medio receptor. Los resultados obtenidos indican que la utilización de citosina como componente funcional representa una nueva estrategia para dotar a los hidrogeles de afinidad por moléculas que, como el ácido transferúlico, cuentan en su estructura con grupos

aromáticos y otros grupos con capacidad para formar puentes de hidrógeno.

En su conjunto, los resultados de esta Tesis Doctoral abren nuevas posibilidades para desarrollar formas de aplicación tópica ocular, tanto líquidas como sólidas, que proporcionen niveles sostenidos de fármaco en córnea y esclera.





Introduction





1. Introduction

Ocular diseases are pathologies which affect the normal functioning of the eye. These conditions may be specific to the organ or due to a collateral effect caused by a disease located elsewhere in the body. An early diagnosis is helpful in finding the right treatment for each situation, but many times the symptoms do not appear or appear late, making it difficult to address the problem. Ocular diseases affect more than 17% of the world's population. The main causes of these visual disabilities are uncorrected refractive errors, cataracts, age-related macular degeneration, glaucoma, diabetic retinopathy, corneal opacity and trachoma. According to World Health Organization (WHO), there are differences in prevalence depending on country and age (**Figure 1.1**). For example, in lower-income countries, cataracts are the predominant cause of blindness, while diabetic retinopathy, glaucoma and macular degeneration are more predominant in countries more economically stable (*Flaxman et al., 2017; World Health Organization 2019*). The main causes of visual impairment and blindness worldwide are shown in **Figure 1.2**. It is

difficult to pinpoint the determinants of corneal disease, but it involves a wide range of infectious and inflammatory diseases that lead to blindness. According to WHO, in 2010 the main causes of visual impairment worldwide were uncorrected refractive errors (43%) and cataracts (33%) and the leading cause of global blindness was cataracts (51%).

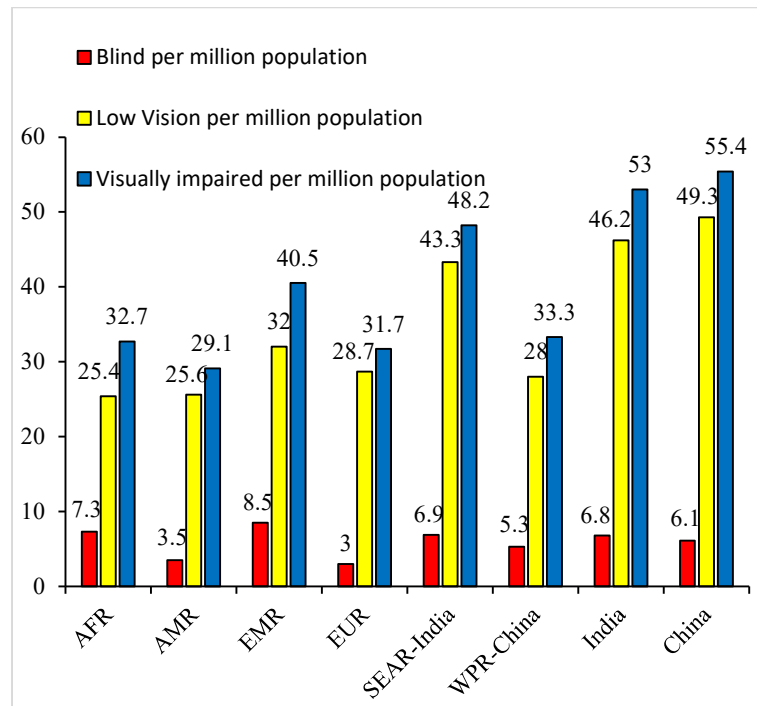


Figure 1.1: Number of people (%) by WHO regions who are blind, have low vision or have some form of visual impairment in 2010. AFR: Africa; AMR: America; EMR: Eastern Mediterranean; EUR: Europe; SEAR: Southeast Asia (without India); WPR: Western Pacific (without China). Figure made from data taken from [“https://www.iapb.org/wp-content/uploads/WHO-Global-Data-on-Visual-Impairments-2010.pdf”](https://www.iapb.org/wp-content/uploads/WHO-Global-Data-on-Visual-Impairments-2010.pdf).

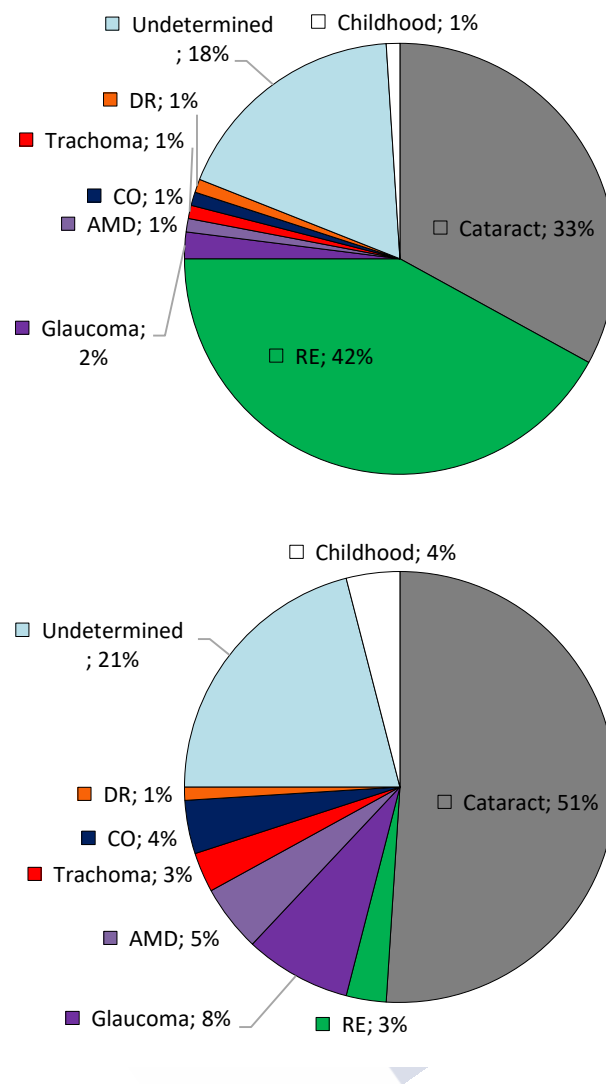


Figure 1.2: Global causes of visual impairment (top) and blindness (bottom) as a percentage of global visual impairment and global blindness in 2010. AMD: age-related macular degeneration; CO: corneal opacities; DR: diabetic retinopathy; RE: uncorrected refractive errors. Figure made from data taken from [“https://www.iapb.org/wp-content/uploads/WHO-Global-Data-on-Visual-Impairments-2010.pdf”](https://www.iapb.org/wp-content/uploads/WHO-Global-Data-on-Visual-Impairments-2010.pdf).

1.1. Ocular anatomy

The eye is one of the most complex organs, with unique anatomical, histological and physiological features. Eyes are the sensory organs responsible for capturing images and transmitting them to the brain, through the optic nerve. Their function is very important, as they receive extremely useful information from the environment. The ocular globe is divided into two zones: anterior and posterior. The anterior segment consists of aqueous humor, conjunctiva, cornea, uvea, crystalline and pupil, and represent approximately one third of the eye. The rest corresponds to the posterior segment, consisting of vitreous humor, retina, optic nerve, choroid, sclera and macula (Gaudana *et al.*, 2009; Cholkar *et al.*, 2013; Souto *et al.*, 2019) (Figure 1.3).

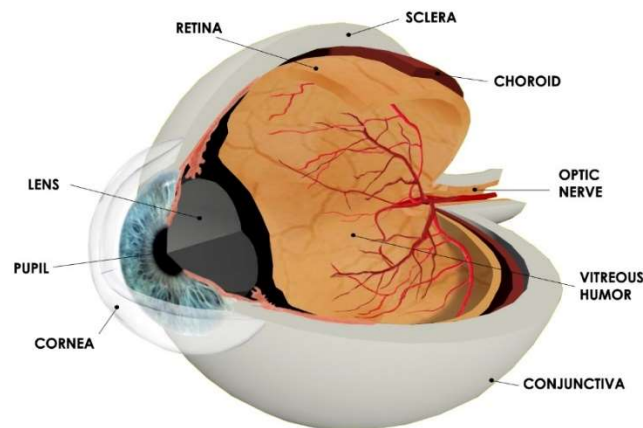


Figure 1.3: Structure of the eyeball. Figure made by the author of this Thesis.

The conjunctiva is a thin mucous membrane, which forms the inside of the eyelids from the corneal limb. It is formed by stratified non-keratinized epithelium. It contains Goblet cells, which are secretory cells, and vascularized connective tissue. Below the conjunctiva is the tarsal plate, formed by meibomian glands that secrete substances that decrease the evaporation of the tear film (*Witt et al., 2018; Pradeep et al., 2019*).

The cornea is the richest innervated tissue in the body, consisting mostly of sensory nerves, which are derived from the ophthalmic branch of the trigeminal nerve. It is in the most anterior part of the eye. It has an average horizontal diameter of 11.5 mm and a vertical diameter of 10.5 mm in an adult eye. The cornea lacks vascular structures; only the peripheral cornea is irrigated by anterior ciliary arteries that reach the limbus. It consists of five layers (from the outside to the inside): epithelium, Bowman's membrane, lamellar stroma, Descemet's membrane and endothelium. The epithelium protects the cornea on its outermost part with a tear film. It consists of surface cells, wing cells and basal cells. The stroma is responsible for maintaining the structure of the cornea and is mostly made up of collagen fibrils and keratocytes. Finally, the corneal endothelium is formed by a single layer of cuboidal cells and is responsible for intracellular ion transport (*Willoughby et al., 2010*) (**Figure 1.4**).

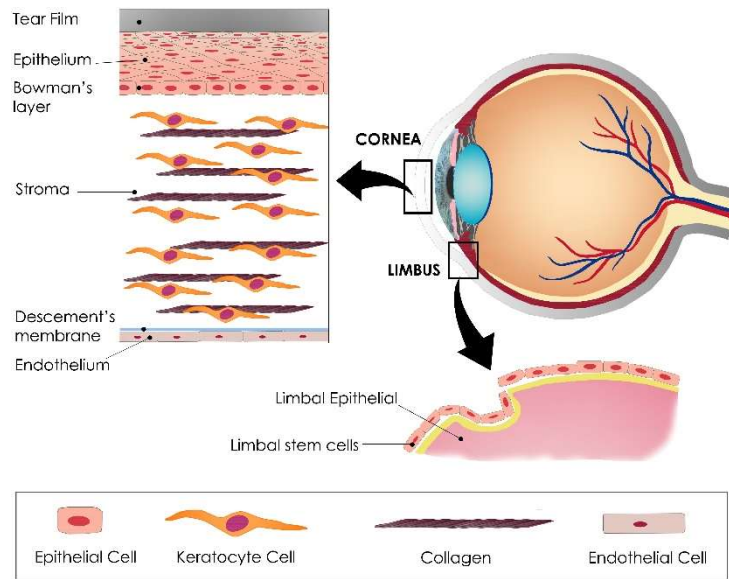


Figure 1.4: Schematic representation of the layers of the cornea and the cells that conform it. Adapted from Masterton et al. (2018). This is an open access article under the CC BY-NC-ND license.

The uvea is located between the retina and the sclera, and is formed by the ciliary body, the choroid and the iris. It is a pigmented vascular layer. The ciliary body covers the anterior sclera. The choroid is the main pigmented vascular tissue of the eyeball. The iris is located between the cornea and the lens, within the aqueous humor, and divides the anterior and posterior chambers with a central aperture, the pupil (Malhotra et al., 2011).

The crystalline or lens is made up of long fibre cells, with proteins and water. It is divided into two parts, nucleus and cortex. It is a transparent and flexible tissue, so that light can pass through it without problems and focus on the retina. It can change the curvature

of the surface when necessary, to adjust the focal distance (*Petrash 2013; Wang et al., 2019*).

The vitreous humor represents 80% of the volume of the eyeball and is divided into three parts: the vitreous nucleus, the vitreous base and the vitreous cortex. It is composed of 99% water, together with inorganic salts, sugars, lipids and proteins. Its function, in addition to providing mechanical support, is to maintain homeostasis in neighbouring tissues, provide nutrients, guarantee optical transparency and protect against the entry of cells or macromolecules that may interfere with the normal function of the eye (*Monteiro et al., 2015*).

The retina is a tissue that covers the internal surface of the eyeball. It consists of six classes of neurons: photoreceptors (cones and rods), bipolar cells, horizontal cells, amacrine cells, ganglion cells and Müller's glia, arranged in several parallel layers. Its function is to convert signals coming from outside into nerve impulses, transmitted from the optic nerve to the brain (*Willoughby et al., 2010*).

The optic nerve is part of the central nervous system. It is made up of retinal ganglion cell axons and supporting glial cells. Its function is to transmit electrical signals from the retina to the brain (*Chen et al., 2017*).

The choroid is a vascular layer located at the back of the uvea and consists of five layers: Bruch's membrane, the choriocapillaris, two vascular layers (Haller's and Sattler's) and the suprachoroidea. It is composed principally of blood vessels. Its main function is to supply

oxygen and nutrients to the retina, but it can also act as a thermoregulator and modulator of intraocular pressure (IOP) (*Nickla et al., 2010*).

Finally, the sclera is a protective and supportive outer layer of the eye. It occupies the area between the cornea margin and the optic nerve, which constitutes more than 80% of the eye's surface. Its structure varies with age, being thicker during the first few years of life. Then, it stretches and becomes stiffer. Sclera is formed by collagen fibres type I (90%) and type III (5%), which are included in the proteoglycan matrix. Its function is to maintain intraocular pressure and is where extraocular muscles meet. In addition, it is the main carrier tissue of the eye (*Malhotra et al., 2011; Coudrillier et al., 2015*).

1.2. Eye-defense mechanisms

Eye anatomy and physiology make it autonomous to defend itself from external agents (*Gaudana et al., 2010*). The eye's defense mechanisms can be classified into three types: mechanical, anatomical and immunological (*Akpek et al., 2003*). There are many factors that, in combination, provide complete protection to the eye, for example, the continuity of corneal and scleral tissue, blinking and tear composition, among others (*McClellan 1997*). The problem arises when these eye defense mechanisms also act as barriers to drug delivery. The main barriers are categorized as lacrimal film, corneal and non-corneal barriers and blood ocular barriers (**Figure 1.5**).

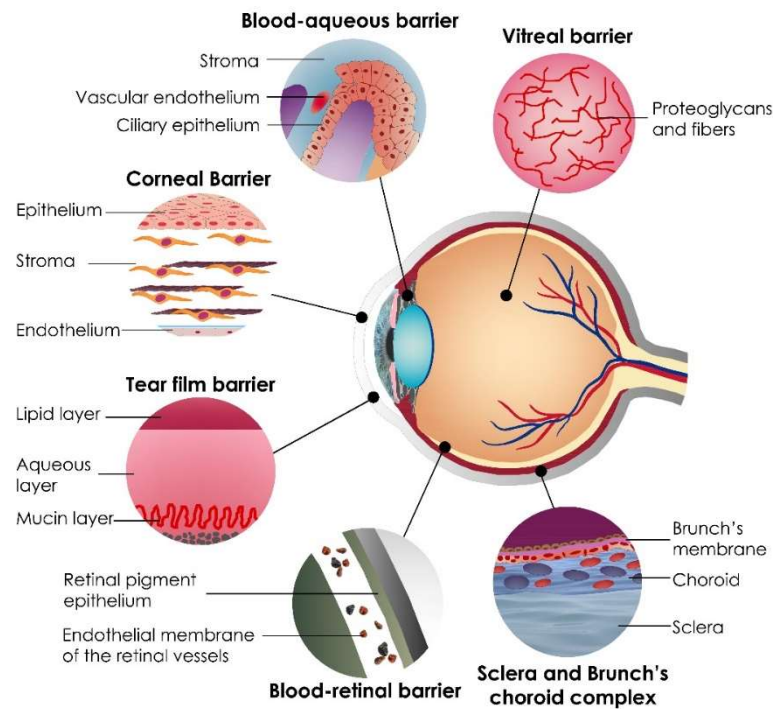


Figure 1.5: Schematic representation of the different defense barriers that the eye presents to the administration of drugs. Adapted from Huang et al. (2018) with permission from Elsevier.

1.2.1. Lacrimal film

It is the first protective barrier of the eye. It consists of proteins, lipids and mucin, with perfect electrolyte composition and optimal nutrient and pH values. The lacrimal fluid is made up of a lipid layer, an aqueous layer and a mucous membrane, from the outside to the inside. Its function is to modulate cell migration and proliferation during healing, as well as to modulate normal cell differentiation and

the secretion of electrolytes and water. The flow of tears is constant, being renewed every 2-20 minutes, so the residence time of any drug on the ocular surface is very low, which reduces its possibility of absorption (*Barar et al., 2009; Huang et al., 2018*).

1.2.2. Corneal barrier

The cornea, with a thickness of 0.5 mm and formed mainly by collagen, is the main barrier to the penetration of molecules into the eye (*Sánchez-López et al., 2017; Huang et al., 2018*). It consists of five layers, each of which has different properties. The outermost layer is the epithelium (stratified, squamous and not keratinized), which may allow the pass of small hydrophobic molecules but hinders the entrance of hydrophilic drugs. Only molecules with a molecular weight below 500 Da can pass through the paracellular pathway (*Barar et al., 2009; Huang et al., 2018*). The stroma (intermediate layer) opposes to the passage of lipophilic molecules due to its high content in hydrated collagen and proteoglycans. The endothelium is the innermost layer and consists of a monolayer of polygonal cells. Like the epithelium, it prevents the passage of hydrophilic molecules to the aqueous humor but allows the passage of small lipophilic molecules (*Barar et al., 2008; Huang et al., 2018*). In the cornea, collagen fibers are present in the Bowman's layer and stroma. In the first one, the fibrils have a diameter between 20-25 nm and their distribution is random, forming leaves 8-12 μm thick. In the stroma, the diameter of collagen fibers varies between 25-35 nm and its

distribution is in parallel, forming flat lamellar bundles (*Komai et al., 1991*). The physicochemical properties of drugs also affect their penetration through the cornea. Adequate balance between lipophilia, molecular weight and degree of ionization is required for a successful passive diffusion. The most common way of passage of drugs through the cornea is transcellular, while the paracellular predominates for hydrophilic or low molecular weight drugs (*Barar et al., 2009; Sánchez-López et al., 2017*).

1.2.3. Non-corneal barriers

The conjunctiva is a thin mucous membrane that covers the eyelids internally and the anterior surface of the sclera. Being formed by blood capillaries and conjunctival lymphatics, productive absorption of a drug is very low, although the permeability is greater than in cornea and also allows the passage of hydrophilic molecules and molecular weights up to 10 kDa (*Sánchez-López 2017; Huang et al., 2018*).

The sclera consists mainly of collagen and mucopolysaccharide. Collagen fibers vary in size from 25 to 230 nm. Although they form lamellar bundles, individual fibrils are more randomly arranged than in the cornea. Thickness varies from 0.5-6 μm . In the outermost part of the sclera, the collagen bundles are narrower and thinner than in the inner part (*Komai et al., 1991*). Sclera has a surface area of about 16 cm^2 and it is more permeable to hydrophilic solutes than other ocular structures, such as the cornea, as they can diffuse through the aqueous

medium between collagen fibrils, rather than through cell membranes. In this case, the radius of the molecules better predicts permeability than molecular weight (MW). Thus, molecules with higher MW but smaller radius cross the sclera better than others of the same MW but larger radius. Molecular charge also influences the transport of molecules; negatively charged molecules are more permeable than those with positive charge, due to the charge of the proteoglycan matrix, which is negative. Overall, drug permeability through sclera is favored compared to cornea (*Barar et al., 2008; Huang et al., 2018*).

1.2.4. Blood ocular barriers

There exist two types of ocular barriers in charge of regulating the solutes that cross towards the internal zones of the ocular globe: the haemato-aqueous barrier (BAB) and the haemato-retinal barrier (BRB).

The BAB is located at the anterior region and consists of the endothelium of the iris/ciliary blood vessels and the non-pigmented ciliary epithelium. Its function is to regulate the intraocular pressure, turning the flow of aqueous humor, to maintain the transparency and chemical composition of the ocular fluids. It also regulates the passage of drugs from the anterior to the posterior segment. The BRB is located at the posterior region of the eye and also consists of two types of cells: capillary endothelial cells of the retina and cells of the retinal pigment epithelium, which form the internal and external BRB, respectively. Its main function is to hinder the diffusion of substances

from the circulatory torrent to the retina. The main limiting property for the passage of substances is the molecular radius. Thus, the permeability decreases as the radius increases. Lipophilia also influences; therefore, only small and lipophilic molecules can pass from the choroid to the retina (*Huang et al., 2018*).

1.3. Ocular drug administration

Drug administration at the anterior segment of the eye can be done in several forms. Topical administration is the most common route for the treatment of diseases of the anterior segment, usually as eye drops or ointments. The following advantages can be mentioned: it is a non-invasive and painless pathway with high patient compliance; very high doses of the drug are not needed; and the effect may be immediate. The main disadvantage is that ocular bioavailability of drugs administered topically is less than 5% due to both physicochemical barriers (the structure of the eye or the composition of the tear) as well as naso-lacrimal drainage, tearing or blinking reflexes or the low volume that can host the cul-de-sac. In addition, it is estimated that the tear volume is 7 μL , and the restoration time of the tear film is fast (2-3 minutes), so that topically administered solutions would be eliminated shortly after instillation (*Awwad et al., 2017; Djebli et al., 2017*). Moreover, systemic side effects may arise, as much of the instilled dose passes into the bloodstream through the conjunctiva and nasal mucosa. In addition, nasolacrimal drainage of certain substances can cause toxic reactions

(*Loftsson et al., 1999; Ribeiro et al., 2015*). This system connects the flow of tears from the eye to the nasal cavity. The part of the drug drained after topical application passes into the lacrimal sac and then into the nasolacrimal duct until it reaches the nose. During this passage, the drug passes through vascularized areas, where it can be absorbed into the systemic circulation, which can lead to undesirable side effects (*Bachu et al., 2018*).

Ophthalmic preparations must meet some specific requirements. The active molecule must have a certain aqueous solubility. In addition, there are several critical parameters that need to be monitored. The ophthalmic formulations must have a tolerable acidity, with an adequate pH around 7.4, although there are some exceptions. They must also be isotonic as well as stable at room temperature. Other critical factors to consider are drug pKa and formulation viscosity. Excipients used during manufacture must be free from toxicity and should not interact with the packaging. All ophthalmic products must be sterile, and injectables must also be free of endotoxins and particles (*Novack et al., 2016; Yellepeddi et al., 2016*) (**Figure 1.6**). Drugs can be administered to the anterior segment of the eye also through intracameral and subconjunctival injections. Both avoid the cornea and hematoencephalic barrier and provide high ocular bioavailabilities. Ocular injections present all the inconveniences associated to injectable formulations, aggravated by the sensitive region where the formulations are delivered, which

causes patient discomfort and has the risk of tissue damage and infection. Finally, the systemic oral route despite being a non-invasive is barely used, since very high doses of drug are necessary to exert an effect at the ocular level and there are many adverse effects on other tissues (Janagam *et al.*, 2017).

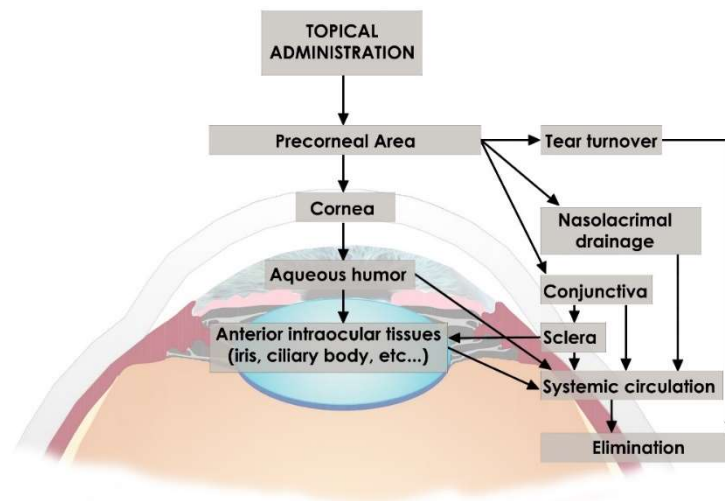


Figure 1.6. Penetration and elimination pathways of drug after topical administration. Adapted from Janagam *et al.* (2017) with permission from Elsevier.

The administration of drugs to the posterior segment of the eye is more complicated. Topical forms, such as drops or ointments, can hardly reach the posterior segment, except if the drug can efficiently enter through the conjunctiva-sclera pathway. Drugs can be administered orally, intramuscularly or intravenously, but the vast majority of drugs cannot cross the barriers, so bioavailability is

reduced to less than 2%. This low bioavailability requires the administration of high doses of drugs, which can trigger systemic toxicity and serious side effects (*Nayak et al., 2018; Varela-Fernandez et al., 2020*).

The intravitreal route allows for the administration of injections or implants. The main risk is the possible infection caused after the injection through the sclera. Other complications that may appear are, for example, elevated intraocular pressure (IOP) or bleeding. Intravitreal implants are aimed at the sustained release of drugs, with the advantage over injections that they do not require constant intervention. Despite the numerous disadvantages of this route, it remains the choice for the direct local treatment of pathologies associated with the posterior segment. Finally, the periocular route, consists of several routes with different functions. For example, the subtenon, subconjunctival, suprachoroid and transscleral routes can be used for drug administration, and the peribulbar, posterior yuxtapapillary, retrobulbar routes are for the application of anesthesia. The periocular route avoids the disadvantages of intravitreal injections, although a high risk is generated by systemic exposure to the drug (*Moisseiev et al., 2017; Nayak et al., 2018*).

1.4. Cornea diseases

The ocular diseases can also be differentiated depending on whether the affected area is the posterior or anterior segment of the eye. Diseases affecting the posterior segment include age-related

macular degeneration (AMD), diabetic retinopathy, macular edema (DME), proliferative vitreoretinopathy (PVR), posterior uveitis or infections caused by cytomegalovirus (CMV). Diseases such as dry eye syndrome, allergic conjunctivitis, anterior uveitis, or cataract may affect the anterior segment (*Bachu et al., 2018*). Corneal injuries are part of the diseases affecting the anterior segment of the eye and rank fifth among the leading causes of blindness worldwide (*Whitcher et al., 2001; Mathews et al., 2018*).

The epidemiology of corneal lesions and diseases is broad and includes ocular trauma, degenerative disorders, inflammatory diseases or infectious diseases, among others.

1.4.1. Ocular trauma

Eye trauma can occur for a range of reasons. Lacerations and perforations may have similar origin but differ in the depth of the lesion, since in lacerations, the stroma is damaged and in perforations, the endothelium is reached. The main causes are those associated with projectiles or sharp objects, as well as strong contusions. This type of trauma accounts for 6.8-14.7% of eye injuries. The best way to prevent this type of injury is with eye protection. The objectives of the treatment are to keep the eyeball hermetically sealed, in order to avoid infections, for example, by surgical repair, trying to restore the original shape of the eye, and finally, to return the organ to its normal function (*Vora et al., 2013; Barrientez et al., 2019*). Pharmacological treatment consists of intravenous administration of broad-spectrum

antibiotics to treat post-traumatic endophthalmitis infections (vancomycin, gentamycin or third generation cephalosporins) (*Willmann et al., 2019*).

Another reason for eye trauma is the contact with foreign bodies, which may lodge under the eyelid or in different parts of the cornea, even going unnoticed initially. Most corneal trauma injuries are due to foreign bodies. The symptoms are usually pain, discomfort or blepharospasm. The first thing to do is to remove the foreign body. Sometimes it is necessary to use a topical anesthetic for the physical examination and for the diagnosis a slit-lamp can be used. Corneal lesions usually heal quickly as long as the foreign body is completely removed (*Barrientez et al., 2019; Willmann et al., 2019*).

Finally, another notable cause of corneal injury is ocular abrasions due to blows or injuries produced by nails or foreign bodies, for example. Ocular inspections may reveal a variety of signs such as swelling, blepharospasm or tearing. Superficial pain may be relieved with a local anesthetic, such as proparacaine. Again, as with foreign bodies, abrasive lesions heal relatively quickly, and only control of pain and avoidance of infections is required. If the lesions are more complex, pharmacological treatment with cycloplexes and anti-inflammatories is used (*Willmann et al., 2019*).

1.4.2. Degenerative disorders

One of the most important degenerative diseases of the cornea is keratoconus. It consists of a progressive bilateral thinning and a

primary ectasia of the cornea, which leads to a loss of visual acuity. Loss of structural integrity results in cone-shaped corneal deformation (*Barrientez et al., 2019*). In keratoconus there is a thinning of the stroma, a rupture of the Bowman layer and iron deposits in the epithelium (*Romero-Jiménez et al., 2010*). In addition, collagen fibers lose elasticity by up to 36% (*Ma et al., 2018*). Corneal topography is the technique that provides earlier and more accurate detection of the disease (*Khaled et al., 2017*). The cause is not fully defined, but it is believed that genetic and environmental factors (contact lenses, allergies, etc.) may contribute to the development of the disease (*Davidson et al., 2014*). In addition, oxidative stress may also contribute to the pathogenesis (*Martin et al., 2019*). The main symptoms of keratoconus are photophobia or decreased visual acuity, among others. In occidental countries, it represents one of the main reasons for keratoplasty (*Khaled et al., 2017*). It generally occurs in adulthood and appears indifferently in men and women and does not distinguish by ethnicity (*Martin et al., 2019*). Prevalence varies greatly between countries and from 50 to 230 per 100,000 (*Khaled et al., 2017; Soiberman et al., 2017*). Treatment varies according to severity. Traditionally, glasses are worn during the onset of the disease. Mild or moderate cases are treated with silicone contact lenses (greater oxygen permeability), and more severe cases may require surgery (*Romero-Jiménez et al., 2010*).

1.4.3. Inflammatory diseases

The main inflammatory disease of the cornea is the dry eye syndrome (DES), also known as keratoconjunctivitis seca, and is directly related to age. Clinically, this disease is divided into two types: inflammation of the ocular surface and tear gland, and neurotrophic deficiency and dysfunction of the meibomian gland. Therefore, it is classified as dry eye by tear deficiency (10% of those affected) or dry eye by increased evaporation of tears (80% of those affected), respectively (*Messmer 2015*). In turn, tear deficiency can be divided into non-Sjogren's syndrome or Sjogren's syndrome; and increased tear evaporation is divided into meibomian gland disease and dry eye related to exposure. The etiology of this disease is very wide, for example, can be the result of inflammatory diseases, unfavorable environmental conditions, hormonal imbalance, improper use of contact lenses, systemic disorders or the use of certain drugs (*Javadi et al., 2011*). DES affects between 5 and 34% of the world's population and increases with age (*Martin et al., 2019*). The classic symptoms that appear are the sensation of grit, burning and dryness, (*Zhu et al., 2019*) and is characterized by eye discomfort, hyperosmolarity of the tear film and inflammation of the ocular surface, among others (*Martin et al., 2019; Radomska-Leśniewska et al., 2019*). The initial management is an improvement in palpebral hygiene, although the outcome is often poor. The use of eye lubricants only serves to mitigate symptoms. The pharmacological treatment

includes cyclosporine A as anti-inflammatory, although its high hydrophobic character poses solubility problems at the ocular level. Lipophilic drugs can be administered, in the form of emulsion, but end up causing irritation and blurred vision. Nowadays, there is no completely effective treatment for this pathology (*Gupta et al., 2020*).

1.4.4. Infectious diseases

Eye infections have different etiologies and can be of bacterial or viral origin. Bacterial infections are more common than other eye infections. Their origin can be the use of contaminated contact lenses, problems during an operation or age, for example, and may be caused by both Gram-positive and Gram-negative bacteria. Some of the most common bacterial infectious diseases are conjunctivitis, blepharitis, endophthalmitis or keratitis (*Teweldemedhin et. al., 2017*). Although not a majority, virus infections also affect the eye. The most common viral infections are conjunctivitis, keratitis, or herpetic diseases.

1.4.5. Prevention and treatment of corneal lesions: antioxidant agents

At the cornea level, inflammation and oxidative stress are responsible for both the origin and development of various age-related eye diseases, such as cataracts, glaucoma, diabetic retinopathy, macular degeneration or dry eye syndrome. These diseases represent the major causes of progressive and irreversible vision loss worldwide (*Abu-Amero et al., 2016; Bungau et al., 2019*). Specifically, age-related macular degeneration alone accounts for 8.7% of blindness

worldwide, and this figure is expected to double in 30 years (*Tan et al., 2019*).

Reactive oxygen species (ROS) are a subproduct of normal anaerobic metabolism. Enzymes such as SOD (superoxide dismutase), CAT (catalase) or GPx (glutathione peroxidase) neutralize these subproducts. When a disequilibrium is generated in the redox haemostasis of the pro- and antioxidant systems due to the incapacity of enzymes to eliminate free radicals, cell necrosis is triggered due to damage to proteins, lipids and DNA, causing degeneration at the ocular level (*Bungau et al., 2019; Tan et al., 2019*).

There are different factors that promote oxidative stress, such as age, exposure to light or metabolic processes, such as hyperglycemia (*Bungau et al., 2019*). The cornea protects the eye from environmental stress by absorbing ultraviolet (UV) light, but prolonged irradiation may cause corneal lesions (*Zernii et al., 2018*). The radiation can end up damaging the anterior segment. The most common acute condition is photokeratitis and in the long-term cataracts, carcinomas, melanomas or other pathologies of the conjunctiva may appear. The most serious consequence of UV radiation is ROS generation. At the ocular level, there are several antioxidants of low molecular weight in both tissues and fluids, such as ascorbic acid, alpha-tocopherol or glutathione, and of high molecular weight, which are the enzymes mentioned above. The cornea, especially the anterior part, can absorb up to 60% of UVA radiation and up to 92% of UVB radiation,

although it is more sensitive to the latter. Although the eye has an antioxidant defense, when there is an increase in UV radiation, there is a prooxidant/antioxidant imbalance that favors the damage (*Cejkova et al., 2004*).

Several carotenoids and polyphenols have antioxidant and anti-inflammatory activities. They decrease the production of ROS, which in turn inhibits tumor necrosis factor α (TNF α) and vascular endothelial growth factor pathways, which helps to suppress p53-dependent apoptosis, eliminating the genesis of inflammatory markers (IL-8, 6, 1 α and endothelial leucocyte adhesion molecule-1) (*Bungau et al., 2019*). One example is resveratrol, which has also been shown to exhibit anti-aging properties at ocular level (*Abu-Amero et al., 2016*). Another compound to highlight is transferulic acid, which besides being a powerful antioxidant, exerts anti-inflammatory and antibacterial effects, among others. Its mechanism of action, in addition to eliminating free radicals, can inhibit the enzymes that catalyze the synthesis of these free radicals (*Zdunska et al., 2018*). At the ocular level, studies have shown that it can be useful for the healing of corneal wounds (*Tsai et al., 2016; Grimaudo et al., 2020*), or to suppress the production of amyloid B in the human lens (*Nagai et al., 2017*).

1.5. Ocular viral infections

It is estimated that 20-70% of conjunctivitis are viral, and of these, 65-90% are caused by adenoviruses. These viral infections

spread through the air, by deposits, or by direct contact with the virus. Conjunctivitis can be classified in two groups: papillary or follicular. The first one manifests itself with flat and compact projections, with numerous eosinophils, lymphocytes, plasma cells and mast cells in the stroma that surrounds a central vascular channel. It is usually associated with a foreign body response or an allergic immune response. Follicular conjunctivitis occurs with prominent follicles in the lower palpebral and forniceal conjunctiva. The most common symptoms and signs during viral conjunctivitis are foreign body sensation, red eyes, itching, sensitivity to light, burning, and watery discharge (*Li et al., 2018; Solano et al., 2019*).

Keratitis is another eye infection caused by a virus; in this case mainly herpes simplex virus (HSV). The number of people affected by this disease worldwide was estimated at 1.5 million. It is the most common cause of unilateral infectious corneal blindness. Unlike bacterial or fungal keratitis, viral keratitis can be recurrent and chronic. There are two other forms of viral keratitis, but they are less common: varicella-zoster virus (VZV) keratitis and cytomegalovirus (CMV) keratitis (*Austin et al., 2017*). The classic symptoms of viral keratitis are eye pain, blurred vision, redness, and photophobia (*Rowe et al., 2013*).

Herpes zoster is a relevant eye infection. It has its origin in the reactivation of the varicella-zoster virus (VZV), a virus of the herpesviridae family (**Table 1.1**). Initially, the disease presents itself

as chickenpox, infecting the sensory ganglia. It usually occurs in the early stages of life. It is very contagious but benign and occurs in the form of blisters spread throughout the body with itching.

Table 1.1. Classification of *Herpesvirus*.

<i>Herpesviridae</i> family		
Sub-family	Types	Virus
Alpha-herpesvirinae	Herpesvirus 1	Herpes simplex 1
	Herpesvirus 2	Herpes simplex 2
	Herpesvirus 3	Varicella Zoster
Beta-herpesvirinae	Herpesvirus 5	Cytomegalovirus
	Herpesvirus 6	Herpesvirus lymphotrope
	Herpesvirus 7	Human herpesvirus
Gamma-herpesvirinae	Herpesvirus 4	Epstein-Barr Virus
	Herpesvirus 8	Kaposi's Sarcoma

The reactivation of the virus, known as herpes zoster or shingles, is more dangerous. It manifests as vesicular eruptions, affecting mostly the thoracic nerve, but also the trigeminal nerve. Factors such as changes in T-cells or a decrease in the neutralization of antibodies, which occur as age progresses, influence the possible reactivation of VZV. The risk is also higher in immunocompromised patients. The data warn that about 50% of adults affected by herpes zoster are at risk of complications. Herpes zoster ophthalmicus represents between 10-20% of cases of zoster and is the second most common complication. The disease begins with symptoms of severe pain and discomfort.

After a few days, skin lesions appear. Complications at the level of the cornea appear in 65% of cases. The acute phase presents with epithelial keratitis (puncture or dendritic) or stromal keratitis, and the late phase with neurotrophic keratopathy or neovascularization of the cornea. The most common manifestations are photosensitivity, decreased vision or perforation, among others (*Zhu et al., 2014*).

1.5.1. Treatment of ocular viral infections

The causal agent of viral conjunctivitis should be identified correctly so that proper treatment can be given. For example, commonly viral conjunctivitis occurs with watery discharge, as opposed to bacterial conjunctivitis that presents mucopurulent discharges. There is no effective treatment in its entirety. Artificial tears, topical antihistamines, or cold compresses are used as palliatives. The effectiveness of ocular antivirals is not high. Topical antibiotics are not indicated since they are not capable of preventing secondary infections, also causing undesired side effects, such as allergy or toxicity. Of all cases of acute conjunctivitis, the herpes simplex virus is responsible for 1.3-4.8%. This type of pathology is usually unilateral, with watery discharge and sometimes even vesicular lesions may appear on the eyelid. The usual treatment consists of topical and oral antivirals. The use of topical corticosteroids should be avoided because they are potentiators of the virus (*Azari et al., 2013*).

On the other hand, topical treatment for viral keratitis caused by herpes simplex virus (HSV) includes antiviral drugs and adjunctive topical corticosteroids. The most commonly used topical antiviral was trifluridine, although its bioavailability was very low and caused surface toxicity at the ocular level, so its use has been reduced. Acyclovir is the first choice for the treatment of keratitis since its effectiveness is high and it is less toxic. New synthetic drugs, such as ganciclovir, have a broader-spectrum antiviral action, i.e., in addition to treating keratitis caused by HSV, it also attacks VZV and CMV. Additionally, topical corticosteroids are sometimes used as adjuvant therapy. On the other hand, acyclovir is also given as an oral adjuvant therapy. Valacyclovir was also seen to have greater oral bioavailability for the treatment of HSV, requiring lower doses (*Austin et al., 2017*).

Finally, herpes zoster ophthalmicus usually appears as a mild case, but antiviral use is still recommended for the first 72 hours after the onset of the rash. Early treatment can lead to a reduction in the duration of the illness as well as acute pain and halve the likelihood of eye disorders. The drugs chosen are acyclovir, valacyclovir and famcyclovir. Although all three have similar efficacies, the more recent ones (valacyclovir and famcyclovir) have higher oral bioavailability. In this case, corticosteroids are also used as adjuvant therapy, especially during the first stage of the disease, to relieve pain and improve healing, but their long-term use should be avoided

because of side effects. If the disease manifests late, antiviral drugs are not effective and topical corticosteroids should be used to reduce inflammation (*Zhu et al., 2014*).

1.6. Micelles and contact lenses as platforms for ocular delivery

The classic methods of ocular administration of drugs (eye drops or ointments) have different drawbacks, as explained in section 1.3. That is the reason of a continuous search for new drug dosage forms, to improve drug ocular bioavailability, combining an efficient controlled release and minimizing pain and discomfort for the patient. Among other platforms, polymeric micelles and soft contact lenses are gaining increasing interest (*Gote et al., 2019*).

1.6.1. Polymeric micelles

The use of nanocarriers is gaining increasing attention for the delivery of ocular drugs (*Gomez-Ballesteros et al., 2019*). Polymeric micelles are formed by amphiphilic copolymers, which spontaneously self-assemble in an aqueous medium, once they exceed the critical micellar concentration (CMC) (*Grimaudo et al., 2019*). Their size can vary between 5-100 nm, and their shapes can also be different. During the process of micelle formation there is an equilibrium of intermolecular forces, such as van der Waals forces, hydrogen bonding and hydrophobic, steric and electrostatic interactions (*Gaucher et al., 2005*). The structure of the micelle comprises an internal hydrophobic core, capable of hosting liposoluble drugs and solubilizing them, and an external hydrophilic shell, in contact with

the external environment, which physically stabilizes the micelle (**Figure 1.7**) (Croy *et al.*, 2006).

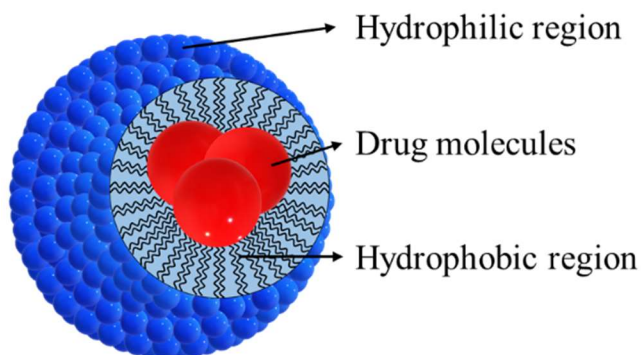


Figure 1.7. Schematic representation of the structure of a polymeric micelle. Figure made by the author of this Thesis.

The encapsulation of drugs in polymeric micelles prevents the interaction with the surrounding environment, which enhances their physicochemical stability. In addition, properties of the external shell, such as viscosity, thickness or porosity, may determine the rate of drug release. The process of drug incorporation is complex and depends on the molecular and physicochemical properties of both parts (micelle and drug). The molecular weight and the hydrophilic-lipophilic balance (HLB) are properties to consider in the copolymer; for similar molecular weights, a decrease in HLB leads to larger nucleus and with greater encapsulation power. On the other hand, for similar HLB, the higher the molecular weight of the copolymer, the more efficient the encapsulation is. Properties of the drug such as molecular weight, radius, lipophilia (partition coefficient, $\log P$),

melting point, tendency to aggregation and the presence of specific functional groups that may interact with the micelle modify the encapsulation efficiency.

There are different methods for the preparation of drug-loaded polymeric micelles. The most direct and simple method consists of dissolving the copolymer in water, stabilizing the micelle dispersion at a suitable temperature (48-72 h) and then adding the drug to be incorporated into the micelles. This method is generally used for micelles formed by copolymers of intermediate HLB. It may require the application of heat to dehydrate the segments that will form the nucleus to form the micelles. Another technique, used for more hydrophobic copolymers, consists of dissolving both components (copolymer and drug) in water-miscible organic solvents. The mechanism of micellar formation will depend on the procedure by which the organic solvent is removed. For example, the mixture may be dialyzed and the slow elimination of the organic phase triggers the formation of micelles; or the organic phase may evaporate, forming a polymeric film, which will be rehydrated with an aqueous solvent, aided by heat, to form the drug-loaded micelles. There are more techniques, such as trapping a hydrophobic drug in an O/W emulsion, casting in solution or lyophilization (*Gaucher et al., 2005*).

Topical formulations of drug-loaded polymeric micelles can be considered as non-invasive delivery systems. These systems can stay in the site of administration long enough for the drug to exert its

therapeutic effect due to properties such as viscosity or mucoadhesion. In general, the contact time of the formulation is directly proportional to its viscosity. The clearance of drugs by blinking or naso-lacrimal drainage is reduced by increasing the viscosity of the system. The use of mucoadhesive components for the formation of the polymer micelles also increases the residence time of the micelles at the administration site due to the formation of covalent bonds with mucin. Polymeric micelles are safe and effective systems and avoid patient discomfort. For the drug to reach the posterior segment of the eye, it can follow the corneal or conjunctival-scleral route (**Figure 1.8**) (Mandal *et al.*, 2017; Grimaudo *et al.*, 2019).

The size of the polymeric micelles in the nanoscale endows them with the ability to pass through structures such as the cornea or the conjunctiva/sclera pathway. The pass of hydrophobic drugs through the hydrophilic stroma may be favored by the encapsulation in nanomicelles. The sclera has a larger area, which allows the polymeric micelles to spread laterally to the posterior segment. From there, the cells of the retinal pigmented epithelium may engulf nanocarriers by endocytosis, opening the possibility of exerting an effect on the ocular tissues of the posterior segment (Hughes *et al.*, 2005; Mandal *et al.*, 2017).

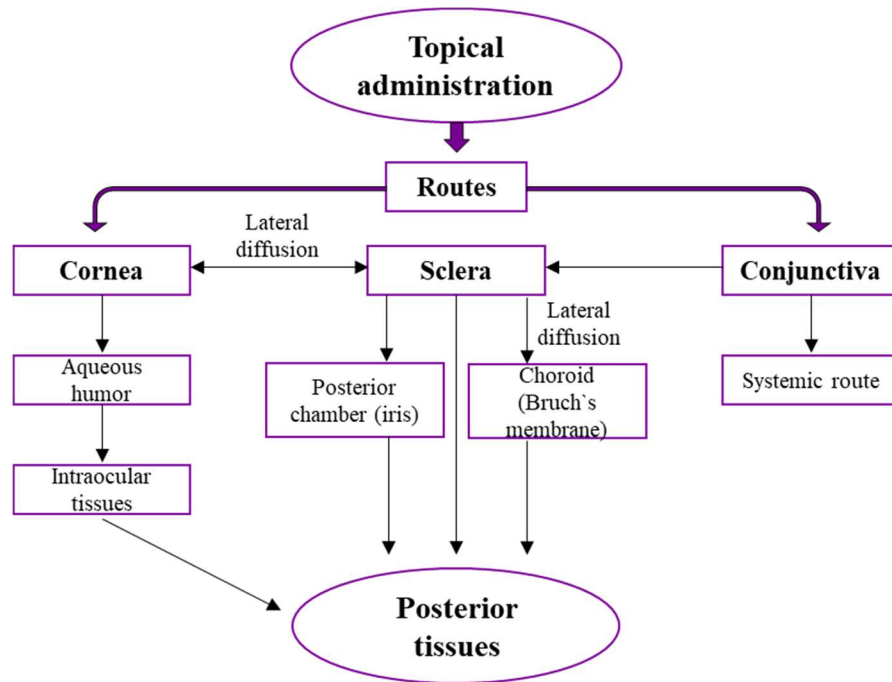


Figure 1.8. Diagram of the different routes after topical ocular administration of medication. Adapted from Hughes et al. (2005) with permission from Elsevier.

1.6.2. Contact lenses

The use of soft contact lenses (SCLs) as drug delivery systems is considered an alternative to the classic forms. The aim is to increase the ocular bioavailability of the drugs administered, while minimizing possible pain during administration and maintaining visual capacity (Gonzalez-Chomon et al., 2013; Alvarez-Lorenzo et al., 2019). SCLs are mainly made of hydroxyethyl methacrylate (HEMA) polymer hydrogels with hydrophilic comonomers, which increase the water content and thus the oxygen permeability. As an alternative, silicone

hydrogel CLs have higher oxygen permeability and can be worn for longer periods of time, but they are less hydrophilic (Xu *et al.*, 2018).

The use of drug-loaded CLs relies on that they can supply a precise dose of drug; they can deliver in a single device two or more active substances in high quantities; they do not damage the ocular surface and do not perturb the vision; they may reduce the number of daily administrations due to sustained release and prolonged permanence time on the eye surface in contact with the cornea; they minimize the amount of drug that passes into the systemic circulation, reducing possible untoward effects; and they can be used for vision correction at the same time as drug treatment is administered. After placement of the CLs over the eye, a physical division is created between the pre-lens and post-lens tear fluid. The drug diffuses from the CL mainly to the post-lens fluid, i.e., in contact with the cornea. Differently, there is no drug diffusion towards the pre-lens fluid since the external face of the CL becomes dry in the time in between successive blinks. The post-lens lacrimal fluid has slower renovation dynamics which favors drug accumulation and therefore higher drug concentrations can be achieved in contact with the cornea. The increase in concentration gradient is the main driven force for drug penetration into the ocular structures (Xu *et al.*, 2018; Alvarez-Lorenzo *et al.*, 2019).

Design of drug-releasing CLs is a challenge because most of the available CLs do not show affinity for drugs or bind them irreversibly.

The different strategies to endow CLs with affinity for drugs are classified into two broad groups, depending on whether the starting material is commercial CLs or ad hoc preparations (*Alvarez-Lorenzo et al., 2019*). If the affinity of the drug for the polymer components is too low, therapeutic levels will not be reached; while if it is too high, the binding will be irreversible and no release will occur (*Gonzalez-Chomon et al., 2013*).

Methods for loading drugs into CLs can be summarized as follows.

- a) Soaking: this method is the simplest. The force that drives the drug into and out of the CLs is molecular diffusion by concentration difference. The amount of drug loaded/released depends on the concentration of the drug, its molecular weight, the thickness of the CLs or its water content, and the length of time it is soaked. The release kinetics will depend on the composition of the hydrogel, i.e. the use of hydrophilic monomers increases drug loading due to a higher swelling and, on the contrary, a higher proportion of hydrophobic monomers may provide more sustained drug release. If the drug is only hosted in the aqueous phase of the hydrogel, a burst release occurs after eye insertion. Only if specific interactions with the network can be established, the loading becomes relevant and controlled release may be achieved. The main disadvantages of this method are that drugs with a high

molecular weight are not able to penetrate the aqueous channels, so they remain on the surface and are released quickly. In addition, the lenses have a low affinity for most ophthalmic drugs, so they are not properly retained within the hydrogel structure and are released very quickly, failing to reach therapeutic levels (*Gonzalez-Chomon et al., 2011; Maulvi et al., 2016*).

- b) Soaking method combined with vitamin E: vitamin E is relatively hydrophobic and the soaking of a CLs in a medium (usually a non-aqueous solvent) containing a mid/low polarity drug and the vitamin E favors the hosting inside the CL. Vitamin E may form an efficient diffusion barrier on the surface able to regulate and prolong drug release, particularly useful for hydrophilic drugs. In addition, vitamin E is a powerful antioxidant, capable of blocking UV radiation and avoiding damage to the surface of the eye, as well as preventing oxidation of susceptible drugs. This barrier is safe and allows the passage of oxygen and ions properly. In addition, the optical properties of the lens are not modified, so vision is not compromised. The main limitations of the use of vitamin E are that it can modify the mechanical properties of the contact lens and that it adsorbs proteins due to its hydrophobic nature (*Peng et al., 2012; Hsu et al., 2013*).

- c) Drug-polymer film embedded contact lens: this method consists of the application of poly(lactic-co-glycolic) acid (PLGA) films on preloaded CLs. PLGA is a biodegradable and biocompatible polymer capable of regulating drug release. The aim is to achieve zero-order release kinetics. This method improves sustained release and increases ocular bioavailability, but as the PLGA layer turns white in contact with water, the transparency of the lens is affected, as well as mechanical properties and oxygen permeability (*Ciolino et al., 2009; Ciolino et al., 2014*).
- d) Ion interactions: one way to increase affinity and improve drug loading and release is by polymerizing CLs with an ionic monomer, after which the CLs is immersed in a drug solution. Another technique, in addition to copolymerization, is the use of adsorption force to achieve a loading of ionic components in the CLs. The result is a hydrogel with side chains of ion groups that can interact with ionic moieties in the drug. The main disadvantages of this technique are that the volume can vary as the drug is released (which may interfere in the optical accuracy), and that it is only valid for one type of drug at a time, that is, it does not work for mixtures of cationic and anionic drugs, nor for neutral drugs (*Uchida et al., 2003; Hsu et al., 2014*).

- e) Cyclodextrin-based contact lens: cyclodextrins (CDs) are widely used to form inclusion complexes through reversible non-covalent interactions with a variety of drugs. There are different techniques to develop CLs grafted with CDs, such as copolymerization of acrylic/vinyl CD derivatives and grafting of CDs onto preformed polymer networks. In general, solutions that contain CDs do not achieve controlled drug release, due to the rapid CD:drug decomplexation that occurs on contact with physiological fluids. But if the CD is bound to a polymer network, the release occurs less rapidly as the dilution is minimized. Factors such as the pH of the medium or the salt concentration must be taken into account when formulating CD:drug complexes, as they can alter the affinity constant (*dos Santos et al., 2008; dos Santos et al., 2009*).
- f) Molecular imprinting: this method consists of creating artificial receptors in the CL structure with the size and the chemical groups more adequate to fit the drug of interest. The technique relies on adding the molecule of interest to the solution of monomers (backbone and functional ones) before the polymerization in order that the monomers can arrange around the template molecules as a function of their affinity. The affinity of these receptors for the drug would determine the strength of the interaction with the CL and thus the release

rate. Critical parameters such as the selection of the functional monomer and its stoichiometry with respect to the template must be considered (*Alvarez-Lorenzo et al., 2010*).

- g) Supercritical fluid impregnation: Supercritical fluids, mainly supercritical CO₂ (scCO₂) can be used to enhanced drug dissolution and penetration into polymer networks (*Garcia-Gonzalez et al., 2015*). The process starts with the dissolution of the drug in the supercritical solvent in contact with the CLs. This technique allows the loading of hydrophilic and hydrophobic drugs at higher amount than conventional soaking in aqueous medium, but no significant improvements in the control of release rate are usually achieved (*Yañez et al., 2011*).
- h) Incorporation of colloidal nanoparticles: the administration of drugs encapsulated in colloidal nanoparticles increases the residence time of the drug in the cornea and prevents the ocular enzymes from metabolizing the drug. Therefore, the addition of nanocarriers to CLs may prolong the action time. Nevertheless, the addition of nanoparticles may obstruct the vision by decreasing the transparency of the lens.
- There are four methods of preparing these systems. The first one consists of preparing the nanoparticles loaded with drug, and their subsequent dispersion in pre-monomer mixtures, to

form CLs. The second method is to add surfactants and drugs to pre-monomer mixtures to form micelles during polymerization. The third method consists of immersing the already formed CL in a suspension of nanoparticles. Finally, the fourth method consists of immobilizing the nanoparticles on the surface of the CL by means of chemical bonds. Different types of nanoparticles can be subjected to these procedures, such as polymer nanoparticles, micelles, liposomes or microemulsions (*Morrison et al., 2014; Ali et al., 2016; Choi et al., 2018*).



1.7. References

Abu-Amero K.K., Kondkar A.A., Chalam K.V. 2016. Resveratrol and ocular diseases. *Nutrients*. 8:200

Akpek E.K., Gottsch J.D. 2003. Immune defense at the ocular surface. *Eye (Lond)*. 17:949-956

Ali J., Fazil M., Qumbar M., Khan N., Ali A. 2016. Colloidal drug delivery system: amplify the ocular delivery. *Drug Deliv*. 23:710-726

Alvarez-Lorenzo C., Anguiano-Igea S., Varela-Garcia A., Vivero-Lopez M., Concheiro A. 2019. Bioinspired hydrogels for drug-eluting contact lenses. *Acta Biomater*. 84:49-62

Alvarez-Lorenzo C., Yañez F., Concheiro A. 2010. Ocular drug delivery from molecularly-imprinted contact lenses. *J Drug Deliv Sci Technol*. 20:237-248

Austin A., Lietman T., Rose-Nussbaumer J. 2017. Update on the management of infectious keratitis. *Ophthalmology*. 124:1678-1689

Awwad S., Mohamed Ahmed A.H.A., Sharma G., Heng J.S., Khaw P.T., Brocchini S., Lockwood A. 2017. Principles of pharmacology in the eye. *Br J Pharmacol*. 174:4205-4223

Azari A.A., Barney N.P. 2013. Conjunctivitis: a systematic review of diagnosis and treatment. *JAMA*. 310:1721-1729

Bachu R.D., Chowdhury P., Al-Saedi Z.H.F., Karla P.K., Boddu S.H.S. 2018. Ocular drug delivery barriers-role of nanocarriers in the treatment of anterior segment ocular diseases. *Pharmaceutics*. 10(1):28

Barar J., Asadi M., Mortazavi-Tabatabaei S.A., Omid Y. 2009. Ocular drug delivery; impact of *in vitro* cell culture models. *J Ophthalmic Vis Res.* 4:238-252

Barar J., Javadzadeh A.R., Omid Y. 2008. Ocular novel drug delivery: impacts of membranes and barriers. *Expert Opin Drug Deliv.* 5:567-581

Barrientez B., Nicholas S.E., Whelchel A., Sharif R., Hjortdal J., Karamichos D. 2019. Corneal injury: clinical and molecular aspects. *Exp Eye Res.* 186:107709

Bungau S., Abdel-Daim M.M., Tit D.M., Ghanem E., Sato S., Maruyama-Inoue M., Yamane S., Kadonosono K. 2019. Health benefits of polyphenols and carotenoids in age-related eye diseases. *Oxid Med Cell Longev.* 2019:9783429

Cejkova J., Stipek S., Crkovska J., Ardan T., Platenik J., Cejka C., Midelfart A. 2004. UV Rays, the prooxidant/antioxidant imbalance in the cornea and oxidative eye damage. *Physiol Res.* 53:1-10

Chen C.A., Yin J., Lewis R.A., Schaaf C.P. 2017. Genetic causes of optic nerve hypoplasia. *J Med Genet.* 54:441-449

Choi S.W., Kim J. 2018. Therapeutic contact lenses with polymeric vehicles for ocular drug delivery: a review. *Materials (Basel).* 11(7):1125

Cholkar K., Dasari S.R., Pal D., Mitra A.K. 2013. 1 - Eye: anatomy, physiology and barriers to drug delivery. In: Mitra, A.K. (Ed.), *Ocular Transporters and Receptors. Their role in drug delivery.* Woodhead Publishing Series in Biomedicine, pp. 1-36

Ciolino J.B., Hoare T.R., Iwata N.G., Behlau I., Dohlman C.H., Langer R., Kohane D.S. 2009. A drug-eluting contact lens. *Invest Ophthalmol Vis Sci.* 50:3346-3352

Ciolino J.B., Stefanescu C.F., Ross A.E., Salvador-Culla B., Cortez P., Ford E.M., Wymbs K.A., Sprague S.L., Mascoop D.R., Rudina S.S., Trauger S.A., Cade F., Kohane D.S. 2014. *In vivo* performance of a drug-eluting contact lens to treat glaucoma for a month. *Biomaterials.* 35:432-439

Coudrillier B., Pijanka J., Jefferys J., Sorensen T., Quigley H. A., Boote C., Nguyen T. D. 2015. Collagen structure and mechanical properties of the human sclera: analysis for the effects of age. *J Biomech Eng.* 137(4):041006

Croy S.R., Kwon G.S. 2006. Polymeric micelles for drug delivery. *Curr Pharm Des.* 12:4669-4684

Davidson A.E., Hayes S., Hardcastle A.J., Tuft S.J. 2014. The pathogenesis of keratoconus. *Eye (Lond).* 28:189-195

Djebli N., Khier S., Griguer F., Coutant A.L., Tavernier A., Fabre G., Leriche C., Fabre D. 2017. Ocular drug distribution after topical administration: population pharmacokinetic model in rabbits. *Eur J Drug Metab Pharmacokinet.* 42:59-68

dos Santos J.F., Alvarez-Lorenzo C., Silva M., Balsa L., Couceiro J., Torres-Labandeira J.J., Concheiro A. 2009. Soft contact lenses functionalized with pendant cyclodextrins for controlled drug delivery. *Biomaterials.* 30:1348-1355

dos Santos J.F., Couceiro R., Concheiro A., Torres-Labandeira J.J., Alvarez-Lorenzo C. 2008. Poly(hydroxyethyl methacrylate-co-

methacrylated-beta-cyclodextrin) hydrogels: synthesis, cytocompatibility, mechanical properties and drug loading/release properties. *Acta Biomater.* 4:745-755

Flaxman S.R., Bourne R.R.A., Resnikoff S., Ackland P., Braithwaite T., Cicinelli M.V., Das A., Jonas J.B., Keeffe J., Kempen J.H., Leasher J., Limburg H., Naidoo K., Pesudovs K., Silvester A., Stevens G.A., Tahhan N., Wong T.Y., Taylor H.R. 2017. Vision loss expert group of the global burden of disease study, global causes of blindness and distance vision impairment 1990-2020: a systematic review and meta-analysis. *Lancet Glob Health.* 5:e1221-e1234

Garcia-Gonzalez C.A., Concheiro A., Alvarez-Lorenzo C. 2015. Processing of materials for regenerative medicine using supercritical fluid technology. *Bioconjug Chem.* 26:1159-1171

Gaucher G., Dufresne M.H., Sant V.P., Kang N., Maysinger D., Leroux J.C. 2005. Block copolymer micelles: preparation, characterization and application in drug delivery. *J Control Release.* 109:169-188

Gaudana R., Ananthula H.K., Parenky A., Mitra A.K. 2010. Ocular drug delivery. *AAPS J.* 12(3):348-360

Gaudana R., Jwala J., Boddu S.H., Mitra A.K. 2009. Recent perspectives in ocular drug delivery. *Pharm Res.* 26:1197-1216

Gomez-Ballesteros M., Andres-Guerrero V., Parra F.J., Marinich J., de-Las-Heras B., Molina-Martinez I.T., Vazquez-Lasa B., San Roman J., Herrero-Vanrell R. 2019. Amphiphilic acrylic nanoparticles containing the poloxamer star Bayfit® 10wf15 as ophthalmic drug carriers. *Polymers (Basel).* 11(7):1213

Gonzalez-Chomon C., Concheiro A., Alvarez-Lorenzo C. 2011. Drug-eluting intraocular lenses. *Materials (Basel)*. 4:1927-1940

Gonzalez-Chomon C., Concheiro A., Alvarez-Lorenzo C. 2013. Soft contact lenses for controlled ocular delivery: 50 years in the making. *Ther Deliv*. 4:1141-1161

Gote V., Sikder S., Sicotte J., Pal D. 2019. Ocular drug delivery: present innovations and future challenges. *J Pharmacol Exp Ther*. 370:602-624

Grimaudo M.A., Amato G., Carbone C., Diaz-Rodriguez P., Musumeci T., Concheiro A., Alvarez-Lorenzo C., Puglisi G. 2020. Micelle-nanogel platform for ferulic acid ocular delivery. *Int J Pharm*. 576:118986

Grimaudo M.A., Pescina S., Padula C., Santi P., Concheiro A., Alvarez-Lorenzo C., Nicoli S. 2019. Topical application of polymeric nanomicelles in ophthalmology: a review on research efforts for the noninvasive delivery of ocular therapeutics. *Expert Opin Drug Deliv*. 16:397-413

Gupta P.K., Asbell P., Sheppard J. 2020. Current and future pharmacological therapies for the management of dry eye. *Eye Contact Lens*. 46 Suppl 2 S64-S69

Hsu K.H., Fentzke R.C., Chauhan A. 2013. Feasibility of corneal drug delivery of cysteamine using vitamin E modified silicone hydrogel contact lenses. *Eur J Pharm Biopharm*. 85:531-540

Hsu K.H., Gause S., Chauhan A. 2014. Review of ophthalmic drug delivery by contact lenses. *J Drug Del Sci Tech*. 24:2 123-135

Huang D., Chen Y.S., Rupenthal I.D. 2018. Overcoming ocular drug delivery barriers through the use of physical forces. *Adv Drug Deliv Rev.* 126:96-112

Hughes P.M., Olejnik O., Chang-Lin J.E., Wilson C.G. 2005. Topical and systemic drug delivery to the posterior segments. *Adv Drug Deliv Rev.* 57:2010-2032

Janagam D.R., Wu L., Lowe T.L. 2017. Nanoparticles for drug delivery to the anterior segment of the eye. *Adv Drug Deliv Rev.* 122:31-64

Javadi M.A., Feizi S. 2011. Dry eye syndrome. *J Ophthalmic Vis Res.* 6:192-198

Khaled M.L., Helwa I., Drewry M., Seremwe M., Estes A., Liu Y. 2017. Molecular and histopathological changes associated with keratoconus. *Biomed Res Int.* 7803029

Komai Y., Ushiki T. 1991. The three-dimensional organization of collagen fibrils in the human cornea and sclera. *Invest Ophthalmol Vis Sci.* 32:2244-2258

Li J., Lu X., Jiang B., Du Y., Yang Y., Qian H., Liu B., Lin C., Jia L., Chen L., Wang Q. 2018. Adenovirus-associated acute conjunctivitis in Beijing, China, 2011-2013. *BMC Infect Dis.* 18:135-018-3014-z

Loftsson T., Jarvinen T. 1999. Cyclodextrins in ophthalmic drug delivery. *Adv Drug Deliv Rev.* 36:59-79

Ma J., Wang Y., Wei P., Jhanji V. 2018. Biomechanics and structure of the cornea: implications and association with corneal disorders. *Surv Ophthalmol.* 63:851-861

Malhotra A., Minja F.J., Crum A., Burrowes D. 2011. Ocular anatomy and cross-sectional imaging of the eye. *Semin Ultrasound CT MR*. 32:2-13

Mandal A., Bisht R., Rupenthal I.D., Mitra A.K. 2017. Polymeric micelles for ocular drug delivery: from structural frameworks to recent preclinical studies. *J Control Release*. 248:96-116

Martin L.M., Jeyabalan N., Tripathi R., Panigrahi T., Johnson P.J., Ghosh A., Mohan R.R. 2019. Autophagy in corneal health and disease: a concise review. *Ocul Surf*. 17:186-197

Masterton S., Ahearne M. 2018. Mechanobiology of the corneal epithelium. *Exp Eye Res*. 177:122-129

Mathews P.M., Lindsley K., Aldave A.J., Akpek E.K. 2018. Etiology of global corneal blindness and current practices of corneal transplantation: a focused review. *Cornea*. 37:1198-1203

Maulvi F.A., Soni T.G., Shah D.O. 2016. A review on therapeutic contact lenses for ocular drug delivery. *Drug Deliv*. 23:3017-3026

McClellan K.A. 1997. Mucosal defense of the outer eye. *Surv Ophthalmol*. 42:233-246

Messmer E.M. 2015. The pathophysiology, diagnosis, and treatment of dry eye disease. *Dtsch Arztebl Int*. 112:71-81

Moisseiev E., Loewenstein A. 2017. Drug delivery to the posterior segment of the eye. *Dev Ophthalmol*. 58:87-101

Monteiro J.P., Santos F.M., Rocha A.S., Castro-de-Sousa J.P., Queiroz J.A., Passarinha L.A., Tomaz C.T. 2015. Vitreous humor in the pathologic scope: insights from proteomic approaches. *Proteomics Clin Appl.* 9:187-202

Morrison P.W., Khutoryanskiy V.V. 2014. Advances in ophthalmic drug delivery. *Ther Deliv.* 5:1297-1315

Nagai N., Kotani S., Mano Y., Ueno A., Ito Y., Kitaba T., Takata T., Fujii N. 2017. Ferulic acid suppresses amyloid beta production in the human lens epithelial cell stimulated with hydrogen peroxide. *Biomed Res Int.* 5343010

Nayak K., Misra M. 2018. A review on recent drug delivery systems for posterior segment of eye. *Biomed Pharmacother.* 107:1564-1582

Nickla D.L., Wallman J. 2010. The multifunctional choroid. *Prog Retin Eye Res.* 29:144-168

Novack G.D., Robin A.L. 2016. Ocular pharmacology. *J Clin Pharmacol.* 56:517-527

Peng C.C., Burke M.T., Chauhan A. 2012. Transport of topical anesthetics in vitamin E loaded silicone hydrogel contact lenses. *Langmuir.* 28:1478-1487

Petrash J.M. 2013. Aging and age-related diseases of the ocular lens and vitreous body. *Invest Ophthalmol Vis Sci.* 54:ORSF54-9

Pradeep T., Waheed A. 2019. Histology, eye. In: *StatPearls Publishing LLC*. <https://www.ncbi.nlm.nih.gov/books/NBK544343/> (accessed June 2020)

Radomska-Lesniewska D.M., Osiecka-Iwan A., Hyc A., Gozdz A., Dabrowska A.M., Skopinski P. 2019. Therapeutic potential of curcumin in eye diseases. *Cent Eur J Immunol.* 44:181-189

Ribeiro A.M., Figueiras A., Veiga F. 2015. Improvements in topical ocular drug delivery systems: hydrogels and contact lenses. *J Pharm Pharm Sci.* 18:683-695

Romero-Jimenez M., Santodomingo-Rubido J., Wolffsohn J.S. 2010. Keratoconus: a review. *Cont Lens Anterior Eye.* 33:157-66

Rowe A.M., St Leger A.J., Jeon S., Dhaliwal D.K., Knickelbein J.E., Hendricks R.L. 2013. Herpes keratitis. *Prog Retin Eye Res.* 32:88-101

Sanchez-Lopez E., Espina M., Doktorovova S., Souto E.B., Garcia M.L. 2017. Lipid nanoparticles (SLN, NLC): overcoming the anatomical and physiological barriers of the eye - Part I - Barriers and determining factors in ocular delivery. *Eur J Pharm Biopharm.* 110:70-75

Soiberman U., Foster J.W., Jun A.S., Chakravarti S. 2017. Pathophysiology of keratoconus: what do we know today. *Open Ophthalmol J.* 11:252-261

Solano D., Czyz C.N. 2019. Viral conjunctivitis. In: *StatPearls Publishing LLC.* <https://www.ncbi.nlm.nih.gov/books/NBK470271/> (accessed June 2020)

Souto E.B., Dias-Ferreira J., Lopez-Machado A., Ettcheto M., Cano A., Camins Espuny A., Espina M., Garcia M.L., Sanchez-Lopez E. 2019. Advanced formulation approaches for ocular drug delivery: state-of-the-art and recent patents. *Pharmaceutics.* 11(9):460

Tan B.L., Norhaizan M.E. 2019. Carotenoids: how effective are they to prevent age-related diseases? *Molecules*. 24(9):1801

Teweldemedhin M., Gebreyesus H., Atsbaha A.H., Asgedom S.W., Saravanan M. 2017. Bacterial profile of ocular infections: a systematic review. *BMC Ophthalmol*. 17:212-017-0612-2

Tsai C.Y., Woung L.C., Yen J.C., Tseng P.C., Chiou S.H., Sung Y.J., Liu K.T., Cheng Y.H. 2016. Thermosensitive chitosan-based hydrogels for sustained release of ferulic acid on corneal wound healing. *Carbohydr Polym*. 135:308-315

Uchida R., Sato T., Tanigawa H., Uno K. 2003. Azulene incorporation and release by hydrogel containing methacrylamide propyltrimethylammonium chloride, and its application to soft contact lens. *J Control Release*. 92:259-264

Varela-Fernandez R., Diaz-Tome V., Luaces-Rodriguez A., Conde-Penedo A., Garcia-Otero X., Luzardo-Alvarez A., Fernandez-Ferreiro A., Otero-Espinar F.J. 2020. Drug delivery to the posterior segment of the eye: biopharmaceutic and pharmacokinetic considerations. *Pharmaceutics*. 12(3):269

Vora G.K., Haddadin R., Chodosh J. 2013. Management of corneal lacerations and perforations. *Int Ophthalmol Clin*. 53:1-10

Wang K., Pierscionek B.K. 2019. Biomechanics of the human lens and accommodative system: functional relevance to physiological states. *Prog Retin Eye Res*. 71:114-131

Whitcher J.P., Srinivasan M., Upadhyay M.P. 2001. Corneal blindness: a global perspective. *Bull World Health Organ*. 79:214-221

Willmann D., Melanson S.W. 2019. Corneal injury. In: *StatPearls Publishing LLC*. <https://www.ncbi.nlm.nih.gov/books/NBK459283/> (accessed June 2020)

Willoughby C. E., Ponzin D., Ferrari S., Lobo A., Landau K., Omid Y. 2010. Anatomy and physiology of the human eye: effects of mucopolysaccharidoses disease on structure and function – a review. *Clin Exp Ophthalmol*. 38: 2-11

Witt J., Mertsch S., Borrelli M., Dietrich J., Geerling G., Schrader S., Spaniol K. 2018. Decellularised conjunctiva for ocular surface reconstruction. *Acta Biomater*. 67:259-269

World Health Organization. Blindness and vision impairment. Available from: <https://www.who.int/en/news-room/fact-sheets/detail/blindness-and-visual-impairment> (accessed June 2020)

Xu J., Xue Y., Hu G., Lin T., Gou J., Yin T., He H., Zhang Y., Tang X. 2018. A comprehensive review on contact lens for ophthalmic drug delivery. *J Control Release*. 281:97-118

Yañez F., Martikainen L., Braga M.E., Alvarez-Lorenzo C., Concheiro A., Duarte C.M., Gil M.H., de Sousa H.C. 2011. Supercritical fluid-assisted preparation of imprinted contact lenses for drug delivery. *Acta Biomater*. 7:1019-1030

Yellepeddi V.K., Palakurthi S. 2016. Recent advances in topical ocular drug delivery. *J Ocul Pharmacol Ther*. 32:67-82

Zdunska K., Dana A., Kolodziejczak A., Rotsztejn H. 2018. Antioxidant properties of ferulic acid and its possible application. *Skin Pharmacol Physiol*. 31:332-336

Zernii E.Y., Gancharova O.S., Tiulina V.V., Zamyatnin Jr A.A., Philippov P.P., Baksheeva V.E., Senin I.I. 2018. Mitochondria-targeted antioxidant SKQ1 protects cornea from oxidative damage induced by ultraviolet irradiation and mechanical injury. *BMC Ophthalmol.* 18:336-018-0996-7

Zhu L., Zhu H. 2014. Ocular herpes: the pathophysiology, management and treatment of herpetic eye diseases. *Virol Sin.* 29:327-342

Zhu S., Gong L., Li Y., Xu H., Gu Z., Zhao Y. 2019. Safety assessment of nanomaterials to eyes: an important but neglected issue. *Adv Sci (Weinh).* 6:180228





Aims





2. Aims

The eye is a peculiar organ, protected by a combination of anatomical, mechanical and immunological barriers. Although it is easily accessible for topical drug administration, the combination of local and systemic barriers prevents a successful drug distribution. Formulations that can combine the patient acceptance of topical formulations and the effectiveness of intraocular injections have been largely prospected.

The aim of this PhD Thesis was to design polymeric micelles and CL with improved features for topical administration of ophthalmic drugs. Specifically, the research focused on the antiviral drugs acyclovir and valacyclovir and the antioxidant agent transferulic acid. These drugs are poorly soluble in water and their therapeutic outcomes could be notably improved if sustained levels on the eye structures are achieved.

According to this general aim, three specific aims were identified and developed as follows.

1) Design of polymeric micelles suitable for the administration of acyclovir. This antiviral agent is the first choice for the treatment of

ocular herpes caused by the herpes simplex virus. This virus can affect all layers of the cornea, producing blurred vision, redness, or tearing. Herpes simplex keratitis (infection and inflammation of the cornea) is the leading cause of infection blindness worldwide. Acyclovir penetrates infected cells and competes with natural nucleosides to incorporate DNA and act as a chain terminator. After anchoring, a suicidal inactivation mechanism occurs, since the terminated DNA binds to the viral DNA polymerase and irreversibly inhibits it, preventing viral replication. Classic topical treatment requires a long application period and results in serious side effects. Oral administration is characterized by having a bioavailability of less than 20%, which is the reason of prescribing high doses for long periods of time.

The hypothesis of this first stage of the Thesis was that the encapsulation of acyclovir in polymeric nanomicelles should increase drug solubility of the drug and promote the accumulation of the drug in cornea and sclera and its access to deeper structures. Soluplus and Solutol copolymers were chosen as amphiphilic copolymers. Soluplus is a biodegradable copolymer of polyvinyl caprolactam-polyvinyl acetate-polyethylene glycol (MW 90000-140000 g/mol, CMC 7.6 mg/L), which forms aqueous dispersions that may undergo in situ gelling at the ocular temperature. This additional feature may increase the residence time at the site of application and enhance the control of drug release. Solutol or macrogol 15-hydroxystearate (MW 963.24

g/mol, CMC 0.005-0.02%) is a non-ionic surfactant, which improves stability and solubility of insoluble drugs. It is stable, highly biocompatible and permeable to the mucosa. To carry out the work, dispersions of each copolymer will be prepared covering a wide range of concentrations and their size, Z potential, capability to host acyclovir and rheological behaviour will be evaluated. Those formulations combining adequate performances will be tested regarding cornea and sclera accumulation and permeability.

2) Design of imprinted hydrogels for antiviral drugs. Seeking for prolonging drug permanence on the ocular surface beyond that the formulations in nanomicelles may allow, the aim of the second step of the Thesis was to design hydrogels suitable for soft CL with affinity for acyclovir and valacyclovir. Among the proposed procedures to endow the hydrogel CLs with affinity for specific molecules, the creation of artificial receptors using the molecular imprinting technique stands out. This technique requires incorporating the substances of interest into the monomers mixture so that these can rearrange according to their affinity. This rearrangement becomes permanent during polymerization. The removal of the template molecules generates cavities with the most appropriate size and chemical groups to host the substance of interest again. Functional monomers suitable for interaction with the antiviral drugs will be first screened using computational modeling. Then hydrogels will be

prepared with various contents in the functional monomer in the presence (imprinted) and absence (non-imprinted) of the drug. The load and release capacities of antiviral drugs will be evaluated, as well as their biocompatibility in chorioallantoic membrane (HET-CAM test). The hydrogels will be characterized in terms of swelling, transmittance and mechanical properties. Finally, the permeability through bovine cornea and sclera of the aqueous solution of the drug and the drug released by the hydrogels will be compared.

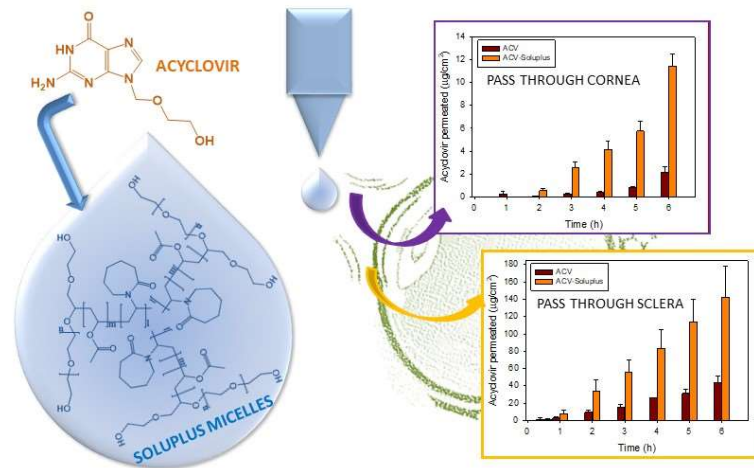
3) Design of cytosine-functionalized bioinspired hydrogels for ocular administration of transferulic acid. Transferulic acid is one of the most powerful natural antioxidants, it scavenges reactive oxygen and nitrogen species (ROS and RNS), and it regulates cytoprotective systems. At the ocular level, it is useful in the treatment of corneal lesions and can suppress the production of amyloid at the crystalline. However ocular formulations for sustained release of transferulic acid have not been developed yet. The creation of artificial receptors using the molecular imprinting technique is not applicable when the molecule of interest is an antioxidant since it would degrade during polymerization and would also interfere with the process. Therefore, the development of hydrogels with an affinity for antioxidants requires the identification of functional groups that can act as receptors without the need of carrying out the polymerization in the presence of the molecule of interest. The mechanism of action of

several drugs relies on their ability to interact with puric bases (adenine and guanine) or pyrimidine bases (thymine, cytosine and uracil) that build up DNA and RNA. The hypothesis of the last part of the Thesis was that the incorporation of a pyrimidine base, such as cytosine, into the structure of a hydrogel should endow it with an affinity for molecules with complementary structure in terms of ability to interact through hydrogen bonding and hydrophobic π - π stacking. The use of nitrogenous base as functional groups has not been previously tested, so a post-polymerization anchoring procedure was developed for their incorporation into the hydrogels. To carry out the study, the hydrogels will be prepared by mixing HEMA with different proportions of glycidylmethacrylate (GMA) and ethylene glycolphenyl methacrylate (EGPEM). GMA can serve as a bridge to immobilize cytosine in hydrogels, while EGPEM may reinforce the interaction between transferulic acid and cytosine forming Rebek molecular complexes. The hydrogels will be functionalized with cytosine and characterized regarding the amount grafted and in terms of degree of swelling, transmittance and mechanical properties. The capability of the hydrogels to load transferulic acid and to sustain its release while preserving the antioxidant activity will be evaluated in detail. HET-CAM test and viability of human corneal epithelial cells (HCEC) will be used for a first assessment of the ocular compatibility of the developed hydrogels. Finally, permeability of transferulic acid

through cornea and sclera when applied in solution and when delivered from the hydrogels will be compared.



*Polymeric micelles for acyclovir ocular delivery:
formulation and cornea and sclera permeability*





3. Polymeric micelles for acyclovir ocular delivery: formulation and cornea and sclera permeability

3.1.Introduction

The eye is considered a unique tissue from an immunological perspective. Several protective elements are present on the ocular surface; for example, mucins that form a dense glycocalyx on the cornea provide a physical barrier that prevents bacterial adhesion, and β -defensins, calprotectin, lysozyme, lipocalin and lactoferrin exhibit antimicrobial features. Eye surface infections appear when the homeostasis is disturbed by both unfavorable environmental conditions and infectious agents, which break down the eye surface and alter the innate immune system of this organ (Caspi, 2013; Pearlman et al., 2013; Lu et al., 2016). Ocular infections can be caused by bacteria and fungi pathogens (Caspi, 2013; Mangoni et al., 2016) or by viruses such as *Herpes simplex*, *Varicella Zoster* or *Cytomegalovirus* (Edwards et al., 2017).

The varicella zoster virus (VZV) causes chickenpox and herpes zoster. The first is a benign disease and the second appears after a

reactivation of the virus and is more dangerous. At the ocular level, it is the second most common complication in the form of keratitis (76.2%), uveitis (46.6%) and conjunctivitis (35.4%) (*Yawn et al., 2013; Zhu et al., 2014*). Cytomegalovirus can cause retinitis, which leads to progressive vision loss and blindness in immunocompromised people (*Scholz et al., 2003*). Herpes simplex virus (HSV) is the most common agent responsible for herpes eye disease (*Rechenchoski et al., 2017*). It is a double-chain DNA virus and there are two types, HSV-1 and HSV-2. Diseases caused by HSV-1 are mostly associated with the eye and orofacial area, while those caused by HSV-2 are related to the genital area. However, both types of viruses can cause pathologies in the same areas of the body. Globally, it is estimated that out of 10 million people affected by HSV, 20% will suffer from vision problems (*Zhu et al., 2014*). Currently, about 67% of the world's population of less than 50 years old suffers from HSV-1, and 11% of people between 15 and 49 years old have HSV-2 infection (*Rechenchoski et al., 2017; World Health Organization, 2017*).

HSV is acquired by direct contact and enters through the mucous membranes or damaged skin. The infection is initiated by adsorption of the viral envelope onto the plasma membrane of the target cell. Once inside, the virus is transported to a pore of the nuclear membrane and the viral DNA is released into the nucleus for transcription and replication processes. The virus then travels by axonal transport to the sensory nerve nodes, where it establishes

latency in neuronal cells. The virus retains its potential to reactivate, resume replication and cause recurrent disease (Zhu *et al.*, 2014; Rechenchoski *et al.*, 2017). Reactivation can be triggered by different reasons, such as fever, exposure to ultraviolet light, stress or menstruation (Roizman *et al.*, 2013). The virus returns to the surface, replicates and causes disease, typically appearing in dense areas with sensory receptors, such as the cornea, oral mucosa, lips or fingertips (Toma *et al.*, 2008). The virus can infect all three layers of the cornea, causing tearing, redness, and blurred vision. The primary infection is asymptomatic and will depend on the patient's immune status (Zhu *et al.*, 2014). HSV-1 is more likely to cause infection and inflammation of the cornea, known as herpes simplex keratitis. This infection is the leading cause of blindness in the world (Karsten *et al.*, 2012). Four distinct categories of this disease can be defined. First, infectious epithelial keratitis, which consists of corneal vesicles, dendritic ulcers, geographic ulcers and marginal ulcers. Secondly, neurotrophic keratopathy, which includes point epithelial erosions and neurotrophic ulcers. In the third category, stromal keratitis occurs. Finally, the fourth category corresponds to endothelitis (Al-Dujaili *et al.*, 2011; Tsatsos *et al.*, 2016). Primary HSV infection does not need to be treated, although an appropriate treatment may shorten the disease, reduce severity, and minimize damage.

Antiviral agents are the cornerstone of anti-HSV treatment (Zhu *et al.*, 2014). Acyclovir (ACV) (**Figure 3.1**) was the first antiviral

developed and is still the first choice. It is a guanine analogue that penetrates into the infected cells and is phosphorylated by a thymidine kinase of the own virus, and then undergoes two more stages of phosphorylation by cell kinases. Acyclovir triphosphate competes with natural triphosphate nucleosides and is incorporated into the DNA chain that is replicating and acts as a chain terminator. This is a suicidal inactivation mechanism, since this terminated DNA binds to viral polymerase DNA and inhibits it irreversibly (*Hung et al., 1984; James et al., 2014*). Thus, the drug prevents viral replication and reduces the severity of symptoms, the frequency of spread and the propagation of disease (*Zhu et al., 2014*).

Treatment for herpetic keratitis combines topical or oral antiviral agents (acyclovir, trifluridine, idoxuridine, vidarabine, brivudine, foscarnet, or ganciclovir) with topical corticosteroids (prednisolone). Corticosteroids have significant secondary effects, such as glaucoma or cataracts, and antivirals are only beneficial if the virus is present. In addition, the treatment periods are very long (10 weeks) (*Knickerbein et al., 2009; Hill et al., 2014; Wilhelmus, 2015; Azher et al., 2017*). Oral bioavailability of acyclovir is limited to 20%, requiring high doses and high frequency of administration (*Tsatsos et al., 2016*). Besides, the physiological and anatomical barriers present in the eye and their protective mechanisms (tearing, blinking or nasolacrimal drainage) are responsible of the low ocular bioavailability (<5%) shown by ophthalmic solutions.

3. Polymeric micelles for acyclovir ocular delivery: formulations and cornea and sclera permeability

Encapsulation of drugs into nanocarriers may enhance ocular bioavailability through a variety of mechanisms, mainly involving improved solubilization, bioadhesion and penetration (*Bachu et al., 2018; Bisht et al., 2018*). In this regard, polymeric nanomicelles may be advantageous because of their spontaneous formation, kinetic and thermodynamic stability, capability to encapsulate a variety of drugs, enhanced permeability through the ocular epithelium, and sustained release. Moreover, some nanomicelles can pass through the sclera and provide therapy to the posterior segment of the eye (*Li et al., 2015; Alvarez-Rivera et al., 2016; Mandal et al., 2017*).

The aim of this work was to test whether encapsulation of acyclovir in Soluplus or Solutol (**Figure 3.1**) polymeric micelles increases its solubility, corneal permeability and sclera penetration. The aqueous solubility of acyclovir is known to be low, and therefore approaches that increase both its solubility and its ability to penetrate through the eye may favor the efficacy of the treatments. Previous studies have focused on the use of acyclovir prodrugs formulated as micelles (*Vadlapudi et al., 2014*), but the interest of direct encapsulation of acyclovir in polymeric micelles for ocular delivery has not been tested in spite of that micelles can increase its solubility (*Tan, 2016*). Soluplus and Solutol are amphiphilic copolymers used to deal with the oral and parenteral formulation of hydrophobic drugs. Soluplus is a biodegradable block copolymer that may act as a matrix in solid solutions and may endow aqueous dispersions with in situ gelling

ability, which may be exploited for both increasing time of permanence on the ocular surface and controlling drug release, as demonstrated for lipoic acid (BASF, 2010; Alvarez-Rivera *et al.*, 2016). Solutol is formed by a mixture of poly(ethylene oxide) esters of 12-hydroxystearic acid and free (30%) polyethylene glycol, serves as non-ionic solubilizer and emulsifier, and also exhibits capability to reverse multidrug resistance (BASF, 2012; Hou *et al.*, 2016).

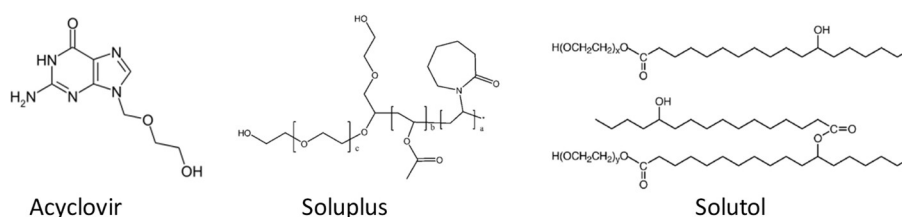


Figure 3.1. Structure of acyclovir and the two copolymers investigated, Soluplus® and Solutol (Kolliphor® HS 15).

3.2. Materials and methods

3.2.1. Materials

Acyclovir was from Farmalabor (Italy); Soluplus® (polyvinyl coprolactam-polyvinyl acetate-polyethylene glycol copolymer, 115000 g/mol, HLB 16) and Solutol (Kolliphor® HS 15, macrogol 15 hydroxystearate, 963.24 g/mol, HLB 16-18) were from BASF (Germany); $\text{CaCl}_2 \cdot 2\text{H}_2\text{O}$ and $\text{NaH}_2\text{PO}_4 \cdot \text{H}_2\text{O}$ from Merck (Germany); NaOH and ethanol absolute from VWR (France); KH_2PO_4 and NaHCO_3 from Panreac (Spain); NaCl, $\text{MgCl}_2 \cdot 6\text{H}_2\text{O}$ and acetonitrile from Scharlau (Spain); KCl from Prolabo (France); phosphate

buffered saline (PBS) from Sigma (Germany); penicillin and streptomycin from Gibco (USA). Water was purified using reverse osmosis (resistivity $>18 \text{ M}\Omega\cdot\text{cm}$, MilliQ, Millipore® Spain). Simulated lacrimal fluid (SLF) was prepared with the following composition: 6.78 g/L NaCl, 2.18 g/L NaHCO_3 , 1.38 g/L KCl, and 0.084 g/L $\text{CaCl}_2\cdot\text{H}_2\text{O}$ with pH 7.5 (*dos Santos et al.*, 2009).

Phosphate buffer pH 7.4 was obtained mixing solution A (50 mL KH_2PO_4 0.2 M) and solution B (39.1 mL NaOH 0.2 M), to 200 mL with H_2O . Carbonate buffer pH 7.2 was prepared by mixing 100 mL of solution A (1.24 g NaCl, 0.071 g KCl, 0.02 g $\text{NaHCO}_4\cdot\text{H}_2\text{O}$ and 0.49 g NaHCO_3) and 100 mL of solution B (0.023 g CaCl_2 and 0.031 g $\text{MgCl}_2\cdot 6\text{H}_2\text{O}$).

3.2.2. Micelles preparation and characterization

Soluplus and Solutol dispersions (1, 4, 8, 12, 16 and 20% w/w) were prepared in triplicate either in water or PBS pH 7.4. The systems were maintained under magnetic stirring for 72 h at room temperature to ensure complete dispersion of the copolymers. Size and Z-potential were measured in triplicate in a Zetasizer® 3000HS (Malvern Instruments, UK), previous filtration of each sample through 0.22 μm membranes (Acrodisc® Syringe Filter, GHP Minispikes, Waters).

3.2.3. Rheological behavior

Evolution of storage (G') and loss (G'') moduli of Soluplus and Solutol (12 and 20% w/w) dispersions in water and in PBS pH 7.4 as a function of temperature (15 to 40 $^{\circ}\text{C}$) was recorded in a Rheolyst AR-

1000N (TA Instruments, UK) rheometer fitted with a Peltier plate and a 6-cm in diameter cone (2 °). The angular frequency was fixed at 5 rad/s and the oscillation stress at 0.1 Pa.

3.2.4. Acyclovir solubilization

Soluplus and Solutol solutions (3 mL) were poured in 5 mL Eppendorf tubes containing acyclovir in excess (50 mg). Solubility of acyclovir in water and PBS pH 7.4 was also recorded. The systems were maintained under magnetic stirring for 72 h, at 300 rpm and room temperature. Then, they were centrifuged at 5000 rpm for 30 min to separate non-solubilized acyclovir. Absorbance of the supernatants was measured at 252 nm (UV/Vis spectrophotometer Agilent 8453, Germany) previous dilution with water:ethanol 50:50 v/v mixtures. Acyclovir concentration was calculated using a calibration curve previously prepared.

The solubility data was used to calculate the following parameters (*Alvarez-Rivera et al., 2016*).

Molar solubilization capacity (moles of drug that can be solubilized per mol of copolymer forming micelles):

$$\chi = \frac{S_{tot} - S_w}{C_{copol} - CM} \quad [\text{Eq. 3.1}]$$

Micelle-water partition coefficient (ratio between the drug concentration in the micelle and the aqueous phase):

$$P = \frac{S_{tot} - S_w}{S_w} \quad [\text{Eq. 3.2}]$$

Molar micelle-water partition coefficient (which eliminates the P dependence on the copolymer concentration, assigning a default concentration of 1M):

$$PM = \frac{\chi^*(1-CM)}{S_w} \quad [\text{Eq. 3.3}]$$

Gibbs standard-free energy of solubilization was estimated from the molar micelle/water partition coefficient (PM) and the micelle-water partition coefficient (P), as follows

$$\Delta G_s = -RT * \ln(PM) \quad [\text{Eq. 3.4}]$$

$$\Delta G_s = -RT * \ln(P) \quad [\text{Eq. 3.5}]$$

In these equations, S_{tot} represents the total solubility of acyclovir in the micellar solution, S_w is the acyclovir solubility in water, CMC is the critical micelle concentration, C_{copol} is the copolymer concentration in each micelle solution, and R is the universal constant of gases.

3.2.5. Micelle stability against dilution

Aliquots of acyclovir-loaded Soluplus (12 %w/w) micelle dispersions prepared in PBS pH 7.4 were poured onto temperature-controlled (35 °C) quartz cells already containing PBS, so the dispersions were diluted 30- or 60-fold. The absorbance of the samples was immediately measured at 252 nm and each 30 seconds during 30 min (UV/Vis spectrophotometer Agilent 8453, Germany). Similar experiments were also carried out in triplicate using water and SLF as dilution medium.

3.2.6. Corneal and sclera permeability assay

Acyclovir permeability assays through cornea and sclera were carried out following the BCOP test protocol (*Alvarez-Rivera et al., 2016; OECD, 2017; Alvarez-Rivera et al., 2018*). Bovine eyes were collected in the first hour after dead, from a local slaughterhouse. They were transported completely immersed in PBS solution with antibiotics added (penicillin 100 IU/mL and streptomycin 100 µg/mL) and maintained in an ice bath. Next, corneas were isolated with 2-3 mm of surrounding sclera, or scleras were isolated. In both cases, tissues were washed with PBS, before mounted on vertical diffusion Franz cells. Donor and receptor chambers were filled with carbonate buffer pH 7.2. The receptor chambers were placed inside a bath at 37 °C and kept under magnetic stirring during 1 h in order to balance ocular tissues. Then, the volume of the donor chamber was completely removed and replaced by drug solutions (2 mL). Acyclovir aqueous solution (0.3 mg/mL) was prepared dissolving the required amount in water. Saturated acyclovir solution in Soluplus micelles (20% w/w) was prepared as reported above; the final drug concentration was 1.34 mg/mL. The chambers were covered with parafilm to prevent evaporation (0.785 cm² area available for permeation). Samples (1 mL) were removed from the receptor chamber at 0.5, 1, 2, 3, 4, 5 and 6 h, replacing the same volume with carbonate buffer each time, and taking care of removing bubbles from the diffusion cells. All experiments were carried out in triplicate.

Acyclovir permeated was quantified by HPLC (Waters 717 Autosampler, Waters 600 Controller, 996 Photodiode Array Detector), fitted with a C18 column (Waters Symmetry C18, 5 μ m, 4.6 \times 250 mm) and operated using Empower2 software. Mobile phase was water:acetonitrile (95:5) at 1 mL/min and 35 °C. The injection volume was 50 μ L and acyclovir was quantified at 251 nm (retention time 4.5 min). Standard solutions were 0.075-15 μ g/mL of acyclovir in water (Volpato *et al.*, 1997). The cumulative amounts of acyclovir permeated per area versus time were fitted to a linear regression, and the steady state flux (J) and the lag time (t_{lag}) were obtained from the slope and the x-intercept of the linear regression, respectively (Al-Ghabeish *et al.*, 2015).

After 6 h permeation test, aliquots of the donor chambers were taken for subsequent analysis. Corneas/scleras were immersed during 24 h in 3 mL of ethanol:water (50:50 v/v) medium, sonicated during 99 min at 37 °C, and centrifuged (1000 rpm, 5 min, 25 °C), and the supernatant filtered (Acrodisc[®] Syringe Filter, 0.22 μ m GHP Minispike, Waters), centrifuged again (14000 rpm, 20 min, 25 °C) and filtered to be measured in HPLC (Volpato *et al.*, 1997).

3.3. Results and Discussion

3.3.1. Micelles preparation and characterization

Soluplus and Solutol micelles were prepared in water and PBS pH 7.4 using copolymer concentrations up to 20% w/w. The pH of the Soluplus solutions in water was acid (pH 3.2) while Solutol solutions

were nearly neutral (pH 6.5). The different pH between copolymer solutions could affect to the acyclovir solubility (pKa 2.27 and 9.25). CMCs of Soluplus and Solutol were reported to be 6.6×10^{-5} mM and 5.19×10^{-2} mM, respectively (*BASF, 2010; BASF, 2012*). The concentrations of each copolymer chosen for the study were well above the CMC values, and ranged between 0.09-1.74 mM for Soluplus, and 10.38-207.63 mM for Solutol (corresponding to 1-20% copolymer concentration).

Size and Z-potential of micelles prepared with 12% copolymer are shown in **Table 3.1**. Soluplus micelles had an average size of 117.4 nm and a polydispersity index of 0.23, while Solutol micelles were much smaller showing an average size of 18.7 nm and a polydispersity index of 0.18. These values are in good agreement with literature (*Hou et al., 2016*). Loading of acyclovir caused a minor increase in the size of Soluplus micelles (137.0 nm), but remarkably increased the size of Solutol ones (134.9 nm). The surface charge of both types of copolymer was similar, being slightly negative or close to zero.

3. Polymeric micelles for acyclovir ocular delivery: formulations and cornea and sclera permeability

Table 3.1. Size, polydispersion index (PDI) and Z-potential of Soluplus and Solutol (12%) micelles in PBS pH 7.4 before and after being loaded with acyclovir (ACV). Mean values and standard deviations in parenthesis; n=3.

Formulations	Particle size (nm)	PDI	Z-potential (mV)
Soluplus	117.4 (1.4)	0.23 (0.01)	-1.73 (0.94)
Solutol	18.7 (4.0)	0.18 (0.02)	-0.57 (0.38)
Soluplus + ACV	137.0 (4.0)	0.30 (0.02)	0.21 (0.85)
Solutol + ACV	134.9 (1.4)	0.26 (0.02)	-1.93 (0.54)

3.3.2. Rheological behavior

Solutol (12 and 20%) dispersions showed viscous-like behavior with negligible G' values in the 15 to 40 °C interval (**Figure 3.2**). The viscosity slightly decreased with the increase in temperature. The complex viscosity values recorded were in the range 0.004 to 0.007 Pa.s, which is slightly higher than pure water.

Differently, Soluplus dispersions showed a remarkable increase in the values of both G' and G'' when temperature surpasses 30 °C or 27 °C in the case of 12 and 20% dispersions, respectively (**Figure 3.2**). The increase was almost linear in the 30 to 37 °C range, and the G'' values at 37 °C were close to 7-40 Pa (the highest values were recorded in PBS) and 1500 Pa for 12 and 20% dispersions, respectively. This behavior agrees well with previous reports on Soluplus dispersions (*Alvarez-Rivera et al., 2016*) and it is quite different from that showed by common in situ gelling copolymer

dispersions that exhibit a sharp increase in G' and G'' at the gelling temperature. The complex viscosity values recorded at 35 °C for Soluplus 12% in water and in PBS were 0.50 and 3.12 Pa.s, respectively, and for Soluplus 20% in water and in PBS were 103.4, and 79.7 Pa.s. These values suggest that the micelle formulations could remain for prolonged time on the ocular surface.

3.3.3. Acyclovir solubilization

Solubility of acyclovir in water was 1.02 mg/mL, a value slightly lower than the values previously reported in literature (*Majumdar et al.*, 2009). Using slightly alkaline medium, such as PBS pH 7.4 or SLF pH 7.5, the solubility increased to 1.44 and 1.56 mg/mL, respectively. This part of the study was aimed to elucidate whether Soluplus and Solutol micelles could encapsulate acyclovir, increasing its apparent solubility. In the range of copolymer concentrations tested, acyclovir solubility positively correlated with Soluplus concentration. The enhancement in solubility was slightly higher in PBS than in water, with apparent solubility values of 2.10 (s.d. 0.07) and 2.05 (s.d. 0.04) mg/mL, respectively, in 20% w/w Soluplus micelle medium.

3. Polymeric micelles for acyclovir ocular delivery: formulations and cornea and sclera permeability

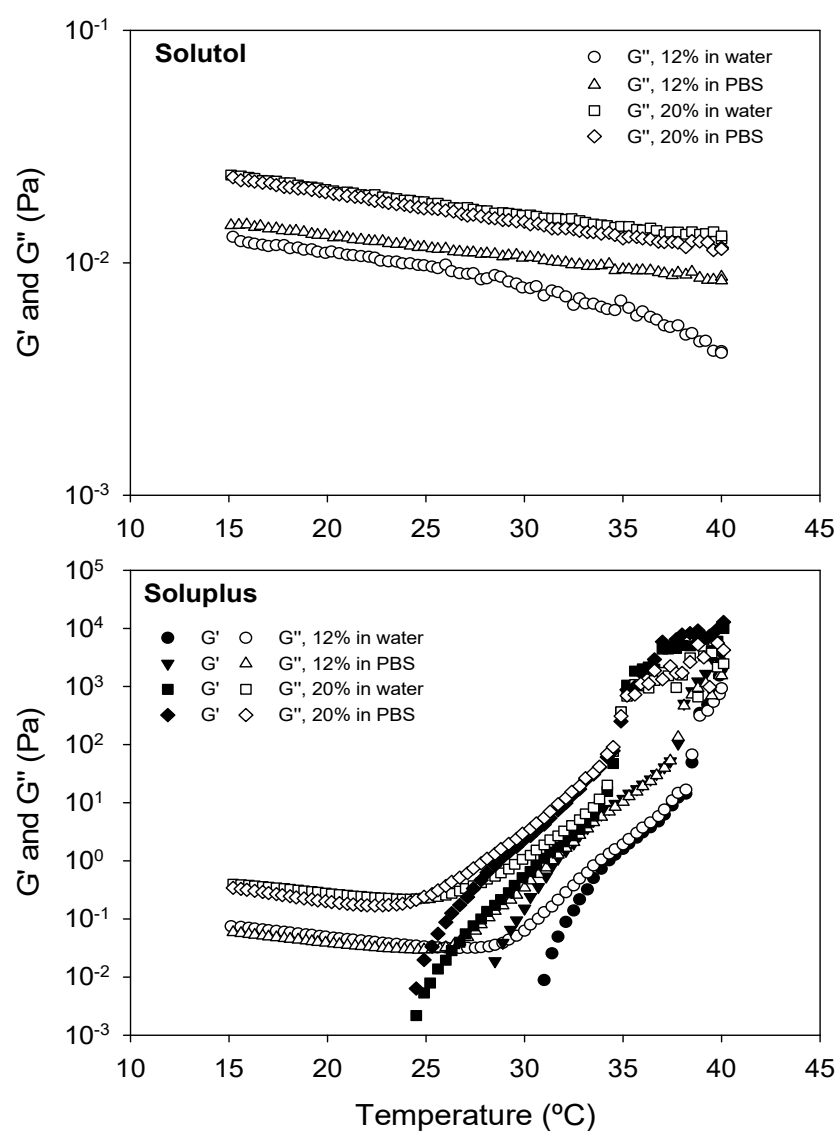


Figure 3.2. Effect of temperature on G' and G'' values of Solutol and Soluplus dispersions.

Differently, acyclovir solubility in 20% w/w Solutol micelles showed a minor increase, being 1.54 (s.d. 0.03) and 1.39 (s.d. 0.06) mg/mL in PBS and water, respectively (**Figure 3.3**).

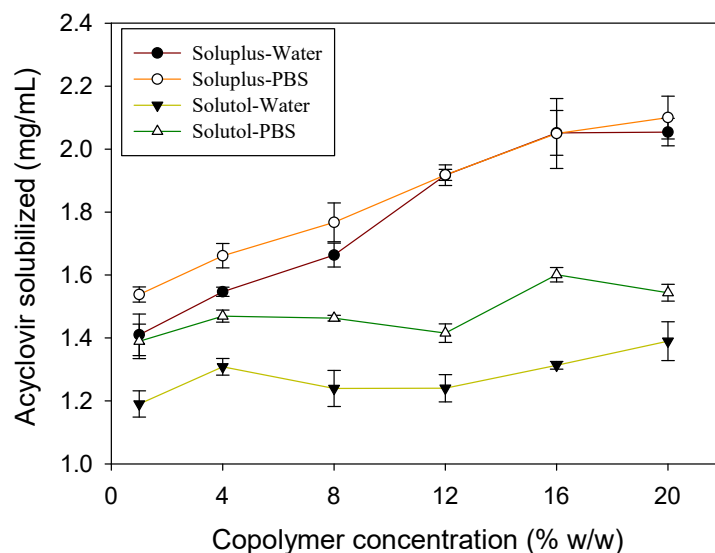


Figure 3.3. Apparent solubility of acyclovir in micelle dispersions of Soluplus and Solutol HS 15, prepared in water and PBS pH 7.4. Error bars represents standard deviation (n=3).

Nevertheless, compared to other drugs formulated in these polymeric micelles, the total increase in solubility was relatively low, with may be related to the polarity of acyclovir (LogP= -1.56) (*Al-Ghabeish et al., 2015; Hou et al., 2016*).

Free energy of solubilization was negative in all cases, which means that the solubilization occurred spontaneously and was thermodynamically favored by the hydrophobicity of micelle core. Previous works have reported on solubilization values of up to 15

mg/ml using O'-O-lauroyl chitosan (*Tan, 2016*). Despite of having similar HLB values, Soluplus composition and architecture as a self-assembled copolymer seem to be more suitable to host acyclovir than the Solutol mixture of poly (ethylene oxide) esters of 12-hydroxystearic acid and free polyethylene glycol. Therefore, Solutol was discarded for subsequent studies.

Parameters used to quantify the efficiency of solubilization are summarized in **Table 3.2**. The micelle-water partition coefficient (P) for Solutol dispersions was below 1, which means that there are more acyclovir molecules solubilized in the aqueous medium than inside the micelles. Differently, an increase in the partition coefficient values was observed for Soluplus as the copolymer concentration increased, indicating that for micelle systems prepared with Soluplus at 16% or higher the amount of acyclovir into the micelles surpasses the amount solubilized in the outer aqueous medium.



Table 3.2. Parameters that characterize the ability of Soluplus (water (A) or PBS (B)), and Solutol (water (C) or PBS (D)) micelles to solubilize acyclovir, estimated using equations (3.1), (3.2), (3.3), (3.4) and (3.5). (ACV: acyclovir; χ : molar solubilization capacity; P : partition coefficient; PM : molar partition coefficient; ΔG : standard-free Gibbs energy of solubilization; mf : molar fraction of drug encapsulated inside the micelle).

(A) WATER							
Soluplus (% w/w)	Soluplus (M)	ACV (M)	χ	P	PM	ΔG (KJ/mol)	mf
1	$8.7 \cdot 10^{-5}$	$6.3 \cdot 10^{-3}$	20.04	0.39	4435.1	-20806.1	0.28
4	$3.5 \cdot 10^{-4}$	$6.9 \cdot 10^{-3}$	6.75	0.52	1494.4	-18110.8	0.34
8	$6.9 \cdot 10^{-4}$	$7.4 \cdot 10^{-3}$	4.12	0.63	911.9	-16887	0.39
12	$1.1 \cdot 10^{-3}$	$8.5 \cdot 10^{-3}$	3.83	0.88	847.1	-16704.1	0.47
16	$1.4 \cdot 10^{-3}$	$9.1 \cdot 10^{-3}$	3.30	1.02	730.1	-16335.8	0.50
20	$1.7 \cdot 10^{-3}$	$9.1 \cdot 10^{-3}$	2.65	1.02	585.5	-15788.9	0.50

(B) PBS pH 7.4							
Soluplus (% w/w)	Soluplus (M)	ACV (M)	χ	P	PM	ΔG (KJ/mol)	mf
1	$8.7 \cdot 10^{-5}$	$6.8 \cdot 10^{-3}$	26.58	0.51	5881.3	-21505.4	0.34
4	$3.5 \cdot 10^{-4}$	$7.4 \cdot 10^{-3}$	8.22	0.63	1817.9	-18596.4	0.39
8	$6.9 \cdot 10^{-4}$	$7.8 \cdot 10^{-3}$	4.79	0.74	1058.9	-17257.4	0.42
12	$1.1 \cdot 10^{-3}$	$8.5 \cdot 10^{-3}$	3.83	0.88	847.9	-16706.5	0.47
16	$1.4 \cdot 10^{-3}$	$9.1 \cdot 10^{-3}$	3.29	1.01	728.7	-16331.4	0.50
20	$1.7 \cdot 10^{-3}$	$9.3 \cdot 10^{-3}$	2.76	1.06	611.5	-15897	0.52

3. Polymeric micelles for acyclovir ocular delivery: formulations and cornea and sclera permeability

(C) WATER

Solutol (% w/w)	Solutol (M)	ACV (M)	χ	P	PM	ΔG (KJ/mol)	mf
1	0.01	$5.3 \cdot 10^{-3}$	$7.4 \cdot 10^{-2}$	0.17	16.4	-6932.8	0.14
4	0.04	$5.8 \cdot 10^{-3}$	$3.1 \cdot 10^{-2}$	0.29	6.9	-4779.3	0.22
8	0.08	$5.5 \cdot 10^{-3}$	$1.2 \cdot 10^{-2}$	0.22	2.6	-2391.1	0.18
12	0.12	$5.5 \cdot 10^{-3}$	$7.9 \cdot 10^{-3}$	0.22	1.8	-1395.3	0.18
16	0.17	$5.8 \cdot 10^{-3}$	$7.9 \cdot 10^{-3}$	0.29	1.7	-1382.7	0.22
20	0.21	$6.2 \cdot 10^{-3}$	$7.9 \cdot 10^{-3}$	0.37	1.8	-1400.8	0.27

(B) PBS pH 7.4

Soluplus (% w/w)	Solutol (M)	ACV (M)	χ	P	PM	ΔG (KJ/mol)	mf
1	0.01	$6.2 \cdot 10^{-3}$	$1.6 \cdot 10^{-1}$	0.36	35.3	-8831.9	0.27
4	0.01	$6.5 \cdot 10^{-3}$	$4.8 \cdot 10^{-2}$	0.44	10.7	-5871.8	0.31
8	0.08	$6.5 \cdot 10^{-3}$	$2.4 \cdot 10^{-2}$	0.44	5.3	-4116.8	0.30
12	0.12	$6.3 \cdot 10^{-3}$	$1.4 \cdot 10^{-2}$	0.39	3.1	-2831.8	0.28
16	0.17	$7.1 \cdot 10^{-3}$	$1.6 \cdot 10^{-2}$	0.57	3.5	-3067.3	0.36
20	0.21	$6.8 \cdot 10^{-3}$	$1.1 \cdot 10^{-2}$	0.52	2.5	-2259.0	0.34

3.3.4. Micelle stability against dilution

Capability of Soluplus (12% copolymer) dispersions to retain acyclovir in the micelles once diluted in water or SLF is depicted in **Figure 3.4**. To carry out this study, the micelle systems were diluted 30- and 60-fold. The absorbance was recorded and monitored for 30 min at constant temperature (35 °C). After dilution, absorbance of Soluplus showed a slight initial decrease followed by a complete and

stable recovery in few minutes. These results mean a rapid rebalancing of micelle-medium partition equilibrium.

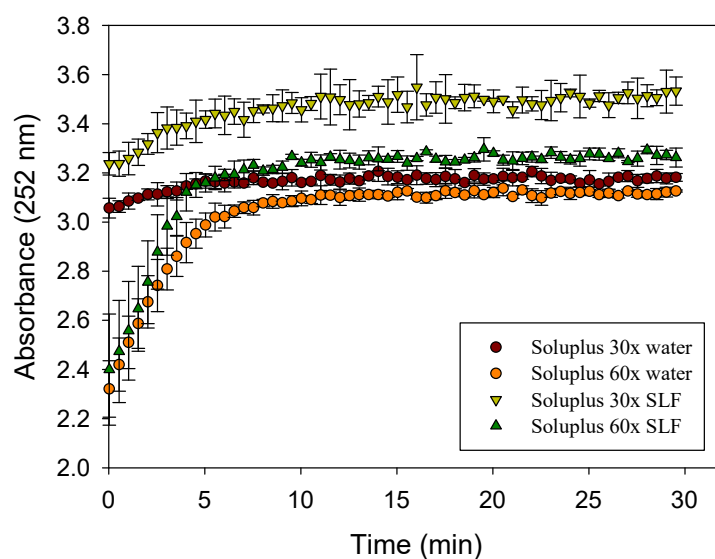


Figure 3.4. Evolution of the absorbance of acyclovir in Soluplus (12 %) dispersions after 30 and 60-fold dilution in water and SLF.

3.3.5. Cornea and sclera permeability assay

Bovine cornea and sclera permeability assays were carried out in vertical (Franz) diffusion cells. The amounts of acyclovir permeated through the tissues to the receptor chamber along 6 hours and those remnants in the receptor chamber at the end of the assay were monitored. After 6h-test, the amounts accumulated in the cornea and the sclera were also quantified. Each experiment was carried out in triplicate using a carbonate buffer pH 7.2 as the receptor medium (37 °C).

In the cornea assay, after 6 h the amounts of acyclovir that crossed the cornea and accumulated in the receptor chamber were $2.16 \mu\text{g}/\text{cm}^2$ (s.d. 0.45) when applied as aqueous solution, and $11.43 \mu\text{g}/\text{cm}^2$ (s.d. 1.04) when formulated in Soluplus micelles (**Figure 3.5**). Therefore, the amount of acyclovir that passed through the cornea in 6 hours was nearly one order of magnitude larger when the drug was formulated in the polymeric micelles.

Acyclovir permeability through the bovine cornea showed a lag time of nearly 4 h when applied as aqueous solution, which decreased to less than 2 h when formulated in Soluplus micelles. After the lag time, an almost linear dependence on time of the cumulative amounts of acyclovir permeated per area unit was recorded ($R^2 > 0.89$); the steady state flux (J) was estimated from the slope to be 0.883 and $2.497 \mu\text{g}/\text{cm}^2 \cdot \text{h}^{-1}$ for acyclovir aqueous solution and micellar formulation, respectively.

This permeability values are lower than those reported for other active substances, e.g. lipoic acid, loaded in Soluplus micelles (*Alvarez-Rivera et al., 2016*), which may be related to the higher polarity of acyclovir. Indeed, acyclovir transport through the cornea has been reported to be limited to passive diffusion. In a study carried out with acyclovir formulated in oily ointments applied onto rabbit cornea, the steady state flux (J) values ranged between 5 and $30 \mu\text{g}/\text{cm}^2 \cdot \text{h}^{-1}$ and the permeability coefficient was $7.29 (\pm 1.31) \cdot 10^{-6} \text{ cm/s}$ (*Al-Ghabeish et al., 2015*).

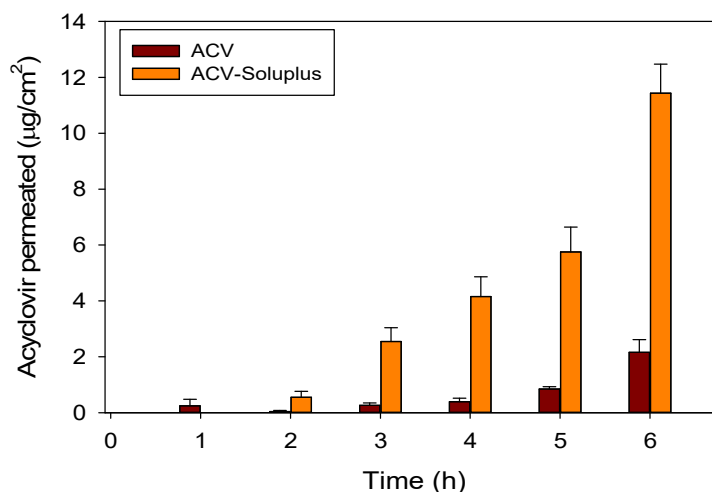


Figure 3.5. Accumulated amounts of acyclovir permeated through bovine cornea during 6 h, for aqueous solution of ACV (0.3 mg/mL) and formulation of ACV in Soluplus 20% micelles (1.34 mg/mL), at 37 °C.

In our case, after 6 h-test the acyclovir concentration in the donor chambers filled with the acyclovir solution (300 µg/mL) decreased to 38.92 µg/mL, while in the donors where the Soluplus formulation was applied (initial concentration 1340 µg/mL) the acyclovir concentration diminished to 156.91 µg/mL. Thus, permeability coefficients were estimated to be in the $4.4 \cdot 10^{-6}$ to $6.3 \cdot 10^{-6}$ cm/s, in good agreement with literature (Majumdar et al., 2009; Hou et al., 2016).

The amounts of acyclovir accumulated in the cornea after 6 h exposition were 2.45 µg/cm² (s.d. 0.68) for acyclovir solution, and 13.97 µg/cm² (s.d. 2.88) for acyclovir-Soluplus formulation.

Permeability through the sclera was also investigated to elucidate whether the drug could be delivered also to the posterior segment.

Although corneal keratopathies are the most common diseases caused by HSV in the eye, these virus can also cause scleritis and episcleritis, two inflammatory diseases of the eyeball (*Heron et al., 2014*). The surface area of absorption in the sclera is larger than in cornea, and for several compounds larger permeability has been recorded for sclera (*Geroski et al., 2000; Loch et al., 2012*). In our case, total acyclovir permeated amounts through sclera after 6 h in contact with the aqueous solution or the micelle formulation were $43.60 \mu\text{g}/\text{cm}^2$ (s.d. 7.69) and $142.62 \mu\text{g}/\text{cm}^2$ (s.d. 35.39), respectively (**Figure 3.6**).

Compared to cornea, the lag time for sclera permeation was considerably shorter and similar for both acyclovir aqueous solution and micellar formulation. The cumulative amounts of acyclovir permeated per area unit showed an almost linear dependence on time too. After 6 h-test the acyclovir concentration in the donor chambers filled with the acyclovir solution ($300 \mu\text{g}/\text{mL}$) decreased to $21.23 \mu\text{g}/\text{mL}$, while in the donors where the Soluplus formulation was applied (initial concentration $1340 \mu\text{g}/\text{mL}$) the concentration diminished to $186.65 \mu\text{g}/\text{mL}$. The permeability coefficients were estimated to be in the $10.5 \cdot 10^{-5}$ to $4.01 \cdot 10^{-5}$ cm/s range.

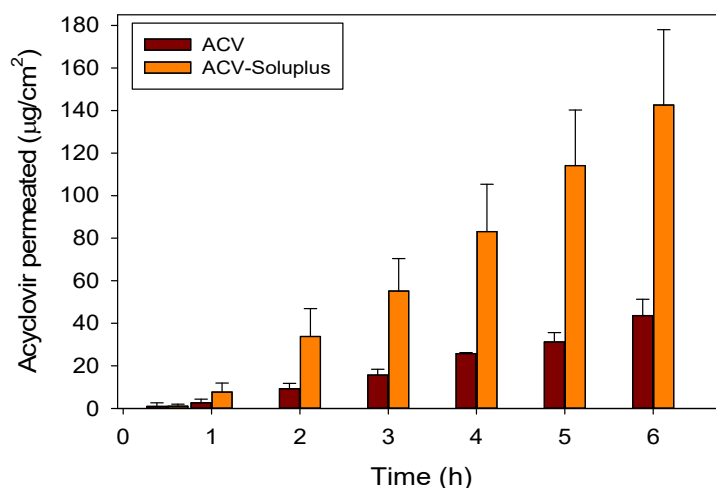


Figure 3.6. Accumulated amounts of acyclovir permeated through bovine sclera during 6 h, for aqueous solution of ACV (0.3 mg/mL) and formulation of ACV in Soluplus 20% micelles (1.34 mg/mL), at 37 °C.

The results showed 10 times greater amounts of drug permeated through the sclera than through the cornea. Since the experiments were carried using similar surface area for both tissues, the differences are clearly related to the greater permeability of sclera, which has a relatively porous structure that allows drug diffusion either as free molecules or after being encapsulated in micelles (*Ahmed et al., 1987; Hamalainen et al., 1997; Tai et al., 2003; Wen et al., 2010; Wen et al., 2013*). Previous studies with cyclosporine encapsulated in Pluronic/TPGS mixed micelles showed that the drug accumulated in the sclera (probably because hydrophobic interactions) and only a small fraction permeated through the receptor (*Grimaudo et al., 2018*). Differently, in the case of acyclovir-Soluplus micelles, there was also

sclera accumulation but most drug could readily diffuse through it, which may favor the access to the posterior eye segment. Compared to acyclovir free in solution, encapsulation in Soluplus micelles was advantageous both in terms of (i) total amount of acyclovir accumulated in the sclera, which was $2.02 \mu\text{g}/\text{cm}^2$ (s.d. 1.61) when applied as aqueous solution, and $13.69 \mu\text{g}/\text{cm}^2$ (s.d. 4.10) when formulated in Soluplus micelles; and (ii) steady state flux (J) obtained from the slope of the amount permeated through the sclera vs. time, which was 8.02 and $26.97 \mu\text{g}/\text{cm}^2 \cdot \text{h}^{-1}$ for acyclovir aqueous solution and micelle formulation, respectively.

3.4. Concluding remarks

Soluplus micelles loaded with acyclovir showed a homogeneous nanometer particle size with slightly negative Z-potential values, which may be adequate to cross cornea and sclera. In addition, this system was shown to be suitable for formulation as eye drops that may undergo in situ gelling since the storage and loss moduli increase as temperature raise from room temperature to ocular temperature. The increase in viscosity of the formulation would prolong its permanence on the eye surface, slowing down the dilution process. The encapsulation of the antiviral drug did not greatly improve its apparent solubility, but it did notably facilitate the penetration through and accumulation in the eye tissues. In particular, the noticeable accumulation of acyclovir at the sclera level may facilitate the access of this drug to the posterior segment of the eye.

3.5. References

Ahmed I., Gokhale R.D., Shah M.V., Patton T.F. 1987. Physicochemical determinants of drug diffusion across the conjunctiva, sclera, and cornea. *J Pharm Sci.* 76:583-586

Al-Dujaili L.J., Clerkin P.P., Clement C., McFerrin H.E., Bhattacharjee P.S., Varnell E.D., Kaufman H.E., Hill J.M. 2011. Ocular herpes simplex virus: how are latency, reactivation, recurrent disease and therapy interrelated? *Future Microbiol.* 6:877-907

Al-Ghabeish M., Xu X., Krishnaiah Y.S., Rahman Z., Yang Y., Khan M.A. 2015. Influence of drug loading and type of ointment base on the *in vitro* performance of acyclovir ophthalmic ointment. *Int J Pharm.* 495:783-791

Alvarez-Rivera F., Concheiro A., Alvarez-Lorenzo C. 2018. Epalrestat-loaded silicone hydrogels as contact lenses to address diabetic-eye complications. *Eur J Pharm Biopharm.* 122:126-136

Alvarez-Rivera F., Fernandez-Villanueva D., Concheiro A., Alvarez-Lorenzo C. 2016. alpha-Lipoic acid in Soluplus® polymeric nanomicelles for ocular treatment of diabetes-associated corneal diseases. *J Pharm Sci.* 105:2855-2863

Azher T.N., Yin X.T., Tajfirouz D., Huang A.J., Stuart P.M. 2017. Herpes simplex keratitis: challenges in diagnosis and clinical management. *Clin Ophthalmol.* 11:185-191

Bachu R.D., Chowdhury P., Al-Saedi Z.H.F., Karla P.K., Boddu S.H.S. 2018. Ocular drug delivery barriers-role of nanocarriers in the treatment of anterior segment ocular diseases. *Pharmaceutics.* 10:28

3. *Polymeric micelles for acyclovir ocular delivery: formulations and cornea and sclera permeability*

BASF, 2010. Soluplus® Technical Information. Available from: <https://pharmaceutical.basf.com/en/Drug-Formulation/Soluplus.html> (accessed May 2018)

BASF, 2012. Solutol® Technical Information. Available from: <https://pharmaceutical.basf.com/en/Drug-Formulation/Kolliphor-HS-15.html> (accessed May 2018)

Bisht R., Mandal A., Jaiswal J.K., Rupenthal I.D. 2018. Nanocarrier mediated retinal drug delivery: overcoming ocular barriers to treat posterior eye diseases. *Wiley Interdiscip Rev Nanomed Nanobiotechnol.* 10:e1473

Caspi R.R. 2013. In this issue: immunology of the eye--inside and out. *Int Rev Immunol.* 32:1-3

dos Santos J.F., Alvarez-Lorenzo C., Silva M., Balsa L., Couceiro J., Torres-Labandeira J.J., Concheiro A. 2009. Soft contact lenses functionalized with pendant cyclodextrins for controlled drug delivery. *Biomaterials.* 30:1348-1355

Edwards R.G., Longnecker R. 2017. Herpesvirus entry mediator and ocular herpesvirus infection: more than meets the eye. *J Virol.* 91:e00115-17

Geroski D.H., Edelhauser H.F. 2000. Drug delivery for posterior segment eye disease. *Invest Ophthalmol Vis Sci.* 41:961-964

Grimaudo M.A., Pescina S., Padula C., Santi P., Concheiro A., Alvarez-Lorenzo C., Nicoli S. 2018. Poloxamer 407/TPGS mixed micelles as promising carriers for cyclosporine ocular delivery. *Mol Pharm.* 15:571-584

Hamalainen K.M., Kananen K., Auriola S., Kontturi K., Urtti A. 1997. Characterization of paracellular and aqueous penetration routes in cornea, conjunctiva, and sclera. *Invest Ophthalmol Vis Sci.* 38:627-634

Heron E., Gutzwiller-Fontaine M., Bourcier T. 2014. Scleritis and episcleritis: diagnosis and treatment. *Rev Med Interne.* 35:577-585

Hill G.M., Ku E.S., Dwarakanathan S. 2014. Herpes simplex keratitis. *Dis Mon.* 60:239-246

Hou J., Sun E., Sun C., Wang J., Yang L., Jia X.B., Zhang Z.H. 2016. Improved oral bioavailability and anticancer efficacy on breast cancer of paclitaxel via novel Soluplus®-Solutol® HS15 binary mixed micelles system. *Int J Pharm.* 512:186-193

Hung S.O., Patterson A., Rees P.J. 1984. Pharmacokinetics of oral acyclovir (Zovirax) in the eye. *Br J Ophthalmol.* 68:192-195

James S.H., Prichard M.N. 2014. Current and future therapies for herpes simplex virus infections: mechanism of action and drug resistance. *Curr Opin Virol.* 8:54-61

Karsten E., Watson S.L., Foster L.J. 2012. Diversity of microbial species implicated in keratitis: a review. *Open Ophthalmol J.* 6:110-124

Knickelbein J.E., Hendricks R.L., Charukamnoetkanok P. 2009. Management of herpes simplex virus stromal keratitis: an evidence-based review. *Surv Ophthalmol.* 54:226-234

Li J., Li Z., Zhou T., Zhang J., Xia H., Li H., He J., He S., Wang L. 2015. Positively charged micelles based on a triblock copolymer

3. *Polymeric micelles for acyclovir ocular delivery: formulations and cornea and sclera permeability*

demonstrate enhanced corneal penetration. *Int J Nanomedicine*. 10:6027-6037

Loch C., Zakelj S., Kristl A., Nagel S., Guthoff R., Weitschies W., Seidlitz A. 2012. Determination of permeability coefficients of ophthalmic drugs through different layers of porcine, rabbit and bovine eyes. *Eur J Pharm Sci*. 47:131-138

Lu L.J., Liu J. 2016. Human Microbiota and Ophthalmic Disease. *Yale J Biol Med*. 89:325-330

Majumdar S., Hingorani T., Srirangam R., Gadepalli R.S., Rimoldi J.M., Repka M.A. 2009. Transcorneal permeation of L- and D-aspartate ester prodrugs of acyclovir: delineation of passive diffusion versus transporter involvement. *Pharm Res*. 26:1261-1269

Mandal A., Cholkar K., Khurana V., Shah A., Agrahari V., Bisht R., Pal D., Mitra A.K. 2017. Topical formulation of self-assembled antiviral prodrug nanomicelles for targeted retinal delivery. *Mol Pharm*. 14:2056-2069

Mangoni M.L., McDermott A.M., Zasloff M. 2016. Antimicrobial peptides and wound healing: biological and therapeutic considerations. *Exp Dermatol*. 25:167-173

OECD, 2017. OECD Guidelines for the Testing of Chemicals, Section 4, Test No. 437. Available from: https://www.oecd-ilibrary.org/environment/test-no-437-bovine-corneal-opacity-and-permeability-test-method-for-identifying-i-chemicals-inducing-serious-eye-damage-and-ii-chemicals-not-requiring-classification-for-eye-irritation-or-serious-eye-damage_9789264203846-en (accessed May 2018)

Pearlman E., Sun Y., Roy S., Karmakar M., Hise A.G., Szczotka-Flynn L., Ghannoum M., Chinnery H.R., McMenamin P.G., Rietsch A. 2013. Host defense at the ocular surface. *Int Rev Immunol.* 32:4-18

Rechenchoski D.Z., Faccin-Galhardi L.C., Linhares R.E.C., Nozawa C. 2017. Herpesvirus: an underestimated virus. *Folia Microbiol. (Praha).* 62:151-156

Roizman B., Whitley R.J. 2013. An inquiry into the molecular basis of HSV latency and reactivation. *Annu Rev Microbiol.* 67:355-374

Scholz M., Doerr H.W., Cinatl J. 2003. Human cytomegalovirus retinitis: pathogenicity, immune evasion and persistence. *Trends Microbiol.* 11:171-178

Tai M.C., Lu D.W., Chiang C.H. 2003. Corneal and scleral permeability of quinolones--a pharmacokinetics study. *J Ocul Pharmacol Ther.* 19:547-554

Tan F. 2016. Preparation of O'-O-lauroyl chitosan and self-assembly micellar solubilization of acyclovir. Available from: <http://dpi-proceedings.com/index.php/dtetr/article/view/9794> (accessed May 2018)

Toma H.S., Murina A.T., Areaux R.G., Jr Neumann D.M., Bhattacharjee P.S., Foster T.P., Kaufman H.E., Hill, J.M. 2008. Ocular HSV-1 latency, reactivation and recurrent disease. *Semin Ophthalmol.* 23:249-273

Tsatsos M., MacGregor C., Athanasiadis I., Moschos M.M., Hossain P., Anderson D. 2016. Herpes simplex virus keratitis: an update of the pathogenesis and current treatment with oral and topical antiviral agents. *Clin Exp Ophthalmol.* 44:824-837

3. Polymeric micelles for acyclovir ocular delivery: formulations and cornea and sclera permeability

Vadlapudi A.D., Cholkar K., Vadlapatla R.K., Mitra A.K. 2014. Aqueous nanomicellar formulation for topical delivery of biotinylated lipid prodrug of acyclovir: formulation development and ocular biocompatibility. *J Ocul Pharmacol Ther.* 30:49-58

Volpato N.M., Santi P., Laureri C., Colombo P. 1997. Assay of acyclovir in human skin layers by high-performance liquid chromatography. *J Pharm Biomed Anal.* 16:515-520

Wen H., Hao J., Li S.K. 2010. Influence of permeant lipophilicity on permeation across human sclera. *Pharm Res.* 27:2446-2456

Wen H., Hao J., Li S.K. 2013. Characterization of human sclera barrier properties for transscleral delivery of bevacizumab and ranibizumab. *J Pharm Sci.* 102:892-903

Wilhelmus K.R. 2015. Antiviral treatment and other therapeutic interventions for herpes simplex virus epithelial keratitis. *Cochrane Database Syst Rev.* 1:CD002898

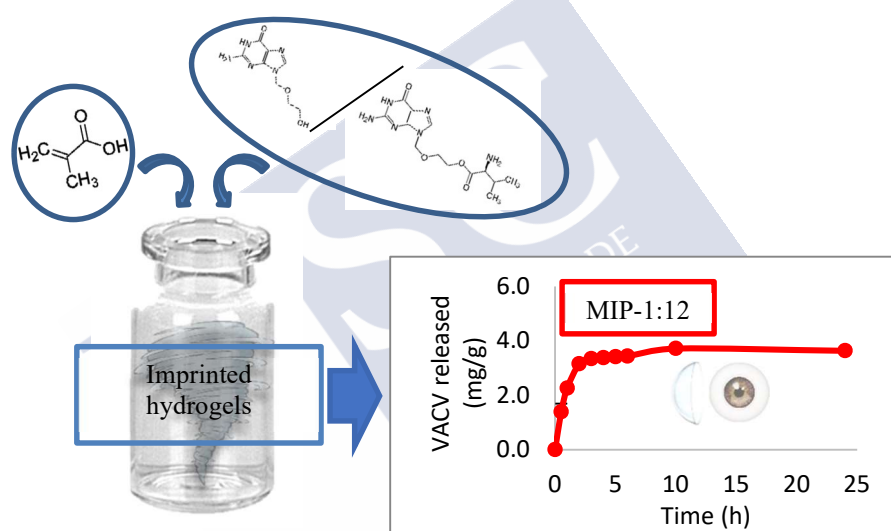
World Health Organization. Herpes simplex virus. Available from: <http://www.who.int/en/news-room/fact-sheets/detail/herpes-simplex-virus> (accessed May 2018)

Yawn B.P., Wollan P.C., St Sauver J.L., Butterfield L.C. 2013. Herpes zoster eye complications: rates and trends. *Mayo Clin Proc.* 88:562-570

Zhu L., Zhu H. 2014. Ocular herpes: the pathophysiology, management and treatment of herpetic eye diseases. *Virol Sin.* 29:327-342



Imprinted hydrogels for ocular administration of acyclovir and valacyclovir





4. Imprinted hydrogels for acyclovir and valacyclovir ocular administration

4.1. Introduction

Herpes simplex virus (HSV) belongs to the genus *Simplexvirus*, within the subfamily *Alphaherpesvirinae*, of the family *Herpesviridae* (Zambrano *et al.*, 2008). Human herpesviruses are approximately 200 nm in diameter and consist of a double-stranded viral DNA nucleus, which is surrounded by a protein capsule, another protein layer surrounding the capsule, and finally a glycoprotein envelope (Whitley *et al.*, 2001; Fatahzadeh *et al.*, 2007). The infection starts when the virus comes into contact with damaged skin or mucous membranes and the incubation period extends to 4 days (Whitley *et al.*, 2001). There are two subtypes of herpes simplex virus, HSV-1 and HSV-2. The main difference is that HSV-1 appears mainly in the orolabial area, while HSV-2 appears mainly in the genital area, although it has been seen that in developed countries, cases of genital conditions due to HSV-1 and orolabial due to HSV-2 are on the increase (Lloyd *et al.*, 2019).

It is estimated that 90% of the world's population is infected with HSV (*Lloyd et al., 2019*). Periodically, the virus can reactivate and travel to the skin or mucous membranes, causing a recurrent symptomatic or asymptomatic infection. Many factors can trigger this reactivation, for example, stress, exposure to heat or cold, menstruation, fever or immunosuppression, among others (*Fatahzadeh et al., 2007*). The clinical manifestations of the infection depends on whether the infection is primary or recurrent, the immune status of the host and the entry portal (*Brady et al., 2004*).

At the ocular level, recurrent HSV represents a serious epidemiological cause of infectious and inflammatory disease. It is estimated that herpes disease affects more than 10 million people, and of these, approximately 2 million suffer vision problems in the affected eye. The most common form of this virus infection is epithelial keratitis and accounts for 50-80% of ocular herpes. Worldwide, about 1 million new or recurrent cases of epithelial keratitis occur annually (*Wilhelmus, 2015*) and it is the most common cause of irreversible blindness in developed countries (*Karsten et al., 2012*). The origin of ocular herpes is probably primary orofacial herpes (HSV-1); about 56-58% of patients with ocular herpes have a history of oral herpes (*Esmann, 2001; Karsten et al., 2012*).

The HSV-1 keratitis is distinguished according to the layer of the cornea affected (epithelium, stroma or endothelium). Epithelial keratitis manifests itself as granular spots with the formation of

epithelial filaments, which form a dotted epithelial keratopathy early on. This is followed by dendritic injury, which leads to the destruction of the basement membrane and the formation of a dendritic ulcer. On the other hand, in stromal keratitis, necrosis and ulceration occur, and the inflammation leads to thinning, neovascularization and scarring of the stroma, as well as lipid deposition. Lastly, in endothelial keratitis, keratic precipitates appear and there is mild or moderate iritis (*Kaye et al., 2006; Tsatsos et al., 2016*). Recurrent disease, i.e., that which occurs in a subject who has been previously infected with HSV-1, is characterized by corneal scarring, thinning and vascularization (*Karsten et al., 2012*).

Current therapy for the treatment of HSV ocular keratitis includes topical, oral or intravenous antiviral agents (*Fatahzadeh et al., 2007; Koganti et al., 2019*). Viral keratitis can become a chronic and recurrent disease, affecting patients' quality of life due to the limited efficacy of available treatments (*Austin et al., 2017; Koganti et al., 2019*). Most of the approved antivirals are acyclic nucleosides and nucleotide analogs, which interrupt virus replication (*Alvarez et al., 2020*). Acyclovir (9-[2-hydroxyethoxymethyl] guanine) (ACV) is a purine nucleoside analogue (guanine) that remains the treatment of choice for HSV-1 infections to date (*Karsten et al., 2012; Koganti et al., 2019*). It is a selective antiviral agent, as it specifically targets virus-infected cells and selectively inhibits the viral DNA polymerase (*Brady et al., 2004; Kalezic et al., 2018*). Nevertheless, the inhibition

of virus replication may not affect the latency, so the infection may have not been solved (*Fatahzadeh et al., 2007; Koganti et al., 2019; Alvarez et al., 2020*). ACV has a good safety profile and is well tolerated by patients, but its oral bioavailability is low (10-20%) and its plasma half-life is short, which involves frequent administration (*Brady et al., 2004; Kaye et al., 2006; Fatahzadeh et al., 2007*). Moreover, there are studies that demonstrate the growing resistance to this drug mainly in immunosuppressed subjects, developed through a mutation of the viral gene thymidine kinase, essential for the phosphorylation of ACV. An additional limitation of oral administration of ACV is renal toxicity in elderly patients, who are unable to excrete the drug properly (*Karsten et al., 2012; Koganti et al., 2019; Alvarez et al., 2020*). An alternative is the topical application of ACV, but its effectiveness depends on its ability to cross the epithelium (*Fatahzadeh et al., 2007*). In comparative studies with other non-selective antiviral agents, ACV ointment has been shown to be more effective and less toxic (*Kalezic et al., 2018*). The problem with topical forms is their low retention time on the eye surface (*Koganti et al., 2019*). Topical ACV is considered the treatment of choice for HSV keratitis in Europe (*Austin et al., 2017*), as opposed to the US, which is trifluridine (a synthetic pyrimidine nucleoside showing ocular toxicity) (*Kalezic et al., 2018*). In some cases, corticosteroids are used as adjuvant therapy to antivirals (*Austin et al., 2017*). The problem is that many side effects can occur in long-

term therapy, including cataract, suppression of the immune response, and possible secondary glaucoma (*Rajasagi et al., 2018; Koganti et al., 2019*).

There are ACV analogues with similar mechanisms of action, but different bioavailability, such as ganciclovir, famciclovir, penciclovir or valacyclovir (*Koganti et al., 2019; Alvarez et al., 2020*). Valacyclovir (L-valine 2-[2-amino-1,6-dihydro-6-oxo-9H-purinyl)methoxy]ethyl ester) (VACV) is a pro-drug for ACV (*Kapanigowda et al., 2016*). VACV is converted to ACV by intestinal and/or hepatic metabolism and 90 % is excreted in urine (*Kumar et al., 2010*). Although the oral bioavailability of VACV is higher than that of ACV (*Kumar et al., 2010; Kalezic et al., 2018*), still the oral administration of VACV does not provide effective concentrations in the eye (*Kang-Mieler et al., 2014*). For example, oral administration of VACV (500 mg/day) does not suppress HSV-1 DNA shedding in tears (*Kumar et al., 2009; Kumar et al., 2010*). Although reports on topical formulations of VACV are still scarce (*Kapanigowda et al., 2016; Kumar et al., 2017*), recent studies have confirmed that VACV binds to the oligopeptide transporter of the corneal epithelium, and that its transcorneal permeability is 3 times higher than that of ACV. It is transformed from a prodrug to a drug by enzymatic hydrolysis in the cornea (*Anand et al., 2002; Kapanigowda et al., 2016*). Also VACV shows higher affinity than ACV for the amino acid transporter $ATB^{O,+}$ present in ocular tissues (*Hatanaka et al., 2004*).

The aim of the second step of the Thesis was to design hydrogels suitable for soft CL with affinity for acyclovir and valacyclovir and that can sustainedly release these drugs on the ocular surface during daily use. Among the proposed procedures to endow the hydrogel CLs with affinity for specific molecules, the creation of artificial receptors using the molecular imprinting technique stands out (*Byrne et al., 2002; Alvarez-Lorenzo et al., 2004*). This technique requires incorporating the substances of interest into the monomers mixture so that the monomers can rearrange according to their affinity. This rearrangement becomes permanent during polymerization. The removal of the template molecules generates cavities with the most appropriate size and chemical groups to host the substance of interest again (*Alvarez-Lorenzo et al., 2004*). Functional monomers suitable for interaction with the antiviral drugs were first screened using computational modeling; methacrylic acid (MAA) showed higher affinity for the drugs than the structural monomer 2-hydroxyethyl methacrylate (HEMA) and other functional monomers (**Figure 4.1**). MAA may interact with the side chain of VACV through not only hydrogen bonding with the ring (as in the case of ACV) but also electrostatic interactions with the amino group. Hydrogels were prepared with various contents in the functional monomer in the presence (imprinted) and absence (non-imprinted) of the drug. The hydrogels will be characterized in terms of swelling, transmittance, mechanical properties, biocompatibility (HET-CAM assay) and

capability to load and release the antiviral drugs. Finally, the permeability through bovine cornea and sclera of the drug released by the hydrogel was evaluated.

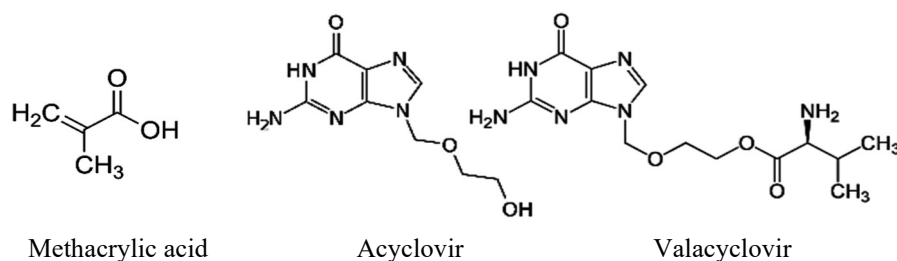


Figure 4.1. Structure of methacrylic acid, acyclovir and valacyclovir.

4.2. Materials and methods

4.2.1. Materials

Acyclovir was purchased from Farmalabor (Italy); valacyclovir, 2,2'-azo-bis(isobutyronitrile) (AIBN), dichlorodimethylsilane, ethyleneglycol dimethacrylate (EGDMA) and methacrylic acid (MAA) were from Sigma-Aldrich (Germany); ethanol absolute and NaOH were from VWR (Belgium); 2-hydroxyethyl methacrylate (HEMA) was from Merck (Germany); acetic acid and NaCl were from Scharlau (Spain); and methanol was from Fisher (Belgium). Ultrapure water (resistivity > 18 MΩ·cm) was obtained by reverse osmosis (MilliQ®, Millipore Spain). Simulated lacrimal fluid (SLF) was prepared with the following composition: 6.78 g/L NaCl, 2.18 g/L NaHCO₃, 1.38 g/L KCl and 0.084 g/L CaCl₂·2H₂O with pH 7.5. Carbonate buffer pH 7.2 was prepared by mixing buffer solution A

(6.2 g/L NaCl, 0.355 g/L KCl, 0.1 g/L NaH₂PO₄·H₂O and 2.45 g/L NaHCO₃) and buffer solution B (0.115 g/L CaCl₂ and 0.155 g/L MgCl₂·6H₂O).

4.2.2. Computational modeling

A preliminary study was carried out using computer modeling to elucidate interactions between the drugs to be studied (ACV and VACV) and functional monomers used in the synthesis of hydrogels. The tested monomers were acryl amide (AAm), 2-aminoethyl methacrylate hydrochloride (AEMA), N-(3-aminopropyl) methacrylamide hydrochloride (APMA), ethyleneglycolphenylether methacrylate (EGPEM), butoxyethyl methacrylate (BEM), hydroxyethyl methacrylate (HEMA) and methacrylic acid (MAAc). The 3D structure of the functional monomers and ACV and VACV was taken from the PubChem database (*Kim et al., 2016*). The Autodock Tools version 4.2.6 software was used to calculate molecular docking. In all cases, the grid was generated with default settings around the monomer and the drug, the smallest conformation was used and the docking was performed using the Lamarckian Genetic Algorithm (*Morris et al., 2009*). Estimated free energy of binding ($\Delta G_{binding}$) and dissociation constant (K_i) values were obtained.

4.2.3. Synthesis of imprinted hydrogels

Different mixtures of monomers were prepared, as shown in **Table 4.1**. The components were added to vials and mixed at room

temperature and under magnetic agitation (300 rpm) until they were completely dissolved. Finally, the initiator (AIBN) was added, and the solutions were stirred for 15 minutes more. The solutions were injected, with needle and syringe, into pre-assembled moulds, consisting of two pre-treated glass plates (12x14 cm) separated by a 0.45 mm thick silicone frame. The pre-treatment of the glass consisted of applying two layers of dichlorodimethylsilane, waiting 10 minutes between each application. The plates were left to dry in a hood for 1 hour and then were thoroughly washed with ethanol and rinsed with water. Finally, they were dried in an oven at 70°C for 1 hour, before being assembled. Polymerization was carried out for 12 hours at 50°C and then for a further 24 hours at 70°C. All hydrogel compositions were prepared in triplicate.

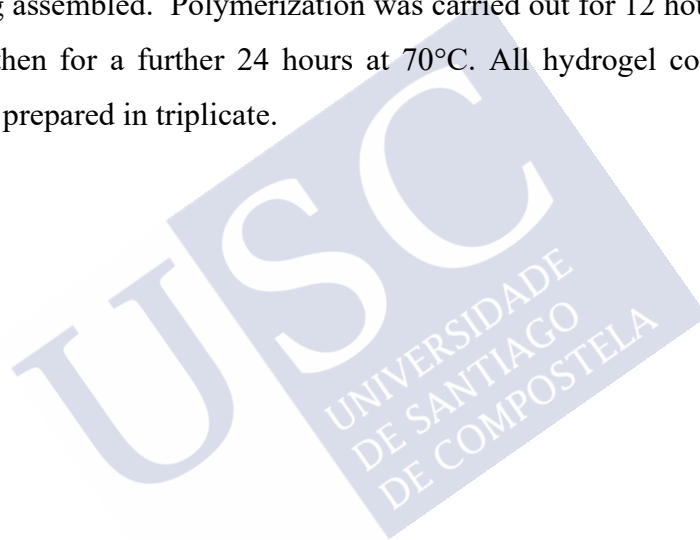


Table 4.1. Composition of the synthesized hydrogels (NIP: non-imprinted hydrogels, MIP: imprinted hydrogels). Final EGDMA, MAA and AIBN concentrations were 8, 200 and 10 mM, respectively.

Hydrogel	HEMA (mL)	EGDMA (μL)	MAA (mL)	ACV (mg)	VACV (mg)	AIBN (mg)
NIP ₀	5	7.55	0	0	0	8.21
NIP ₂₀₀	5	7.55	0.084	0	0	8.21
MIP _{ACV}	5	7.55	0	45	0	8.21
MIP _{1:5}	5	7.55	0.084	45	0	8.21
MIP _{1:10}	5	7.55	0.084	23	0	8.21
MIP _{1:15}	5	7.55	0.084	15	0	8.21
MIP _{VACV}	5	7.55	0	0	25	8.21
MIP _{1:6}	5	7.55	0.084	0	50	8.21
MIP _{1:12}	5	7.55	0.084	0	25	8.21
MIP _{1:32}	5	7.55	0.084	0	10	8.21

4.2.4. Drug removal

After polymerization, each hydrogel sheet was immersed in 500 mL of boiling water for 15 minutes in order to remove unreacted monomers and facilitate cutting into discs (10 mm in diameter). Washing was then performed, except for a few discs of each type of hydrogel, which were reserved for direct drug release test, as explained below. For the washing, the discs were immersed in water, under magnetic agitation (300 rpm) and at room temperature. The media was replaced every 24 hours until no signal was measured, which was monitored spectrophotometrically in the range of 190-800 nm (UV-Vis spectrophotometer, Agilent 8534, Germany). When no

spectrophotometric signal was detected, the hydrogels were dried in an oven at 70°C for 24 hours and stored protected from light and humidity. In parallel, the amount of ACV (MIP_{ACV}, MIP_{1:5}, MIP_{1:10} and MIP_{1:15}) and VACV (MIP_{VACV}, MIP_{1:6}, MIP_{1:12} and MIP_{1:32}) removed in each washing step was monitored spectrophotometrically at 252 and 253 nm, respectively.

4.2.5. Direct drug release test from boiled hydrogels

Discs of each type of hydrogel were individually placed in 5 mL of SLF and kept under oscillating agitation (300 rpm) and at 35 °C. At preset times (0.5, 1, 2, 6 and 24 h), 3 mL of medium were removed and absorbance was measured by spectrophotometry at 252 nm (ACV) and 253 nm (VACV) (UV-Vis spectrophotometer, Agilent 8453, Germany), returning the samples to the release vial. The experiments were carried out in triplicate. The amounts of drug released were calculated using the previously prepared calibration curves and referred to the unit of mass of the dry disc. The calibration curves were prepared by dissolving ACV (30 µg/mL) in ethanol:water (50:50, v/v) mixture, and VACV (50 µg/mL) in water. Dilutions of 2, 3, 5, 10, 15, 20, 25 and 30 µg/mL were made for ACV, and 1.25, 2.5, 5, 10, 15, 20, 25, 30, 40 and 50 µg/mL for VACV. The calibration curve was prepared from absorbances recorded at 252 and 253 nm, respectively (UV-Vis spectrophotometer, Agilent 8453, Germany).

4.2.6. Drug loading and release from conditioned hydrogels

The ACV load was tested on the hydrogels NIP₀, NIP₂₀₀, MIP_{ACV}, MIP_{1:5}, MIP_{1:10} and MIP_{1:15}. Washed and dry discs of each type were placed in triplicate in tubes with 15 mL of drug solution. The loading solution was prepared by dissolving ACV (0.3 mg/mL) in water and kept under magnetic agitation (300 rpm), at room temperature for 72h. The loading tubes were kept under oscillating agitation (300 rpm), at RT (23-25 °C), for 4 days. The absorbances of each sample were measured by spectrophotometry at 252 nm (UV-Vis spectrophotometer, Agilent 8453, Germany), diluting the sample (0.2:5) with ethanol:water mixture (50:50, v/v). The calculation of the total drug load on the discs was estimated by the difference between the initial and final amount of drug in solution, and was calculated using the previously prepared calibration curve, referring the loaded amounts to the unit of mass of the dry disc.

The VACV load was evaluated on the hydrogels NIP₀, NIP₂₀₀, MIP_{VACV}, MIP_{1:6}, MIP_{1:12} and MIP_{1:32}. Three dry discs of each type were placed in tubes with 5 mL of drug solution. The loading solution was prepared by dissolving VACV (0.3 mg/mL) in a 0.1 mM NaOH solution and was kept under magnetic agitation (300 rpm), at RT (23-25 °C), for 15 minutes. The loading tubes were kept under the same conditions of agitation, temperature, and time as for the ACV. The absorbances of each sample were measured spectrophotometrically, at 253 nm, for the calculation of the total load, in the same way.

The drug network/water partition coefficient ($K_{N/W}$) was calculated for each hydrogel from the total amount of drug loaded using the following equation:

$$\text{Loading (total)} = \frac{V_s + K_{N/W} * V_p}{W_p} * C_0 \quad [\text{Eq. 4.1}]$$

where V_s is the volume of water absorbed by the hydrogel, V_p the volume of dry polymer, W_p the weight of the dry hydrogel, and C_0 the concentration of drug in the loading solution.

The loaded discs were removed from the tubes and rinsed with water. The surface water was removed with filter paper and then the discs were immediately placed in release tubes with 15 and 10 mL of SLF (for ACV and VACV, respectively), under oscillating agitation (300 rpm) and at 35 °C. The release kinetics were evaluated at 1, 2, 4, 6, 8 and 24 h, for ACV, and at 0.5, 1, 2, 3, 4, 5, 6, 10 and 24 h, for VACV. The samples were taken following the same protocol as in section 4.1.4.

4.2.7. Degree of swelling

The degree of swelling was monitored in water and SLF for hydrogels NIP₀, NIP₂₀₀, MIP_{VACV}, MIP_{1:6}, MIP_{1:12} and MIP_{1:32}, in triplicate. The study was carried out at RT (23-25 °C) and the increment in weight of the hydrogels was recorded at predetermined times (0.5, 1, 2, 4, 8 and 24 h), after being submerged in 4 mL of the corresponding medium. In each measurement, the disc was removed from the vial, superficially dried with filter paper, weighed and

returned to the vial. The degree of swelling was calculated with the following equation:

$$\text{Swelling degree (\%)} = \frac{W_t - W_0}{W_0} * 100 \quad [\text{Eq. 4.2}]$$

where W_0 and W_t represent the weight of the dried and swollen hydrogel, respectively.

4.2.8. Light transmittance

The light transmission (%) of the hydrated discs in the swelling test (SLF) was measured in a spectrophotometer (Agilent Cary 60 UV-Vis) in triplicate, recording the transmittance from 200 to 800 nm.

4.2.9. Mechanical properties

The mechanical properties of the NIP₀, NIP₂₀₀, MIP_{VACV}, MIP_{1:6}, MIP_{1:12} and MIP_{1:32} discs, swollen in water, were tested in triplicate at RT (23-25 °C). Each hydrogel was cut into 16 x 9 mm strips and attached to the upper and lower clamps, with a 7 mm gap, on a TA.XT Plus Texture Analyzer (Stable Micro Systems, Ltd., UK), equipped with a 5 kgf load cell. The crosshead speed which the stress-strain plots were recorded was 0.1 mm s⁻¹. For the calculation of Young's modulus (E), the slope of the straight line part of the tensile strength (force per cross-sectional area) and the engineering stress (change of active length divided by original length) were used, as follows (*Tranoudis et al., 2004; Bhamra et al., 2017*).

$$E = \frac{F/A_0}{\Delta L/L_0} \quad [\text{Eq. 4.3}]$$

4.2.10. HET-CAM test

The chorioallantoic membrane hen egg test (HET-CAM) was performed by incubating fertilized hen eggs (50-60 g) at 37°C and 60% RH for 9 days. On the ninth day of incubation a circular cut was made on the top of the egg of approximately 1 cm diameter with a rotary saw (Dremel 300, Breda, The Netherlands). The shell was removed, and the inner membrane was moistened with 0.9% NaCl for 30 min (time during which the egg remained inside the climatic chamber). The membrane was then removed to expose the chorioallantoic membrane (CAM) (Alvarez-Rivera *et al.*, 2019).

The test was performed by placing in each CAM a hydrogel of each type in triplicate, previously hydrated for 24 h in loading solution. An aqueous solution of NaOH 0.1N and NaCl 0.9% (300 µL) in triplicate was used as negative and positive controls, respectively. The blood vessels were observed under white light for 5 min, to detect possible bleeding, vascular lysis or coagulation.

4.2.11. Bovine corneal and scleral permeability test

The fresh bovine eyes were collected from the local slaughterhouse and transported according to the BCOP test protocol (OECD, 2009; Alvarez-Rivera *et al.*, 2019). During transport, the eyes were kept immersed in PBS with added antibiotics (penicillin 100 IU/ml and streptomycin 100 µg/ml), in an ice bath. The corneas and scleras were isolated, using a scalpel. The tissues were washed with 0.9% NaCl and mounted in vertical diffusion cells (Franz cells). To

balance the tissues, the donor and receptor chambers were filled with carbonate buffer pH 7.2 and placed in a bath at 37 °C, with magnetic stirring, for 30 minutes. After that time, the volume of the donor chamber was removed and replaced by the analysis samples, in triplicate. The corneas and scleras were exposed to NIP₀ and MIP_{1:12} discs that had been soaked for 4 days in a VACV solution (0.3 mg/mL in NaOH 0.1 mM). The discs were covered with in 2 mL of 0.9% NaCl. In parallel, corneas and scleras were exposed to 2 mL of a VACV solution (50 µg/mL in NaOH 0.1 mM) as a control, for 6 h. The donor chambers were covered with parafilm to avoid evaporation. Samples of 1 mL were extracted from the receptor chamber at pre-established times: 0.5, 1, 2, 3, 4, 5 and 6 h, replacing the same volume removed with carbonate buffer pH 7.2 each time, taking care to eliminate possible bubbles formed in the diffusion cell.

The amount of VACV permeated into the receptor chamber was quantified by HPLC (Autosampler Waters 717, Waters Controller 600, Photodiode Detector 996), equipped with a C18 column (Waters Symmetry C18, 5 µm, 4.6×250 mm) and operated with the Empower2 software. The mobile phase consisted of acetic acid (1:1000):methanol (90:10 vol/vol) with a flow rate of 1 mL/min. The injection volume was 50 µL and the column was kept at 30 °C. The VACV was quantified at 251 nm (retention time 3 min). The calibration was performed with standard solutions of VACV (6.25-0.19 µg/mL) in carbonate buffer pH 7.2 (*Palacios et al., 2005*). The accumulated

amounts of VACV permeate per area vs. time were adjusted for the linear regression, and the steady state flow (J) and the time delay (t_{lag}) were obtained from the slope and x-intercept of the linear regression, respectively (Al-Ghabeish *et al.*, 2015).

After 6 h of the test, a sample was taken from the donor chamber for further analysis. In addition, the corneas/scleras were removed, rinsed with 0.9% NaCl and immersed in 3 mL of an ethanol:water mixture (50:50 v/v) overnight. They were then sonicated for 99 minutes at 37°C, centrifuged (1000 rpm, 5 min, 25°C), filtered and re-centrifuged (14000 rpm, 20 min, 25°C) (Volpato *et al.*, 1997). The coefficient of permeability of the drug through the cornea and sclera was calculated as the ratio of J and the concentration of VACV in the donor chamber (Al-Ghabeish *et al.*, 2015). The amounts extracted from the corneas/scleras were measured by HPLC as explained above.

4.3. Results and Discussion

4.3.1. Computational modeling

Results of computational modeling are summarized in **Table 4.2** and **4.3**. For both drugs, the interaction with MAA was predicted to be more energetically favourable than for other monomers. Therefore, MAA was chosen as functional monomer to prepare the hydrogels.

Table 4.2. Computational modeling results of ACV and the monomers HEMA, Aam, AEMA, APMA, BEM and EGPEM.

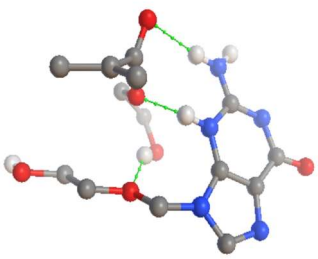
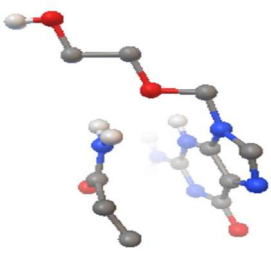
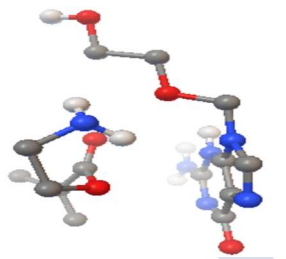
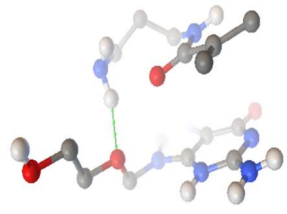
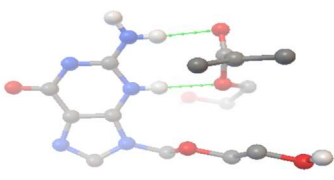
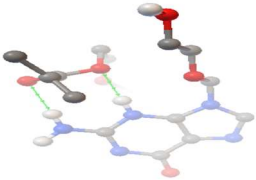
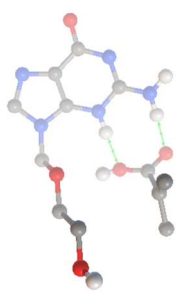
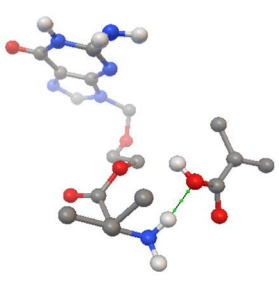
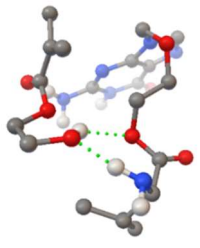
<p>HEMA+ACV</p>  <p>$\Delta G_{binding}$: -1.72 Kcal/mol Ki: 54.63 mM</p>	<p>Aam+ACV</p>  <p>$\Delta G_{binding}$: -1.78 Kcal/mol Ki: 49.66 mM</p>
<p>AEMA+ACV</p>  <p>$\Delta G_{binding}$: -0.89 Kcal/mol Ki: 223.2 mM</p>	<p>APMA+ACV</p>  <p>$\Delta G_{binding}$: -0.76 Kcal/mol Ki: 278.14 mM</p>
<p>BEM+ACV</p>  <p>$\Delta G_{binding}$: -1.24 Kcal/mol Ki: 124.19 mM</p>	<p>EGPEM+ACV</p>  <p>$\Delta G_{binding}$: -2.15 Kcal/mol Ki: 26.44 mM</p>

Table 4.3. Computational modeling results of ACV and VACV, and the monomer MAA. The interaction of VACV with HEMA is also shown.

<p>MAA+ACV</p>  <p>$\Delta G_{binding}$: -3.50 Kcal/mol Ki: 4.55 mM</p>	<p>MAA+VACV</p>  <p>$\Delta G_{binding}$: -3.10 Kcal/mol Ki: 5.35 mM</p>
<p>HEMA+VACV</p>  <p>$\Delta G_{binding}$: -1.85 Kcal/mol Ki: 43.68 mM</p>	

4.3.2. Synthesis of hydrogels and drug removal

Imprinted and non-imprinted hydrogels were synthesized combining HEMA with MAA as functional monomer. The drug was added at different levels, in ascending ratios of ACV:MAA (1:5, 1:10, and 1:15 mol/mol) and VACV:MAA (1:6, 1:12, and 1:32 mol/mol), as explained in **Table 4.1**. The use of MAA as comonomer should

enhance drug-hydrogel interactions through hydrogen bonding of the acrylic acid group with the rings of the drugs (ACV and VACV) and electrostatic interactions with VACV side chain. Maximum amounts of drug added during polymerization were limited by the poor solubility of the drugs in the monomers solution.

VACV was easily removed from the hydrogels during the washing process in boiling water. However, hydrogels synthesized with ACV showed lower drug removal values than the amounts added during synthesis. This could be due to the limited solubility of the ACV in water (**Figure 4.2**).

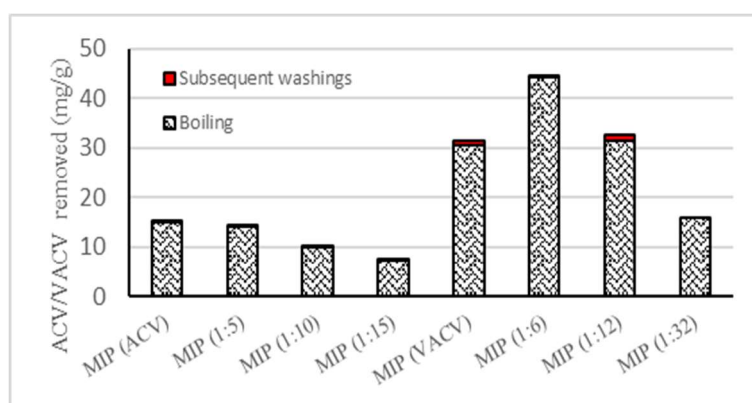


Figure 4.2. Amounts of ACV and VACV removed during washing in boiling water and subsequent washings.

4.3.3. Direct drug release test from boiled hydrogels

A direct release in SLF was carried out for hydrogels after boiling (without further washing), in order to determine their ability to release the remaining ACV and VACV added during polymerization. The

hydrogels polymerized with ACV (MIP_{ACV} , $\text{MIP}_{1:5}$, $\text{MIP}_{1:10}$, $\text{MIP}_{1:15}$) released about 0.20 mg of drug per gram of disc. That amount released was much lower than the total amount added during synthesis (45, 45, 23 and 15 mg of ACV, respectively) and practically no differences were observed between the different types of hydrogel. On the other hand, the hydrogels polymerized using VACV as template (MIP_{VACV} , $\text{MIP}_{1:6}$, $\text{MIP}_{1:12}$, $\text{MIP}_{1:32}$) released the small amount of VACV remaining in a sustained way for 24 h (VACV was mostly removed during the boiling process). A similar release experiment was performed with non-imprinting hydrogels and, as expected, no signal was recorded at the wavelength used for drug quantification (**Figure 4.3**).

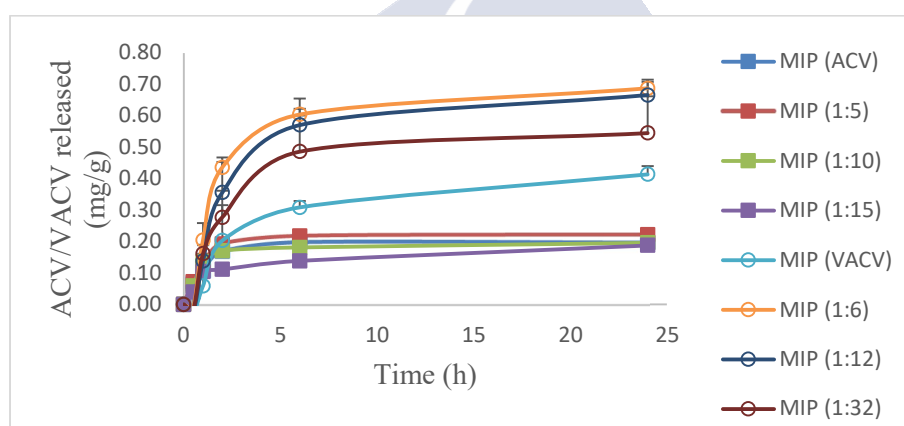


Figure 4.3. Release profiles of ACV and VACV from the imprinted discs that were previously boiled in water (15 min) and dried to constant weight. The drug released corresponds to that used as a template during synthesis. The data is shown as mg of drug per g of dry hydrogel.

4.3.4. Drug loading in washed hydrogels

ACV imprinted hydrogels (**Figure 4.4**) showed low capability to reload the drug. The presence of MAA did not significantly favor the subsequent loading capacity of the hydrogel. Differently, MAA notably enhanced the loading of VACV and a clear difference was observed between imprinted and non-imprinted hydrogels (**Figure 4.5**). The MAA functionalization significantly improved the total amount of VACV loaded by the discs after 4 days immersed in the loading solution. The higher affinity of the hydrogels for VACV can be explained by the stronger interaction of MAA with the amino group of the lateral chain.

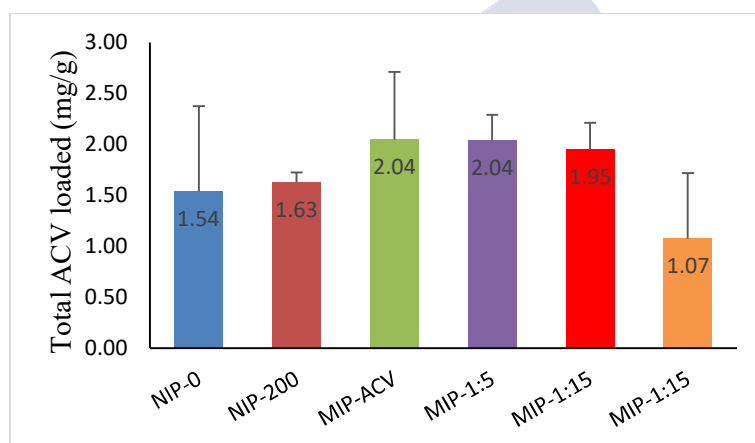


Figure 4.4. Total amounts of ACV loaded by the hydrogels immersed in the drug solution (0.3 mg/mL) for 4 days.

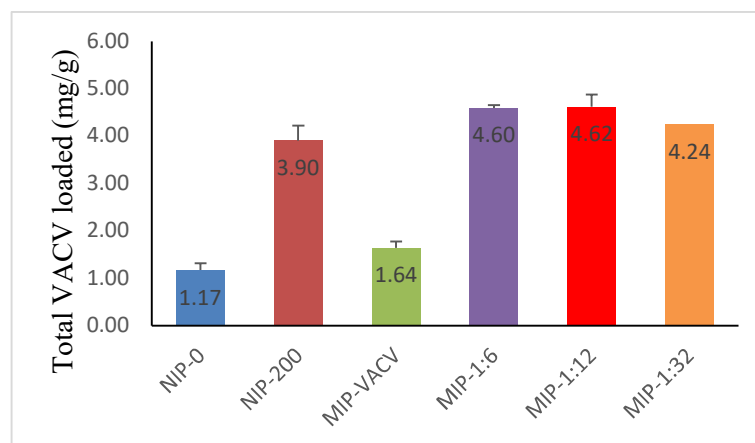


Figure 4.5. Total amounts of VACV loaded by the hydrogels immersed in the drug solution (0.3 mg/mL) for 4 days.

The network/water partition coefficient ($K_{N/W}$) was calculated for both imprinted and non-imprinted hydrogels, in order to analyze the increase in affinity achieved by the MAA functionalization. The control hydrogels i.e. NIP without MAA (NIP_0) had $K_{N/W}$ values of 3.0 (s.d. 0.4). The values obtained for the hydrogels imprinted without MAA (MIP_{VACV}) were 4.4 (s.d. 0.4). The values were all higher than 1, confirming that the drug was hosted in both the water phase and the polymer network. The rest of the hydrogels showed much higher values: NIP_{200} (11.3; s.d. 1.0) = $MIP_{1:32}$ (12.3; s.d. 0.3) < $MIP_{1:6}$ (13.4; s.d. 0.1) = $MIP_{1:12}$ (13.5; s.d. 0.8). Interestingly, simple addition of VACV to the HEMA monomers (MIP_{VACV} hydrogels imprinted without MAA) slightly increased the amount of drug loaded which mean that the drug molecules may create channels in the network that facilitate subsequent loading. Nevertheless, this effect was much

lower than that achieved when truly imprinted networks were prepared. MIP_{1:6} and MIP_{1:12} showed the highest loading capability. MIP_{1:32} were less efficient since there is an excess of MAA mers per drug molecule, which means that most MAA groups are randomly distributed along the hydrogel network (*Hiratani et al., 2002*).

4.3.5. Drug release

Drug-loaded discs (as explained above) were immersed in SLF to evaluate the capability of the hydrogels to control the release. In general, the release could be extended for 10 h. For the discs loaded with ACV, the plateau was reached after approximately 6 h of testing, with a maximum amount released of 0.6 mg/g of disc (**Figure 4.6**). Again, the discs imprinted with ACV were only capable of releasing half the amount of drug loaded, and the release profiles were similar to each other, with no significant differences in the amount of ACV released between the different types of hydrogel. These hydrogels were discarded for subsequent tests because of the irreversible binding of a relevant portion of the drug, which may compromise attaining the minimum level required for antiviral activity (IC₅₀: 1.92 µg/mL) (*Brezani et al., 2018*).

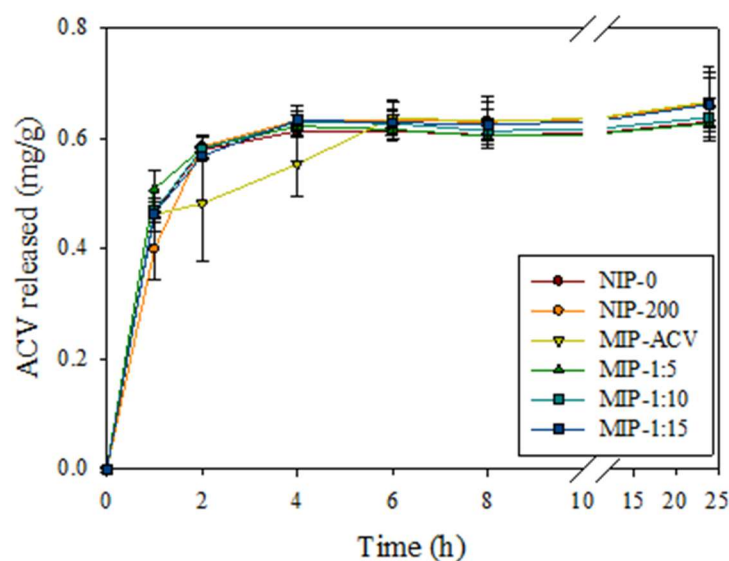


Figure 4.6. Acyclovir released in SLF for 24 h. Data were represented in mg of drug per g of dry hydrogel.

Differently, the discs loaded with VACV showed a sustained release profile for 10 hours. In general, the hydrogels were able to release most of the amount of drug loaded. Specifically, hydrogels functionalized with MAA and imprinted with 25 mg of VACV (MIP_{1:12}) showed better release profiles than their homologous without MAA (MIP_{VACV}), with a clear difference in VACV released (**Figure 4.7**). No significant differences were found between MIP_{1:12} and MIP_{1:6}. The functionalization with MAA clearly improves the capacity of the drug to incorporate and release from hydrogels and the molecular imprinting technique (MIP) improves that capacity.

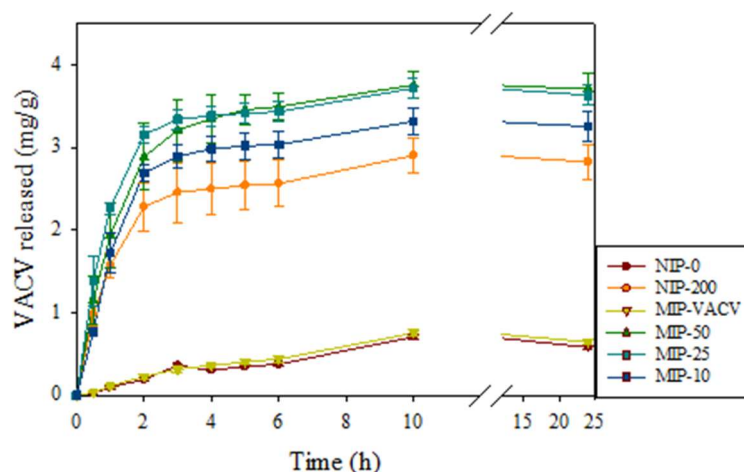


Figure 4.7. Valacyclovir released in SLF for 24 h. Data were represented in mg of drug per g of dry hydrogel.

4.3.6. Hydrogel characterization

Hydrogels NIP₀, NIP₂₀₀, MIP_{VACV}, MIP_{1:6}, MIP_{1:12} and MIP_{1:32} were characterized in terms of swelling degree, transmittance and mechanical properties. The degree of swelling in water and SLF was measured. All the hydrogels absorbed medium rapidly, reaching swelling equilibrium within one hour. The hydrogels swollen in water reached values close to 60%, as well as those not functionalized with MAA swollen in SLF. HEMA-MAA networks (both non-imprinted and imprinted) swollen in SLF were able to absorb up to 90% due to ionization of MAA (**Figure 4.8**). The uptake values are in the range typical of hydrophilic contact lenses.

4. Imprinted hydrogels for acyclovir and valacyclovir ocular administration

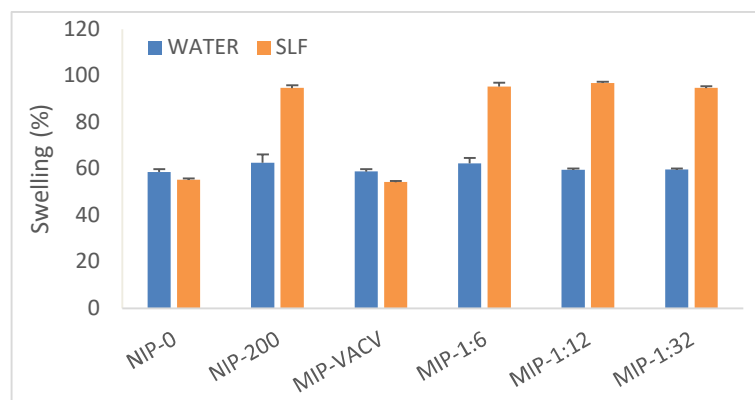


Figure 4.8. Uptake of water and simulated lacrimal fluid (SLF) by the hydrogels after being soaked for 24 h ($n = 3$; mean values and standard deviation).

All hydrogels showed excellent light transmission properties (Figure 4.9), with % transmittance values above 90% in the visible light range (400-800 nm).

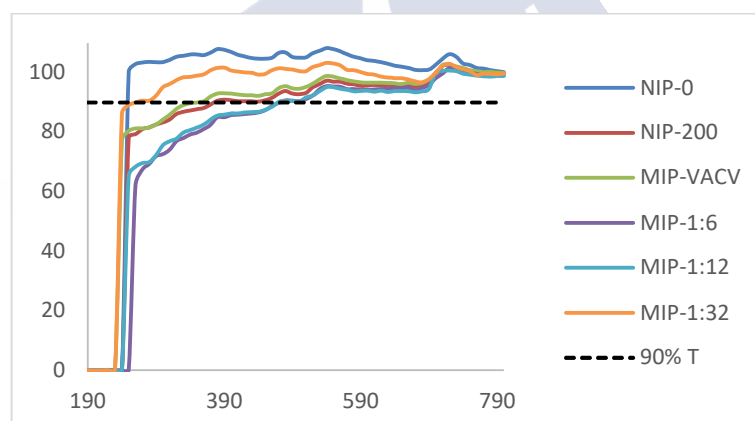


Figure 4.9. Light transmission profiles of the swollen discs in SLF. The acceptance value of 90% transmittance is represented by a dashed line.

Concerning the mechanical properties, the tensile strength tests showed that all types of hydrogel had a Young's modulus greater than 0.50 MPa (**Table 4.4**), except the NIP₀ control hydrogel. These values are within the typical range of hydrophilic contact lenses, so they should be clinically valid.

Table 4.4. *Young's modulus values calculated for the different types of hydrogel (0.45 mm thick and 9 mm wide).*

Hydrogel	Young modulus (MPa)
NIP ₀	0.547
NIP ₂₀₀	0.358
MIP _{VACV}	0.536
MIP _{1:6}	0.623
MIP _{1:12}	0.538
MIP _{1:32}	0.548

4.3.7. HET-CAM test

Irritation analysis by HET-CAM test was performed by exposing the chorioallantoic membrane to hydrogels NIP₀, NIP₂₀₀, MIP_{VACV}, MIP_{1:6}, MIP_{1:12} and MIP_{1:32} previously loaded with VACV solution (0.3 mg/mL). No hemorrhage, lysis or coagulation was observed for any of the six types of hydrogel, behaving in the same way as the negative control (NaCl 0.9%) (**Figure 4.10**).

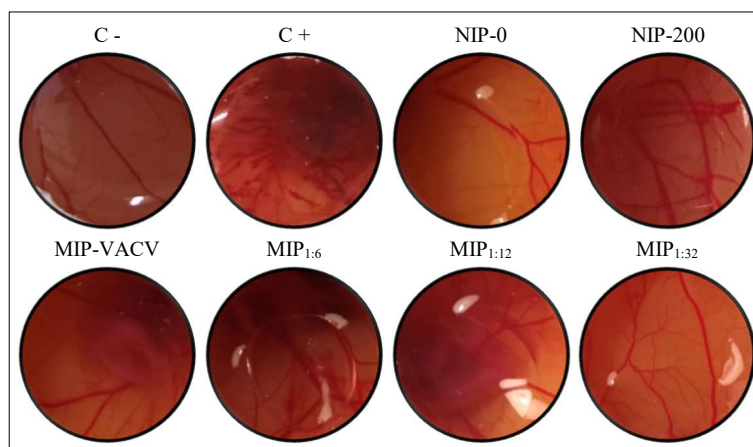


Figure 4.10. Pictures of chorioallantoic membranes during the HET-CAM test after 5 minutes of contact with VACV loaded hydrogels. The - and + controls refer to 0.9% NaCl and 0.1 N NaOH solutions, respectively.

4.3.8. Bovine corneal and scleral permeability test

The permeation ability of the VACV released from MIP_{1:12} hydrogels through bovine cornea and sclera was evaluated. NIP₀ hydrogels were evaluated as control, as well as an aqueous solution of the drug (100 µg/mL). At corneal level, permeated VACV was below the limit of quantification. Nevertheless, the accumulation of VACV in the cornea was remarkable (**Figure 4.11**), being 129.2 µg/cm² for the VACV released from the MIP_{1:12} hydrogel. Similar values were recorded for the drug in solution or released from control hydrogels. These findings indicated a high affinity for cornea tissue. Compared with VACV formulated in lipid nanocarriers as eye drops applied to goats that led to 30 µg drug per cm² of cornea (*Kumar et al., 2017*),

the values of VACV accumulated in the present study were remarkably higher.

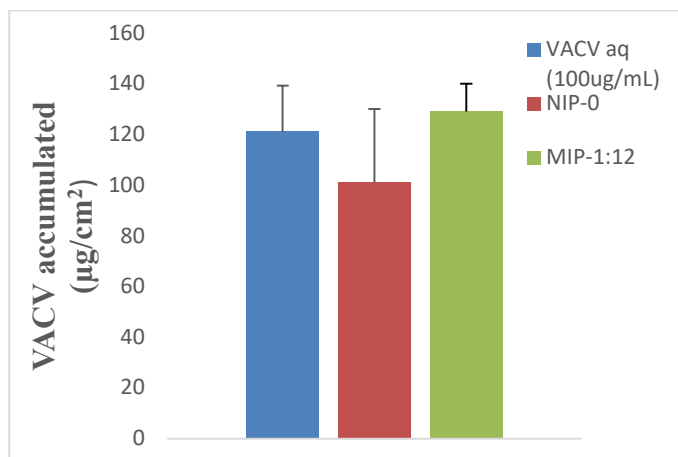


Figure 4.11. Amounts of VACV accumulated inside the cornea, administered through aqueous solution of VACV (100 µg/mL; blue bars), loaded in NIP₀ (red bars) or MIP_{1:12} (green bars) hydrogels.

Regarding the sclera tests, the permeated VACV could be quantified from the first measurement at 0.5 h (**Figure 4.12**). The steady state flow (J) was estimated from the first 5 h of the test to be 0.69 µg/cm²/h for MIP_{1:12} and 1.28 µg/cm²/h for the aqueous solution of VACV (VACV aq). The hydrogel NIP₀ was only able to permeate detectable amounts of VACV after 6 h of testing. The amounts remaining in the donor chamber after 6 h were 42% and 30% for VACV aq. and MIP_{1:12}, respectively. These values were used to calculate the average permeation coefficient (P) through the sclera, being 4.13·10⁻⁶ cm/s for MIP_{1:12} and 4.22·10⁻⁶ cm/s VACV aq. These values indicate that the VACV can permeate through the sclera once

released from the CL, as free drug in solution does. The accumulated drug values in the sclera were also quantified, being $137.35 \mu\text{g}/\text{cm}^2$ and $85.50 \mu\text{g}/\text{cm}^2$ for the aqueous solution and MIP_{1:12}, respectively (**Figure 4.13**). This means that imprinted hydrogels loaded with VACV can act as drug-release platforms, with the advantage of sustained release over aqueous solutions.

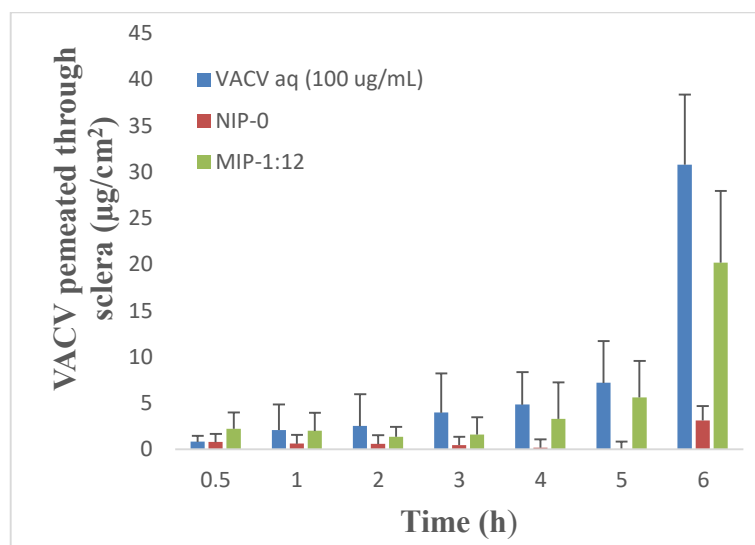


Figure 4.12. Amounts of VACV permeated through the sclera, administered through aqueous solution of VACV ($100 \mu\text{g}/\text{mL}$; blue bars), loaded in NIP₀ (red bars) or MIP_{1:12} (green bars) hydrogels.

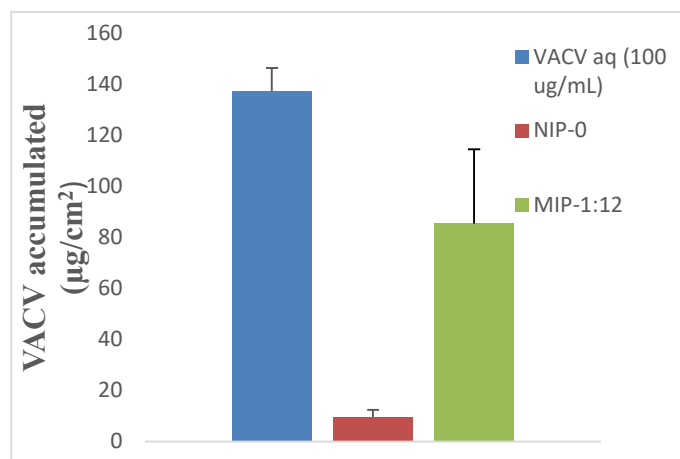


Figure 4.13. Amounts of VACV accumulated inside the sclera, administered through aqueous solution of VACV (100 µg/mL; blue bars), loaded in NIP₀ (red bars) or MIP_{1:12} (green bars) hydrogels.

4.4. Concluding remarks

Acyclovir and valacyclovir behaved differently when incorporated into HEMA-based hydrogels, despite their similar chemical structure and a priori similar binding energy with MAA. The limited solubility of ACV in the monomer mixture together with the weaker interactions through hydrogen bonding with the network may explain why ACV-imprinted hydrogels were not effective in terms of drug loading and release. Moreover, the small amount loaded was not completely released in SLF probably because the hydrophobicity of the drug. Differently, the use of MAA as functional monomer remarkably increased the affinity for VACV through electrostatic interactions between the acrylic acid group of the monomer and the drug lateral chain. The use of VACV as template during

polymerization facilitated the arrangement of the polymer network, creating specific cavities that contributed to enhance the drug's affinity for hydrogel in subsequent loading. The degree of swelling, light transmission and mechanical properties showed common values to daily wear contact lenses. In addition, no potential eye irritation was observed in HET-CAM assay. VACV-imprinted hydrogels can release drug in a sustained manner for 10 h which is a common time of wearing of disposable CL. At the sclera level, VACV-loaded hydrogels showed permeability values equivalent to those achieved for the aqueous solution of the drug, as well as therapeutically relevant amounts accumulated in sclera. VACV permeability through the sclera suggests the possibility of delivery to the posterior segment. Therefore, hydrogels containing MAA and imprinted with VACV are suitable candidates for the preparation of drug-eluting contact lenses.

4.5. References

Al-Ghabeish M., Xu X., Krishnaiah Y.S., Rahman Z., Yang Y., Khan M.A. 2015. Influence of drug loading and type of ointment base on the *in vitro* performance of acyclovir ophthalmic ointment. *Int J Pharm.* 495:783-791

Alvarez D.M., Castillo E., Duarte L.F., Arriagada J., Corrales N., Farias M.A., Henriquez A., Agurto-Munoz C., Gonzalez P.A. 2020. Current antivirals and novel botanical molecules interfering with herpes simplex virus infection. *Front Microbiol.* 11:139

Alvarez-Lorenzo C., Concheiro A. 2004. Molecularly imprinted polymers for drug delivery. *J Chromatogr B Analyt Technol Biomed Life Sci.* 804:231-245

Alvarez-Rivera F., Serro A.P., Silva D., Concheiro A., Alvarez-Lorenzo C. 2019. Hydrogels for diabetic eyes: naltrexone loading, release profiles and cornea penetration. *Mater Sci Eng C Mater Biol Appl.* 105:110092

Anand B.S., Mitra A.K. 2002. Mechanism of corneal permeation of L-valyl ester of acyclovir: targeting the oligopeptide transporter on the rabbit cornea. *Pharm Res.* 19:1194-1202

Austin A., Lietman T., Rose-Nussbaumer J. 2017. Update on the management of infectious keratitis. *Ophthalmology.* 124:1678-1689

Bhamra T.S., Tighe B.J. 2017. Mechanical properties of contact lenses: the contribution of measurement techniques and clinical feedback to 50 years of materials development. *Cont Lens Anterior Eye.* 40:70-81

Brady R.C., Bernstein D.I. 2004. Treatment of herpes simplex virus infections. *Antiviral Res.* 61:73-81

Brezani V., Lelakova V., Hassan S.T.S., Berchova-Bimova K., Novy P., Kloucek P., Marsik P., Dall'Acqua S., Hosek J., Smejkal K. 2018. Anti-Infectivity against Herpes Simplex Virus and selected microbes and anti-Inflammatory activities of compounds isolated from Eucalyptus globulus Labill. *Viruses.* 10(7):360

Byrne M.E., Park K., Peppas N.A. 2002. Molecular imprinting within hydrogels. *Adv Drug Deliv Rev.* 54:149-161

Esmann J. 2001. The many challenges of facial herpes simplex virus infection. *J Antimicrob Chemother.* 47 Suppl T1:17-27

Fatahzadeh M., Schwartz R.A. 2007. Human herpes simplex virus infections: epidemiology, pathogenesis, symptomatology, diagnosis, and management. *J Am Acad Dermatol.* 57:737-63; quiz 764-6

Hatanaka T., Haramura M., Fei Y.J., Miyauchi S., Bridges C.C., Ganapathy P.S., Smith S.B., Ganapathy V., Ganapathy M.E. 2004. Transport of amino acid-based prodrugs by the Na^+ - and Cl^- -coupled amino acid transporter $\text{ATB}^{0,+}$ and expression of the transporter in tissues amenable for drug delivery. *J Pharmacol Exp Ther.* 308:1138-1147

Hiratani H., Alvarez-Lorenzo C. 2002. Timolol uptake and release by imprinted soft contact lenses made of N,N-diethylacrylamide and methacrylic acid. *J Control Release.* 83:223-230

Kalezic T., Mazen M., Kuklinski E., Asbell P. 2018. Herpetic eye disease study: lessons learned. *Curr Opin Ophthalmol.* 29:340-346

Kang-Mieler J.J., Osswald C.R., Mieler W.F. 2014. Advances in ocular drug delivery: emphasis on the posterior segment. *Expert Opin Drug Deliv.* 11:1647-1660

Kapanigowda U.G., Nagaraja S.H., Ramaiah B., Boggarapu P.R., Subramanian R. 2016. Enhanced trans-corneal permeability of valacyclovir by polymethacrylic acid copolymers based ocular microspheres: *in vivo* evaluation of estimated pharmacokinetic/pharmacodynamic indices and simulation of aqueous humor drug concentration-time profile. *J Pharm Innov.* 11:82-91

Karsten E., Watson S.L., Foster L.J. 2012. Diversity of microbial species implicated in keratitis: a review. *Open Ophthalmol J.* 6:110-124

Kaye S., Choudhary A. 2006. Herpes simplex keratitis. *Prog Retin Eye Res.* 25:355-380

Kim S., Thiessen P. A., Bolton E. E., Chen J., Fu G., Gindulyte A., Han L., He J., He S., Shoemaker B. A., Wang J., Yu B., Zhang J., Bryant S. H. 2016. PubChem substance and compound databases. *Nucleic Acids Research.* 44, D1202–D1213

Koganti R., Yadavalli T., Shukla D. 2019. Current and emerging therapies for ocular herpes simplex virus type-1 infections. *Microorganisms.* 7:10.3390/microorganisms7100429

Kumar M., Hill J.M., Clement C., Varnell E.D., Thompson H.W., Kaufman H.E. 2009. A double-blind placebo-controlled study to evaluate valacyclovir alone and with aspirin for asymptomatic HSV-1 DNA shedding in human tears and saliva. *Invest Ophthalmol Vis Sci.* 50:5601-5608

Kumar M., Kaufman H.E., Clement C., Bhattacharjee P.S., Huq T.S., Varnell E.D., Thompson H.W., Hill J.M. 2010. Effect of high versus low oral doses of valacyclovir on herpes simplex virus-1 DNA shedding into tears of latently infected rabbits. *Invest Ophthalmol Vis Sci.* 51:4703-4706

Kumar R., Sinha V.R. 2017. Lipid nanocarrier: an efficient approach towards ocular delivery of hydrophilic drug (valacyclovir). *AAPS PharmSciTech.* 18:884-894

Lloyd J., Copaciu R., Yahyabeik A., DeWit C., Cummings K., Lacey M., Su Q. 2019. Characterization of polyclonal antibodies to herpes simplex virus types 1 and 2. *J Histotechnol.* 42:202-214

Morris G. M., Huey R., Lindstrom W., Sanner M. F., Belew R. K., Goodsell D. S., Olson A. J. 2009. AutoDock4 and AutoDockTools4: Automated Docking with Selective Receptor Flexibility. *J Comput Chem.* 30(16):2785–2791

OECD, Test No. 437: Bovine Corneal Opacity and Permeability Test Method for Identifying Ocular Corrosives and Severe Irritants. 2009 (accessed Jun 2020)

Palacios M.L., Demasi G., Pizzorno M.T., Segall A.I. 2005. Validation of an HPLC method for the determination of valacyclovir in pharmaceutical dosage. *J Liq Chromatogr Rel Technol.* 28:751-762

Rajasagi N.K., Rouse B.T. 2018. Application of our understanding of pathogenesis of herpetic stromal keratitis for novel therapy. *Microbes Infect.* 20:526-530

Tranoudis I., Efron N. 2004. Tensile properties of soft contact lens materials. *Cont Lens Anterior Eye.* 27:177-191

Tsatsos M., MacGregor C., Athanasiadis I., Moschos M.M., Hossain P., Anderson D. 2016. Herpes simplex virus keratitis: an update of the pathogenesis and current treatment with oral and topical antiviral agents. *Clin Exp Ophthalmol.* 44:824-837

Volpato N.M., Santi P., Laureri C., Colombo P. 1997. Assay of acyclovir in human skin layers by high-performance liquid chromatography. *J Pharm Biomed Anal.* 16:515-520

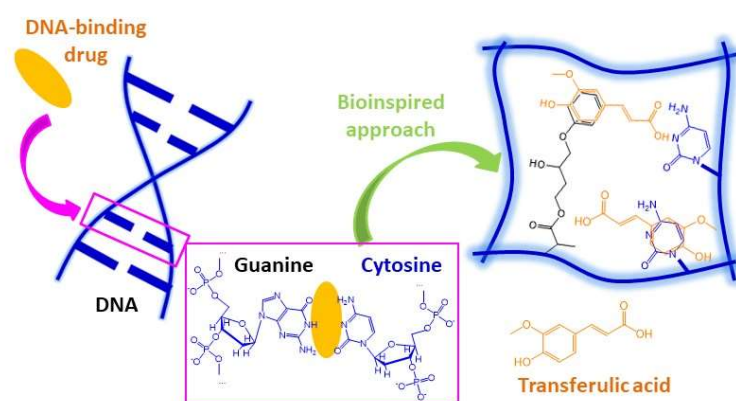
Whitley R.J., Roizman B. 2001. Herpes simplex virus infections. *Lancet*. 357:1513-1518

Wilhelmus K.R. 2015. Antiviral treatment and other therapeutic interventions for herpes simplex virus epithelial keratitis. *Cochrane Database Syst Rev*. 1:CD002898

Zambrano A., Solis L., Salvadores N., Cortes M., Lerchundi R., Otth C. 2008. Neuronal cytoskeletal dynamic modification and neurodegeneration induced by infection with herpes simplex virus type 1. *J Alzheimers Dis*. 14:259-269



Cytosine-functionalized bioinspired hydrogels for ocular delivery of antioxidant transferulic acid





5. Cytosine-functionalized bioinspired hydrogels for ocular delivery of antioxidant transferulic acid

5.1. Introduction

Delivery of drugs to the eye structures is still a quite challenging task. The complex anatomy and physiology of the eye limit the access of drugs when they are administered through a systemic route (e.g. orally), and also when topical administration is chosen (*Srinivasarao et al., 2018*). In spite of being one of the most exposed organs, the privileged protection system of the eye readily clears the drug from the ocular surface through different mechanisms, such as blinking and nasolacrimal drainage. Cornea structure is also a formidable barrier for the access of the drug into the inner eye structures (*Awwad et al., 2017*). All these hurdles compromise the efficacy of conventional pharmacological treatments, especially eye drops (*Yellepeddi et al., 2016*).

A wide variety of drug delivery strategies are being developed to improve topical ocular therapy, ranging from in situ gelling formulations to engineered nanocarriers (*Ribeiro et al., 2012; Bravo-*

Osuna et al., 2016; Imperiale et al., 2018). In this regard, the use of contact lenses (CLs) as drug delivery platforms has received a great deal of attention (*Gonzalez-Chomon et al., 2013; Tieppo et al., 2014*). CLs are used worldwide by millions of people to correct optical problems. Therefore, their biocompatibility with the eye surface during prolonged periods of time has been largely demonstrated. Thus, if CLs could be endowed with ability to host drugs and release them in a sustained way on the ocular surface, they could act as therapeutic ocular bandages that favor drug accumulation in the post-lens lacrimal, increasing drug diffusion rate into cornea and sclera (*Gause et al., 2016*). Regrettably, common components (monomers) of CLs lack of affinity for most ocular drugs and thus the amounts loaded may be insufficient and the release rate too fast (*Hui et al., 2017*). To overcome this problem, encapsulation of drugs into nanocarriers or films to be added to the CLs matrix, coating of the CLs with hydrophobic/erodible layers capable of regulating drug release, and application of the molecular imprinting technology may help improving the therapeutic performance (*Alvarez-Rivera et al., 2018; Lee et al., 2018; Ross et al., 2019; Ubani-Ukoma et al., 2019*). Bioinspired strategies have been shown to be particularly useful for the identification of monomers that can endow CLs with affinity for a given drug (*Alvarez-Lorenzo et al., 2019*). Efficient bioinspired approaches rely on mimicking the receptors for the drug in our body, creating ad hoc artificial receptors in the CLs matrix. Namely, most

commercially available drugs have been designed for selective and reversible interaction with a target structure in human cells. Such drug-target binding is responsible for the inhibition/activation of a biochemical process, which triggers the pharmacological effect. Well-conformed artificial receptors can be obtained by mimicking the components of the site where the drug has to fit into the physiological receptor and their conformation in the space. Applying this strategy, CLs with affinity for anti-allergic drugs, carbonic anhydrase inhibitors, epalrestat and hyaluronic acid have been obtained by recreating, respectively, the physiological histamine H1-receptor, (Tieppo *et al.*, 2012; Gonzalez-Chomon *et al.*, 2016) the carbonic anhydrase active site, (Ribeiro *et al.*, 2011; Ribeiro *et al.*, 2011) the aldose reductase binding site, (Alvarez-Rivera *et al.*, 2018) or the hyaluronic acid binding protein CD44 (Ali *et al.*, 2009).

In most cases, the recreation of the biomimetic receptor requires the drug molecules to be added to the mixture of backbone monomers (main constituents of the CLs) and functional monomers, i.e., those with chemical groups that resemble the amino acids of the physiological receptor. It is expected that the drug molecules act as templates during polymerization facilitating the adequate spatial configuration of the monomers. After polymer synthesis the template drug molecules are removed to reveal the biometric receptors. This molecular imprinting technology is adequate for drugs that can withstand the polymer synthesis conditions. However, there are some

active substances that do not only degrade during polymerization but that can even hinder the polymerization itself (*Kadoma et al., 2008*). This is the case of efficient antioxidants that interfere with the production of free radicals for polymer synthesis. Therefore, there is an unmet need of developing CLs that can act as platforms for sustained release of antioxidants. Antioxidants are receiving increasing attention for the prevention and/or treatment of several age-related and light-induced eye diseases (*Bungau et al., 2019*). Topical administration of antioxidants was demonstrated to relieve symptoms of glaucoma, diabetic cataracts, retinal photodeterioration, dry eye syndrome and photorefractive keractomy, and it may even protect the eye from anti-inflammatory drug-induced cataracts (*Kojima et al., 2002; Engin, 2009; Ribeiro et al., 2013*).

The aim of this work was to develop a bioinspired strategy for the design of hydrogels suitable as CLs that can uptake large amounts of antioxidants. Many active substances, such as the vast majority of cytostatic agents and relevant antimicrobials and antivirals, owe their therapeutic action to their ability to interact with the nucleotides that build up DNA and RNA (*Agudelo et al., 2016; Sadeghi et al., 2016*). Thus, the five nitrogenous bases adenine (A), uracil (U), guanine (G), thymine (T), and cytosine (C) have been identified as target sites for a variety of drugs. Nevertheless, the use of the nitrogenous bases as functional monomers in artificial receptors has been barely explored. Monomers of cytosine have been prepared to endow acrylic polymers

with improved adhesion properties (Zhang *et al.*, 2016) and to provide polysaccharides with fluorescent capabilities (Oza *et al.*, 2012). Only recently, the nitrogenous bases have been proposed as components of traps of palladium ions for removal from aqueous medium (Yoshikawa *et al.*, 2008) and of carriers for the antiviral drug acyclovir (Roleira *et al.*, 2015). Drug binding to nitrogenous bases usually occurs through cooperative effects of hydrogen bonding and π - π stacking interactions (Pan *et al.*, 2018). Therefore, the present work relies on the hypothesis of that cytosine may act as binding monomer for antioxidants having complementary chemical structure in terms of hydrogen bonding and π - π stacking ability, which in turn should endow cytosine-functionalized CLs with capability to host and release antioxidant agents (**Figure 5.1**).

This hypothesis was challenged against transferulic acid (TA) or 4-hydroxy-3-methoxycinnamic acid (**Figure 5.1**), which is one of the smallest and more potent natural antioxidant agents (Srinivasan *et al.*, 2007). It is abundant in vegetables and medicinal herbs, e.g. *Angelica sinensis*, *Cimicifuga heracleifolia* and *Lignsticum chuangxiong* (Trombino *et al.*, 2013). TA is more easily absorbed into the body and stays in the blood longer than any other phenolic acid, although its oral bioavailability is still below 20% with a C_{max} of 2-3 μ M (Mancuso *et al.*, 2014). In addition to their very low toxicity, TA is very efficient scavenger of both reactive oxygen species (ROS) and reactive nitrogen species (RNS) and it up-regulates cytoprotective

systems (*Trombino et al., 2013; Mancuso et al., 2014*). A variety of systemic therapeutic effects have been claimed for TA, including inhibition of vascular smooth muscle cell proliferation and migration (*Hou et al., 2004; Zdunska et al., 2018*). In the ocular field, TA has demonstrated capability to accelerate cornea wound healing (*Tsai et al., 2016*) and to suppress amyloid β production in human lens (*Nagai et al., 2017*). To carry out the work, hydrogels were prepared from mixtures of 2-hydroxyethyl methacrylate (HEMA), glycidyl methacrylate (GMA) and ethyleneglycolphenylether methacrylate (EGPEM) (**Figure 5.1**). GMA was used as bridge to immobilize cytosine after hydrogel synthesis, while EGPEM was added to reinforce hydrophobic interactions with TA. Interestingly, nucleotide-like monomers and monomers similar to EGPEM have been shown to form molecular clefts with two convergent binding arms having in between a space suitable for host-guest interactions (*Roleira et al., 2015; Mbarek et al., 2019*). Then, the hydrogels were characterized in terms of suitability for CLs and capability to host TA and sustain its release in lacrimal fluid while maintaining the antioxidant activity. Finally, as a proof of concept, bioinspired TA-loaded CLs were evaluated *ex vivo* regarding TA accumulation and permeability in cornea and sclera and compared to the non-bioinspired ones. In terms of safety, it should be noted that purines and pyrimidines (e.g. cytosine) have shown therapeutic potential in dry eye treatment and wound healing, and therefore if any non-grafted cytosine would

remain in the hydrogel, non-toxic effects on the eye structures are expected (Gendaszewska-Darmach *et al.*, 2011; Guzman-Aranguez *et al.*, 2014).

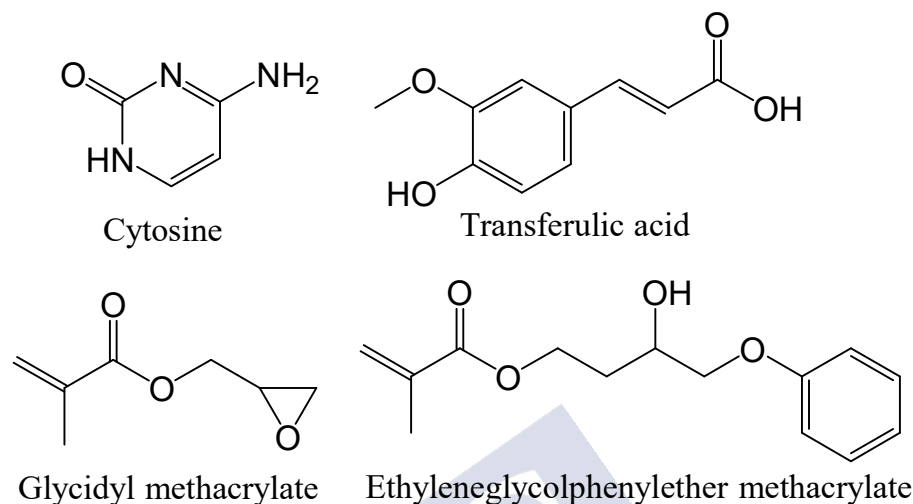


Figure 5.1. Structure of cytosine, transferulic acid and monomers used in the hydrogel synthesis.

5.2. Materials and methods

5.2.1. Materials

Transferulic acid (TA) was purchased from AlfaAesar (Kandel, Germany). Ethyleneglycol dimethacrylate (EGDMA), glycidyl methacrylate (GMA), ethyleneglycolphenylether methacrylate (EGPEM), 2,2'-azo-bis(isobutyronitrile) (AIBN), dichlorodimethylsilane, cytosine, 2,2'-azobis(2-amidino-propane) dihydrochloride (AAPH) and Trolox were from Sigma-Aldrich (Steinheim, Germany). 2-Hydroxyethyl methacrylate (HEMA) was

from Merck (Darmstadt, Germany); chloroform and NaCl were from Scharlau (Barcelona, Spain); 1,4-dioxan was from Panreac (Barcelona, Spain); and NaOH from VWR (Leuven, Belgium). Ultrapure water (resistivity $> 18 \text{ M}\Omega \cdot \text{cm}$) was obtained by reverse osmosis (MilliQ®, Millipore Spain). Simulated lacrimal fluid (SLF) was prepared with the following composition: 6.78 g/L NaCl, 2.18 g/L NaHCO_3 , 1.38 g/L KCl and 0.084 g/L $\text{CaCl}_2 \cdot 2\text{H}_2\text{O}$ with pH 7.5 (see section 3.2.1).

5.2.2. Hydrogel synthesis

Hydrogels were prepared from monomers mixtures summarized in **Table 5.1**. EGDMA (8 mM), GMA (0, 100, 200, 400 or 600 mM) and EGPEM (0, 100 or 200 mM) were added to HEMA and the mixtures were maintained under magnetic stirring (300 rpm; RT 20-23 °C) for 15 min. AIBN (10 mM) was then added and the mixtures were magnetically stirred for 15 min. Finally, each solution was injected into pre-assembled moulds (using needle and syringe) which consisted of two pre-treated glass plates (10x10 cm), separated by a silicone frame of 0.45 mm thickness and fixed with metal clips. Glass plates were treated by soaking (a few seconds) in 200 mL of dichlorodimethylsilane solution (2% v/v in chloroform) and dried at RT (20-23 °C) overnight inside a hood. Then, they were placed into an oven at 70 °C for 2 h and washed with soap (phosphates free) and milliQ water, and dried at 70 °C for 2 h. Monomers polymerization

was carried out at 50 °C for 12 h and then at 70 °C for 24 h more. All hydrogel compositions were prepared at least in duplicate.

Table 5.1. Composition of the hydrogels. In all cases, AIBN (9.85 mg) was added after monomers mixing.

Hydrogel	HEMA (mL)	EGDMA (μL)	GMA (μL)	EGPEM (μL)
G0E0	8	12.1	0	0
G0E100	8	12.1	0	150
G100E0	8	12.1	110	0
G100E100	8	12.1	110	150
G0E200	8	12.1	0	300
G200E0	8	12.1	220	0
G200E200	8	12.1	220	300
G400E0	8	12.1	430	0
G400E200	8	12.1	430	300
G600E0	8	12.1	640	0
G600E200	8	12.1	640	300

5.2.3. Functionalization with cytosine

After polymerization, synthesized hydrogels were functionalized with cytosine adapting a previously reported protocol (**Figure 5.2**) (Yoshikawa *et al.*, 2008). One sheet of each type of hydrogel was immersed in 100 mL of a water:dioxane (1:1) mixture and then 1.11 g of cytosine was added. The container was hermetically closed and kept in an orbital agitator bath (30 osc/min) at 80 °C for 24 h. In parallel, other hydrogel sheet was subjected to the same treatment, but without addition of cytosine. After functionalization, the hydrogels were cut into discs (10 mm in diameter) with a punch and washed in milliQ water (1 L) under magnetic stirring (200 rpm), changing the

medium every 24 h, until the absence of monomers. Finally, the discs were dried at 50 °C for 24 h.

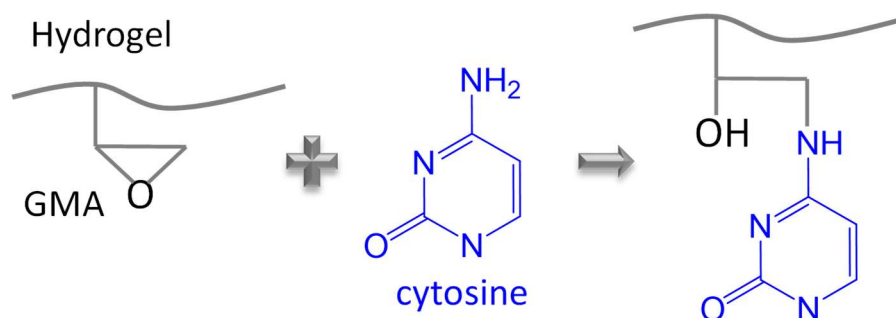


Figure 5.2. Scheme of the reaction between the GMA mers in the hydrogel and cytosine molecules.

5.2.4. Hydrogels characterization

5.2.4.1. FTIR-ATR analysis

The spectra were recorded in a FTIR Varian model 670-IR equipped with a PIKE GladiATR Diamond Crystal Attenuated Total Reflectance accessory. 64 scans were recorded and a resolution of 4 cm⁻¹.

5.2.4.2. Elemental analysis

Elemental analysis was recorded in a Fisons EA 1108 equipment (Italy).

5.2.4.3. Swelling degree

The degree of swelling was monitored in water and SLF for each type of hydrogel in triplicate, at room temperature (RT, 20-23 °C). The discs were weighed and placed into vials with 4 mL of water or

SLF, and the weight increase was recorded at pre-established times. In each measurement, the disc was removed from the vial, the surface was blotted with filter paper, and the disc was weighed and returned to the vial. Swelling degree was calculated as follows:

$$\text{Swelling degree (\%)} = \frac{W_t - W_0}{W_0} \cdot 100 \quad [\text{Eq. 5.1}]$$

where W_0 and W_t represent the weight of the dry and swollen disc, respectively.

5.2.4.4. Light transmittance

Light transmittance (%) of discs swollen in water and in SLF was measured, in triplicate, from 190 to 800 nm in a UV-Vis spectrophotometer (Agilent 8453, Germany).

5.2.4.5. Mechanical properties

Swollen G0E0-0, G400E200-0 and G400E200-C hydrogels were tested in quadruplicate at RT. Each hydrogel (strips of 16x9 mm) was fixed to the upper and lower clamps with a gap of 4 mm in a TA.XT Plus Texture Analyzer (Stable Micro Systems, Ltd., UK) fitted with a 30 Kgf load cell. The stress-strain plots were recorded at a crosshead speed of 0.1 mm/s. Young's modulus, E , was calculated from the slope of the straight line portion of the tensile strength (force per cross-sectional area) versus the engineering strain (the change in active length divided by the original length), as follows (*Tranoudis et al., 2004; Bhamra et al., 2017*):

$$E = \frac{F/A_0}{\Delta L/L_0} \quad [\text{Eq. 5.2}]$$

5.2.5.TA loading

Dry discs of each type of hydrogel were weighed in triplicate and placed in Eppendorf tubes containing 5 mL of aqueous solution of TA (0.01 mg/mL) prepared with 0.05% EDTA, as a solution stabilizer. The tubes were kept under orbital shaking (300 rpm) at 25 °C. The amount of TA loaded was determined spectrophotometrically (UV-Vis Agilent 8453, Germany) at 320 nm at 0.5, 1, 2, 4, 6, 8, 24 and 48 h. At each time point, 2.5 mL of sample were removed, the absorbance measured in the spectrophotometer and the sample returned to the vial. The amount of TA loaded was estimated from the difference between the initial and final amount of TA in the solution, using a previously validated calibration curve.

The network/water partition coefficient ($K_{N/W}$) of TA was calculated using the following equation (*Alvarez-Rivera et al., 2018*):

$$Amount\ loaded = \left(\frac{V_s + K_{N/W} * V_p}{W_p} \right) * C_0 \quad [Eq. 5.3]$$

where V_s is the volume of water sorbed by the hydrogel, V_p the volume of dried polymer, W_p the weight of dry hydrogel and C_0 the concentration of the drug in the loading solution.

5.2.6.TA release

TA-soaked discs were rinsed with water, blotted with filter paper, and placed in vials with 5 mL of SLF. The vials were kept under orbital shaking (300 rpm) at 35 °C. At pre-established times (0.5, 1, 2, 4, 6, 8 and 24 h) 2.5 mL were taken from the release medium, the

absorbance was measured at 320 nm (UV-Vis Agilent 8453, Germany) and the sample returned to the corresponding vial. The amounts released were calculated multiplying the concentrations by the volume, and the values were referred to the initial weight of each hydrogel disc.

5.2.7. HET-CAM test

The Hen's Egg Test on Chorio-Allantoic Membrane (HET-CAM) was carried out as a preliminary biocompatibility test as previously described (*Alvarez-Rivera et al., 2016*). Briefly, fertilized eggs were incubated for 9 days and then a circular cut (ca. 1 cm in diameter) was made in the shell of the egg with a rotary saw (Dremel 300, Breda, The Netherlands). The CAM was exposed, and one hydrogel disc was carefully placed on it. The discs were previously loaded with TA as described above. 0.9% NaCl and 0.1 N NaOH solutions were used as negative and positive controls, respectively. Hemorrhage, vascular lysis and coagulation of CAM vessels were monitored for 5 min.

5.2.8. Cytocompatibility assay

In vitro cytocompatibility of G0E0-0, G400E200-0 and G400E200-C hydrogels was evaluated against Human Corneal Epithelial Cells (HCEC; ATCC® PCS-700-010™). The cell line was cultured in Keratinocyte-Serum Free medium (Gibco, UK), supplemented with hydrocortisone (500 ng/mL), insulin (5 ug/mL), penicillin/streptomycin 1% and antifungal 1%, prior treatment of the flask with a Fibronectin-BSA-Bovine collagen I coating solution.

HCEC (20,000 cells/well) were seeded in 48-well plate in Keratinocyte-Serum Free medium and grown for 24 h at 37 °C (95% RH and 5% CO₂). Discs were loaded for 24 hours in a solution of TA 10 µg/mL, cut in four pieces, and then sterilized in autoclave (steam heat) in the same solution, at 121 °C during 15 min. Then, one disc piece was placed in each well during 24 h. Aqueous drug solution (10 µg/mL) was also added in triplicate (previous sterilization) and negative controls included cells without treatment. After 24 h in cell culture, discs and drug solution were removed from the wells, and cell viability assay was carried out following manufacturer instructions using WST-1 (Roche, Switzerland). Absorbance was read at 450 nm (UV Bio-Rad Model 680 microplate reader, USA). Cell viability (%) was calculated as follows:

$$Cell\ viability(\%) = \frac{Abs_{exp}}{Abs_{negative\ control}} \cdot 100 \quad [Eq. 5.4]$$

5.2.9. Antioxidant activity

The antioxidant activity of non-loaded and TA-loaded G400E200-0 and G400E200-C hydrogels was measured using the ORAC (oxygen radical antioxidant capacity) test (*Lucas-Abellan et al., 2011*) with some modifications. TA-loaded hydrogels (soaked in 5 mL of 10 µg/mL TA solution for 48 h) and non-loaded hydrogels were placed in 5 mL of SLF during 6 h. Aliquots (70 µL) were then removed from each vial for the antioxidant activity assay. To minimize assay read time the sodium fluorescein (ACROS organic, Belgium), and AAPH concentrations were optimized to ensure the reactions were completed.

A solution of fluorescein (3 μM) was prepared in 75 mM sodium phosphate buffer (pH 7.4). A 96-well flat-bottomed black plate was used and each sample (70 μL) was deposited in triplicate in the wells of the microplate, with 100 μL of the fluorescein solution. A blank was prepared with fluorescein (100 μL) and SLF (70 μL). Also, eight calibration solutions using Trolox (10, 20, 30, 40, 50, 60, 70 and 80 μM , in SLF) as antioxidant (70 μL) were tested in parallel. The mixtures were pre-incubated for 30 min at 37 $^{\circ}\text{C}$ and then 30 μL of AAPH solution (final concentration 40 mM in SLF) was quickly added using a multichannel pipette. A negative control was also prepared with fluorescein and SLF (without AAPH). The fluorescence was recorded every 2 min for 120 min ($\lambda_{\text{exc}} = 485 \text{ nm}$, $\lambda_{\text{em}} = 520 \text{ nm}$) in an OPTIMA FLUOstar microplates reader (BMG Labtech, USA). Only the 60 inner wells were used in order to avoid a temperature effect; the outer rows were filled with 200 μL of distilled water.

5.2.10. Cornea and sclera penetration and accumulation

TA permeability tests were carried out with TA-loaded G400E200-0 and G400E200-C hydrogels as well as a TA aqueous solution (10 $\mu\text{g/mL}$), using bovine cornea and sclera according to a previously described protocol (see section 3.2.6). The eyes were provided by a local slaughterhouse and transported immersed in PBS supplemented with antibiotics (penicillin 100 IU/mL and streptomycin 100 $\mu\text{g/mL}$), in an ice bath. In each eye either the sclera or the cornea (leaving 2-3 mm of surrounding sclera) was isolated using a scalpel.

The tissues were washed with PBS before being mounted on vertically diffusing Franz cells. In order to balance the tissues, the donor and recipient chambers were filled with carbonate buffer pH 7.2, and then placed in a water bath at 37 °C, for 30 min under magnetic stirring. Subsequently, the volume of the entire donor chamber was removed and replaced by the test samples (in triplicate): 2 mL of aqueous solution of TA (10 µg/mL), or G400E200-0 discs and G400E200-C discs immersed in 2 mL of 0.9% NaCl. The area available for permeation was 0.785 cm². The chambers were covered with parafilm to prevent evaporation. At preset time (1, 2, 3, 4, 5 and 6 h) 1 mL of sample was removed from the receptor chamber and replaced with the same volume of carbonate buffer, taking care to remove any bubble from the diffusion cells.

The permeated TA was quantified by HPLC (Waters 717 Autosampler, Waters 600 Controller, 996 Photodiode Array Detector), equipped with a C18 column (Waters Symmetry C18, 5 µm, 4.6×250 mm) and operated with Empower2 software. The mobile phase was methanol:acetonitrile:phosphate buffer (20:15:65) at 1 mL/min and 35 °C. The buffer was prepared with KH₂PO₄ 0.68 g/L adjusted with phosphoric acid solution to pH 3.0–3.1. The injection volume was 50 µL and TA was quantified at 320 nm (retention time 5 min). The standard solutions were 0.009–10.0 µg/mL of TA in carbonate buffer. The cumulative amounts of permeated TA per area vs time were adjusted for linear regression, and the steady state flow (J) and delay

time (t_{lag}) were obtained from the slope and x-intercept of the linear regression, respectively (Al-Ghabeish *et al.*, 2015).

After 6 hours of testing, a sample of the donor chamber was taken for further analysis. In addition, the corneas and sclera were visually examined to ensure that they were not damaged during the assay. The corneas and sclera were subsequently placed in 3 mL of an ethanol:water solution (50:50 v/v) overnight, sonicated for 99 min at 37 °C, centrifuged (1000 rpm, 5 min, 25 °C), filtered and centrifuged again (14000 rpm, 20 min, 25 °C) (Volpato *et al.*, 1997). The coefficient of permeability of the drug through the cornea and sclera was calculated as the ratio of J and the concentration of TA in the donor chamber (Al-Ghabeish *et al.*, 2015).

5.3. Results and discussion

5.3.1. Hydrogels synthesis and cytosine grafting

A set of hydrogels was prepared by combining GMA and EGPEM at various proportions as summarized in **Table 5.1**. The hydrogels were coded as GxEy, where x represented the content in GMA in mM and y corresponded to the content in EGPEM in mM in the monomers mixture. G0E0 hydrogels were prepared without any functional monomer to be used as controls. Cytosine monomer was not prepared because of the many steps required for the process, which may alter its structure, (Zhang *et al.*, 2016) and also to avoid structural changes in the HEMA hydrogels that could compromise their subsequent use as CLs. Thus, differently, GMA was added to the monomers mixture for

the post-synthesis grafting of cytosine. GMA is known to react through the glycidyl group with molecules bearing hydroxyl or amine functionalities (*dos Santos et al., 2009*). The protocol for the reaction of cytosine with pendant GMA mers was adapted from a previously reported one, using cytosine in excess (*Yoshikawa et al., 2008*). Some hydrogels were prepared with EGPEM monomer to gain an insight into the possibility of reinforcing the binding of TA by forming artificial receptors that resemble molecular clefts of Rebek (*Mbarek et al., 2019; Roleira et al., 2015*). Cooperative binding of TA could occur if cytosine and EGPEM are placed at the adequate distance, which in turn depends on their proportion in the hydrogel network. Preliminary elucidation of cytosine-TA interactions by means of AutoDock software confirmed the feasibility of hydrogen bonds and hydrophobic interactions (**Figure 5.3**).

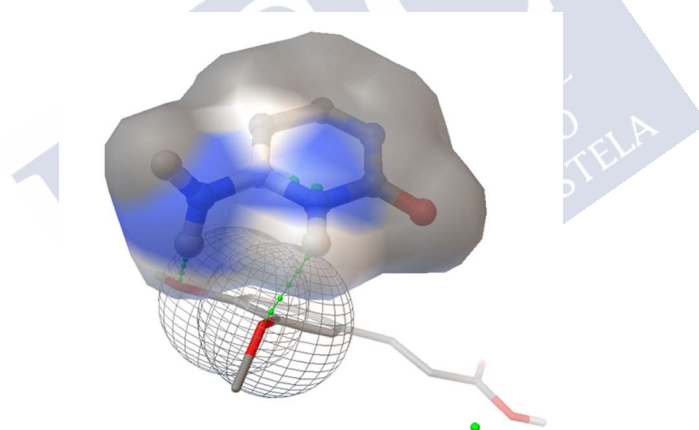


Figure 5.3. AutoDock modeling of cytosine-TA interactions (AutoDock 4.2; The Scripps Research Institute, La Jolla, CA, USA). Estimated free energy of binding - 2.21 Kcal/mol.

5. Cytosine-functionalized bioinspired hydrogels for ocular delivery of antioxidant transferulic acid

Grafting of cytosine to the hydrogels was confirmed by visualization under UV light (366 nm, **Figure 5.4**) since cytosine is highly fluorescent (*Oza et al., 2012*). Pictures of the same hydrogel discs under white light (upper panel) and UV light (lower panel) clearly revealed the presence of cytosine in those prepared with GMA and functionalized with cytosine. Relevantly, the intensity increased with the content in GMA.

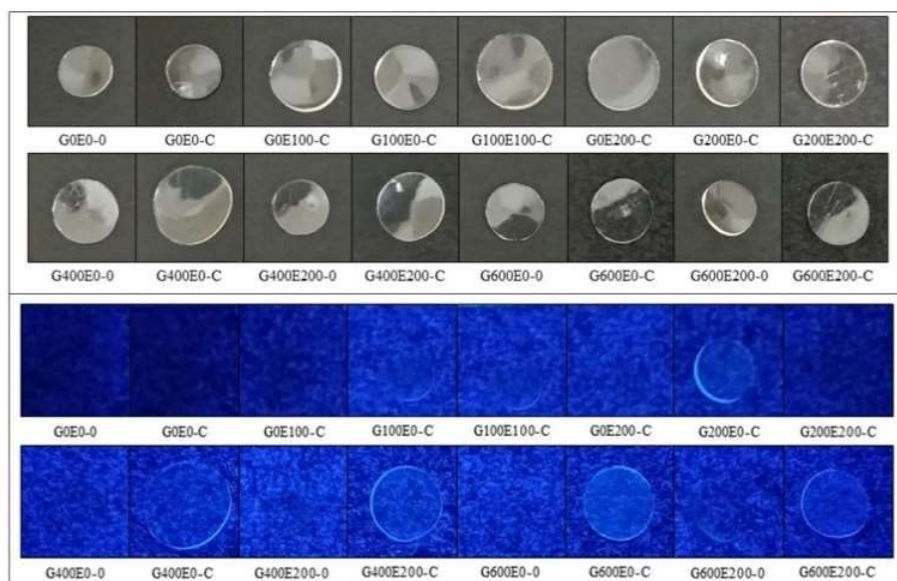


Figure 5.4. Pictures of the hydrogels under white light (upper panels) and UV light (lower panels). Codes (as in **Table 5.1**) ended in 0 identify hydrogels that were processed in the absence of cytosine, while those ended in C referred to hydrogels treated with cytosine.

FTIR-ATR spectra of the hydrogels showed the bands typical of polyHEMA networks (**Figure 5.5**) (*Jantas et al., 2010*). The presence of GMA mers was evidenced by the characteristic adsorption peaks at

906 cm^{-1} , 850 cm^{-1} and 692 cm^{-1} due to stretching vibrations of the epoxide ring (Yang *et al.*, 2012). Moreover, the grafting of cytosine was confirmed by the strong band at 1655 cm^{-1} of its amide carbonyl group (Oza *et al.*, 2012). Elemental analysis revealed reaction yields of about 26%; that is, G400E200-C hydrogels had 0.375 %N instead of the theoretical 1.413 %N, which means that this hydrogel contains 0.088 mmol cytosine per gram instead of expected 0.346 mmol/g if every GMA mer reacted with one cytosine molecule. This yield indicates that cytosine was not only grafted at the surface but also inside the hydrogel.

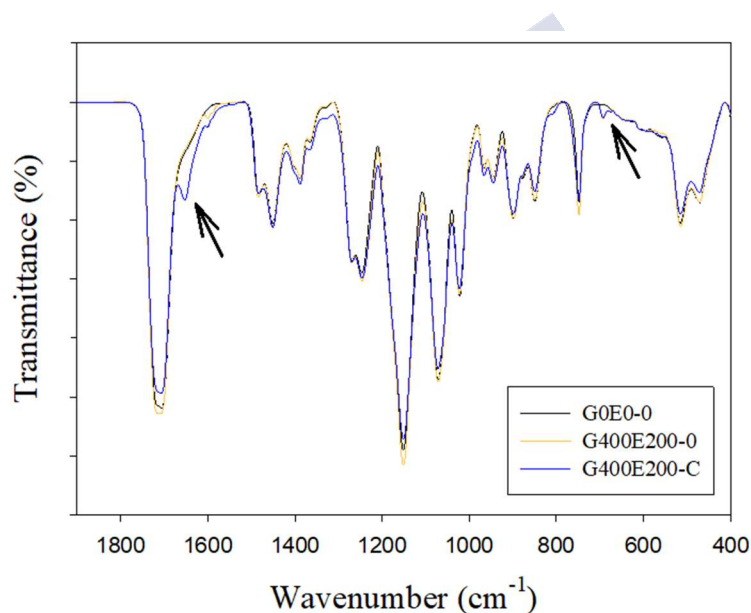


Figure 5.5. FTIR-ATR spectra of G0E0-0, G400E200-0 and G400E200-C hydrogels. The arrows correspond to 692 and 1655 cm^{-1} .

5.3.2. Swelling, light transmission and mechanical properties

Swelling of the discs was evaluated both in water and SLF, obtaining similar results (**Figure 5.6**).

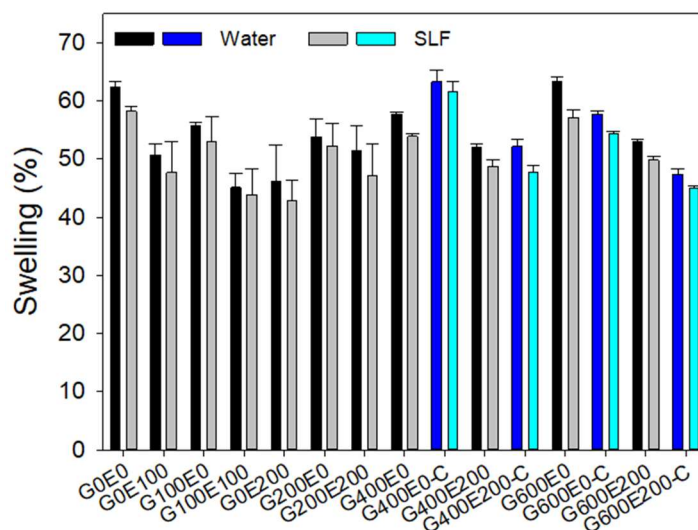


Figure 5.6. Swelling degree in water and in simulated lacrimal fluid (SLF) of hydrogels before (black and grey bars, respectively) and after (dark blue and light blue bars, respectively) functionalization with cytosine ($n=3$; mean values and standard deviation).

All discs sorbed water rapidly and the swelling equilibrium was reached in one hour. Those hydrogels prepared with EGPEM (hydrophobic monomer) had lower swelling degree although still above 45%, which means that all hydrogels are suitable for hydrophilic contact lenses. Swollen discs showed excellent light transmission properties (**Figure 5.7**). Functionalization with cytosine made the hydrogels to absorb more in the UV range, which may help to protect the eye from harmful radiation. All hydrogels fulfil the

requirement of having transmittance values above 90% in the visible range.

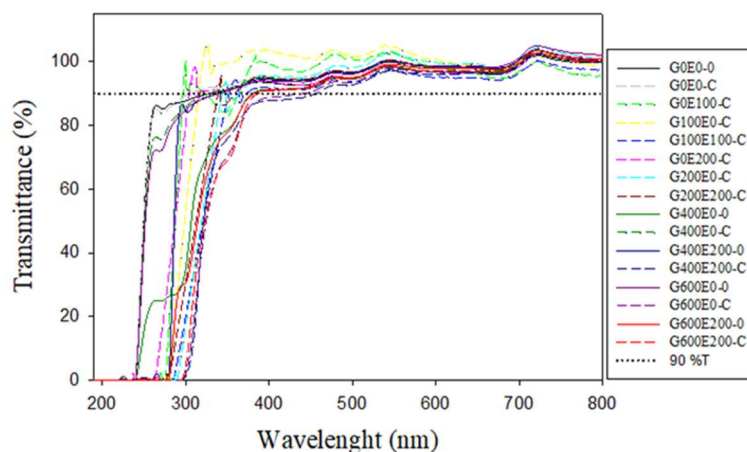


Figure 5.7. Light transmittance patterns recorded for hydrogel discs before (continuous lines) and after (dashed lines) functionalization with cytosine after swelling in SLF. Acceptance value of 90% transmittance is shown as a dotted line.

Regarding mechanical properties, the tensile strength tests revealed that G400E200-0 and G400E200-C had Young's Modulus (0.50, s.d. 0.03 MPa and 0.56, s.d. 0.06 MPa) larger than those recorded for control G0E0 hydrogels (0.43, s.d. 0.02 MPa) (statistically significant differences; ANOVA F2,6d.f. =10.8; $p < 0.05$). In any case these values are in the range of those typical of hydrophilic contact lenses and the differences are not expected to have clinical repercussion (Tranoudis *et al.*, 2004; Bhamra *et al.*, 2017).

5.3.3. TA loading

Hydrogel discs were soaked in TA aq. solution and the amount uptaken was monitored for 48 h (**Figure 5.8**).

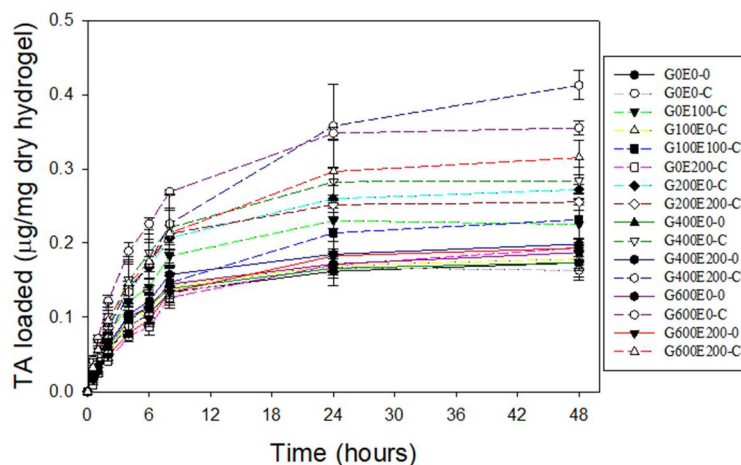


Figure 5.8. Amount of TA loaded by hydrogel discs before (continuous lines) and after (dashed lines) functionalization with cytosine during soaking in a 5 mL of aqueous solution of TA (0.01 mg/mL) prepared with 0.05% EDTA, at 25 °C. Mean values and standard deviations ($n=3$).

Total amount loaded is shown in **Figure 5.9**. Non-functionalized hydrogels completed the loading in the first 8 h, while the functionalized hydrogels continued the sorption for 24 h. The hydrogels that exhibited the highest loading were G400E200-C and required 48 h to complete the loading. These findings indicated that TA was hosted not only in the aqueous phase of the hydrogel (the swelling equilibrium was reached in 1 h) but also through specific interactions with the network.

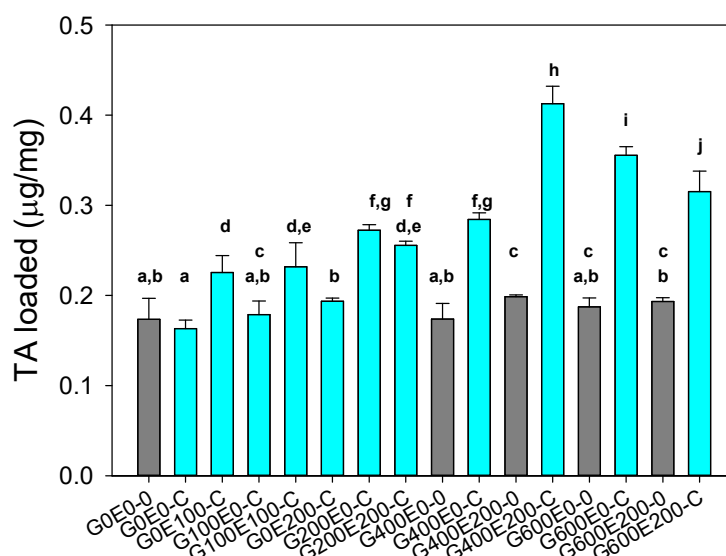


Figure 5.9. Total amount of TA loaded by the hydrogels after 48 h soaking in a 5 mL of aqueous solution of TA (0.01 mg/mL) prepared with 0.05% EDTA, at 25 °C. Mean values and standard deviations (n=3). The data were statistically compared (ANOVA $p < 0.001$; multiple range test $p < 0.001$). Equal letter denotes homogenous groups. Grey bars correspond to hydrogels without cytosine (codes ending in 0), while light blue bars refer to hydrogels functionalized with cytosine (codes ending in C).

Compared to the hydrogels prepared without functional monomers that were used as reference before (G0E0-0) and after (G0E0-C) treatment with cytosine, no improvement in TA loading was recorded for hydrogels synthesized with GMA and/or EGPEM before functionalization with cytosine. Also, hydrogels prepared with the lowest content in GMA 100 mM and functionalized with cytosine (G100E0-C) did not show improvements. Differently, the incorporation of higher GMA proportions and the combination with

EGPEM increased two to three times the loading (ANOVA, $F_{15,32df} = 73.59$; $p < 0.001$). Combining GMA 400 mM and EGPEM 200 mM (G400E200-C) a clear synergy in the uptake occurred. Further increase in GMA up to 600 mM (G600E0-C) enhanced the loading compared to GMA 400 mM (G400E0-C) which correlated with the availability of more binding sites for cytosine as GMA increased. However, addition of EGPEM 200 mM (G600E200-C) did not further improve the loading but had a small detrimental effect. This latter finding may be related to the fact of that G600E200-C hydrogels swelled less than G600E0-C and also less than G400E200-C (**Figure 5.6**), which could cause some hindrance to the penetration of cytosine (during functionalization) and TA (during loading).

The increase in affinity achieved with the functionalization with cytosine was quantified by means of the network/water partition coefficient, $K_{N/W}$. Control hydrogels had $K_{N/W}$ values of 17.9 (s.d. 2.5); values above 1 indicate that the drug is hosted not only in the aqueous phase of the hydrogel but mainly through interactions with the network (*Alvarez-Rivera et al., 2018*). Significantly higher values of $K_{N/W}$ were recorded for some cytosine-functionalized hydrogels ranking in the order G100E100-C (24.3; s.d. 2.83) = G200E200-C (26.7; s.d. 0.5) < G200E0-C (28.5; s.d. 0.7) = G400E0-C (29.7; s.d. 1.8) < G600E200-C (33.1; s.d. 2.4) < G600E0-C (37.3; s.d. 1.0) < G400E200-C (43.5; s.d. 2.1). This finding indicates that an adequate

combination of cytosine and EGPEM moieties allows forming adequate receptors for TA.

5.3.4.TA release

Once loaded, the hydrogels were immersed in plenty volume of SLF at 35 °C to attain sink conditions. Also, the vials were maintained under oscillatory movement to avoid static fluid layers around the discs that could delay the release and led to false sustained profiles (Tieppo *et al.*, 2014; Alvarez-Rivera *et al.*, 2019). Compared to non-functionalized hydrogels, cytosine-functionalized networks exhibiting the highest $K_{N/W}$ were also able to provide more sustained release with less intense burst in the first hour (**Figure 5.10**). It should be noted that these cytosine-functionalized hydrogels released larger amounts of TA, as depicted in **Figure 5.11**, which should be beneficial from a therapeutic point of view. Relevantly, they provided sustained release for 24 h, covering the wearing of a daily-disposable CLs. Indeed, only G400E200-C and G600E200-C hydrogels showed a burst release below 25% in the first 30 min and TA percentage released below 60% at 4 hours. The burst release could be related to TA molecules only interacting at the surface of the hydrogel, while those that are tightly hosted inside the hydrogel allow for more prolonged release.

5. Cytosine-functionalized bioinspired hydrogels for ocular delivery of antioxidant transferulic acid

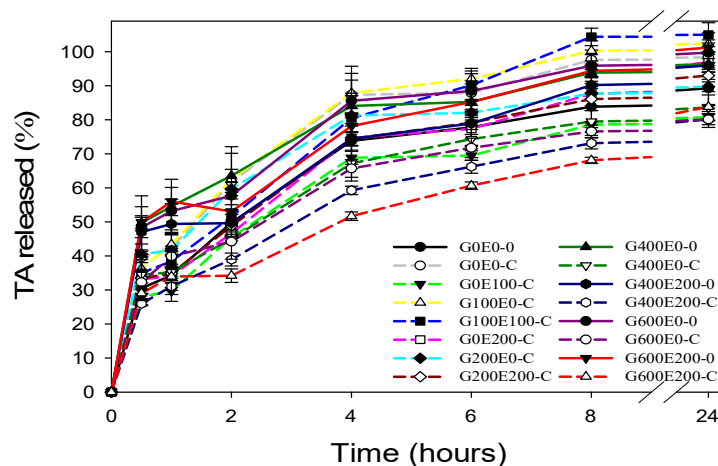


Figure 5.10. TA release profiles in simulated lacrimal fluid at 35 °C from non-functionalized (continuous lines) and cytosine-functionalized (dashed lines) hydrogels (loaded with the amounts shown in Figure 5.9). Mean values and standard deviations ($n=3$).

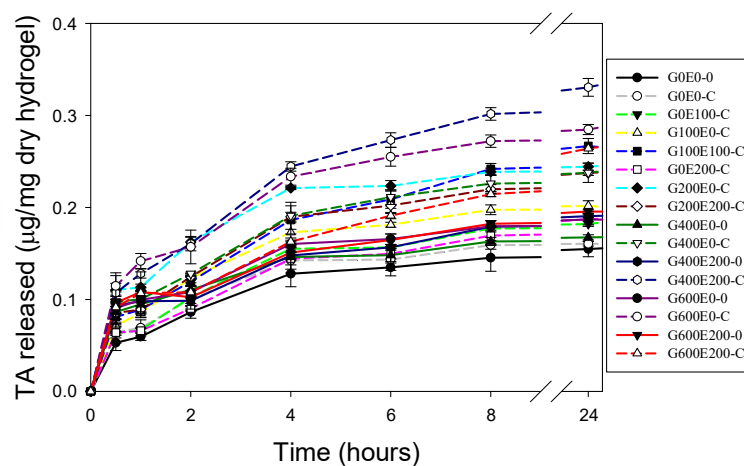


Figure 5.11. Amount of TA released in simulated lacrimal fluid at 35 °C by non-functionalized (continuous lines) and cytosine-functionalized (dashed lines) hydrogels (loaded with the amounts shown in Fig. S2). Mean values and standard deviations ($n=3$).

5.3.5. Biocompatibility

As a preliminary screening of biocompatibility, compatibility of the TA-loaded hydrogels with both Human Corneal Epithelial Cells (HCEC) and chorioallantoic membrane was investigated. The WST-1 test performed with HCEC revealed that the discs and the TA aqueous solution at the concentration used for loading ($10 \mu\text{g/mL} \cong 51.5 \mu\text{M}$) are highly cytocompatible, showing cell viability levels above 80% after 24 h of direct contact (**Figure 5.12**).

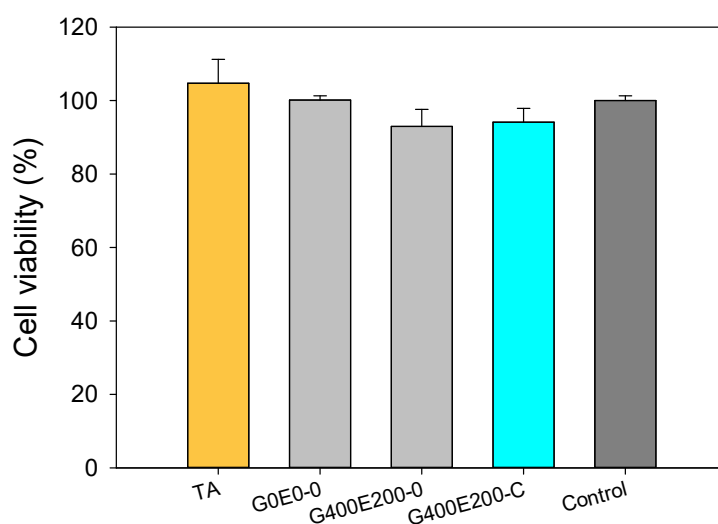


Figure 5.12. Viability of Human Corneal Epithelial Cells (HCEC) after direct contact for 24 h with TA aqueous solution ($10 \mu\text{g/mL}$) or TA-loaded G0E0-0, G400E200-0, and G400E200-C hydrogels, compared to cells in the absence of treatment (control).

This finding is in good agreement with previous reports using these cells and also the *in vivo* irritation test in rabbit eyes, which

suggested that TA concentration up to 100 μM is safe for dry eye syndrome (DES) treatment (*Chen et al., 2017*). Relevantly, no hydrogel caused haemorrhage, vascular lysis or coagulation during the HET-CAM test (**Figure 5.13**). Therefore, neither TA loading nor functionalization with cytosine compromise the biocompatibility of the designed HEMA-based hydrogels.

5.3.6. Antioxidant activity

The next step was to verify that TA maintained its antioxidant activity after the loading and release steps. A biologically relevant source of radicals, 2,2'-azobis(2-amidino-propane) dihydrochloride (AAPH), was chosen to carry out the standardized ORAC test (*Lucas-Abellan et al., 2011*). This method quantifies the capability of a substance to protect fluorescein from degradation by free radicals. Therefore, the slower the decrease of fluorescein fluorescence, the higher the antioxidant capacity.

The SLF release medium in which non-loaded and TA-loaded hydrogels were soaked was analyzed. Non-loaded cytosine-functionalized hydrogels were tested to verify that there were no leaching substances that could cause an artefact (false antioxidant activity) during the test.

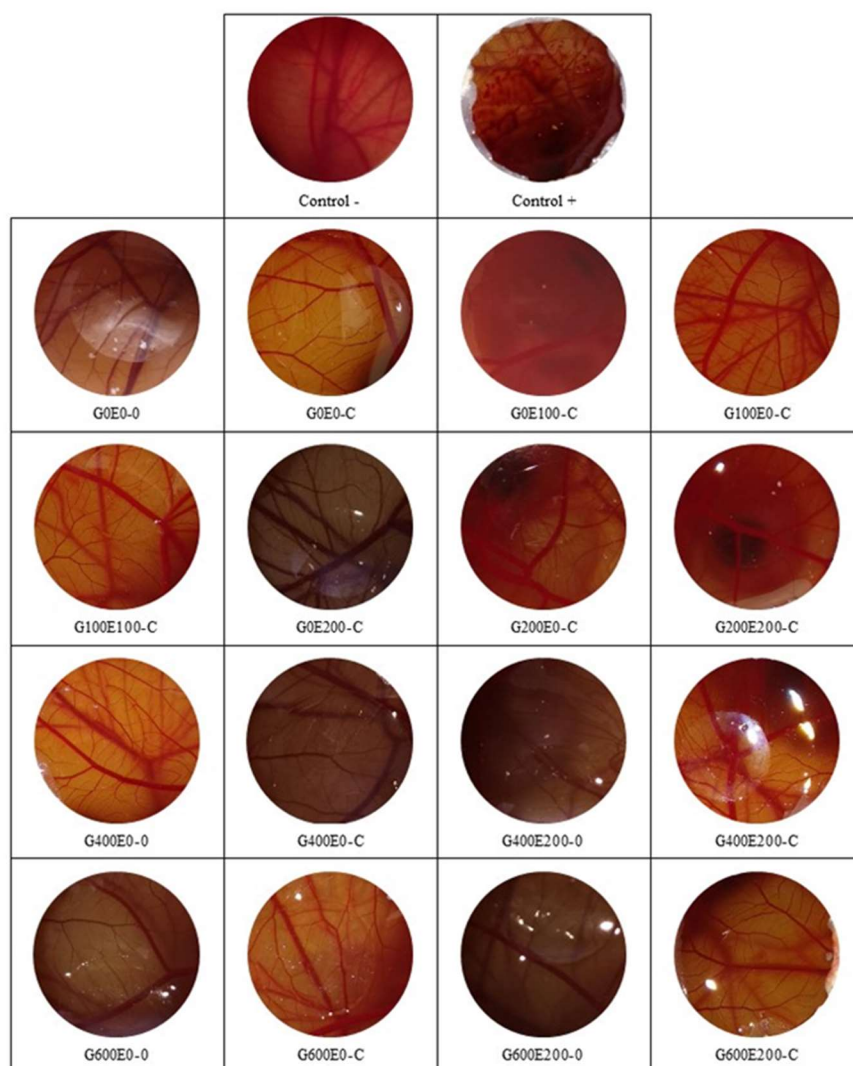


Figure 5.13. Pictures of chorioallantoic membranes during the HET-CAM test after 5 min contact with TA-loaded non-functionalized and cytosine-functionalized hydrogels. Control - and + refer to 0.9% NaCl and 0.1 N NaOH solutions, respectively.

The results were expressed as Trolox equivalent antioxidant capacity (TEAC) for comparative purposes. As expected, non-loaded hydrogels resulted in close to zero (or even negative) values, indicating that they did not release any antioxidant substance.

Differently, TA-loaded G400E200-C led to the highest antioxidant activity, equivalent to 53.28 ± 2.44 μM Trolox, compared to its cytosine-free homologue TA-loaded G400E200-0 that had an activity of 37.48 ± 1.53 μM Trolox. This finding corroborates the usefulness of cytosine to endow the hydrogels with enhanced capability to host TA and, which is even more remarkable, that the TA-cytosine interaction has nondetrimental effect on TA antioxidant activity. Indeed, the antioxidant activity expressed as $\mu\text{molTolox}/\mu\text{molTA}$ gave values in the 4.8-5.0 range, which is in close agreement with previous reports on antioxidant materials containing TA (Snelders *et al.*, 2013).

5.3.7. Cornea and sclera penetration

Finally, the most promising bioinspired G400E200-C hydrogel and its cytosine-free homologue G400E200-0 were evaluated regarding their capability to provide therapeutic amounts of TA to the eye structures. The concentrated TA solution (10 $\mu\text{g/mL}$) used for soaking was tested as control. As expected, permeability through cornea was slower than through sclera for any formulation (**Figure 5.14**). In the case of cornea, all formulations, including the TA solution, showed a lag time of more than 2 hours. With the few values

quantifiable, the steady state flux (J) was estimated to be 0.089 and 0.036 $\mu\text{g}/(\text{cm}^2\cdot\text{h})$ for TA when administered as free in solution and when included in the G400E200-C hydrogel, respectively. G400E200-0 hydrogel only led to measurable amounts permeated after 6 h contact. This different performance can be related to the different amounts provided by each hydrogel to the donor compartment, reaching 2.2 (s.d. 0.2) $\mu\text{g}/\text{mL}$ in the case of G400E200-C and 1.4 (s.d. 0.1) $\mu\text{g}/\text{mL}$ in the case of G400E200-0. It should be noted that in the case of TA solution more than 50% TA remained in the donor after 6 h in contact with cornea (5.3, s.d. 0.4 $\mu\text{g}/\text{mL}$).

These concentration values were used to estimate the mean TA permeability coefficient, P , to be 0.0168 cm/h (i.e. $4.6\cdot 10^{-6}$ cm/s) for TA free in solution and 0.0164 cm/h (i.e. $4.5\cdot 10^{-6}$ cm/s) for TA included in the G400E200-C hydrogel. This means that once released from the CLs, TA can permeate through the cornea as when it was administered as free in solution. Therefore, the differences in amount permeated are directly related to the different amounts loaded by the contact lenses, which highlights the benefit of the bioinspired strategy.

5. Cytosine-functionalized bioinspired hydrogels for ocular delivery of antioxidant transferulic acid

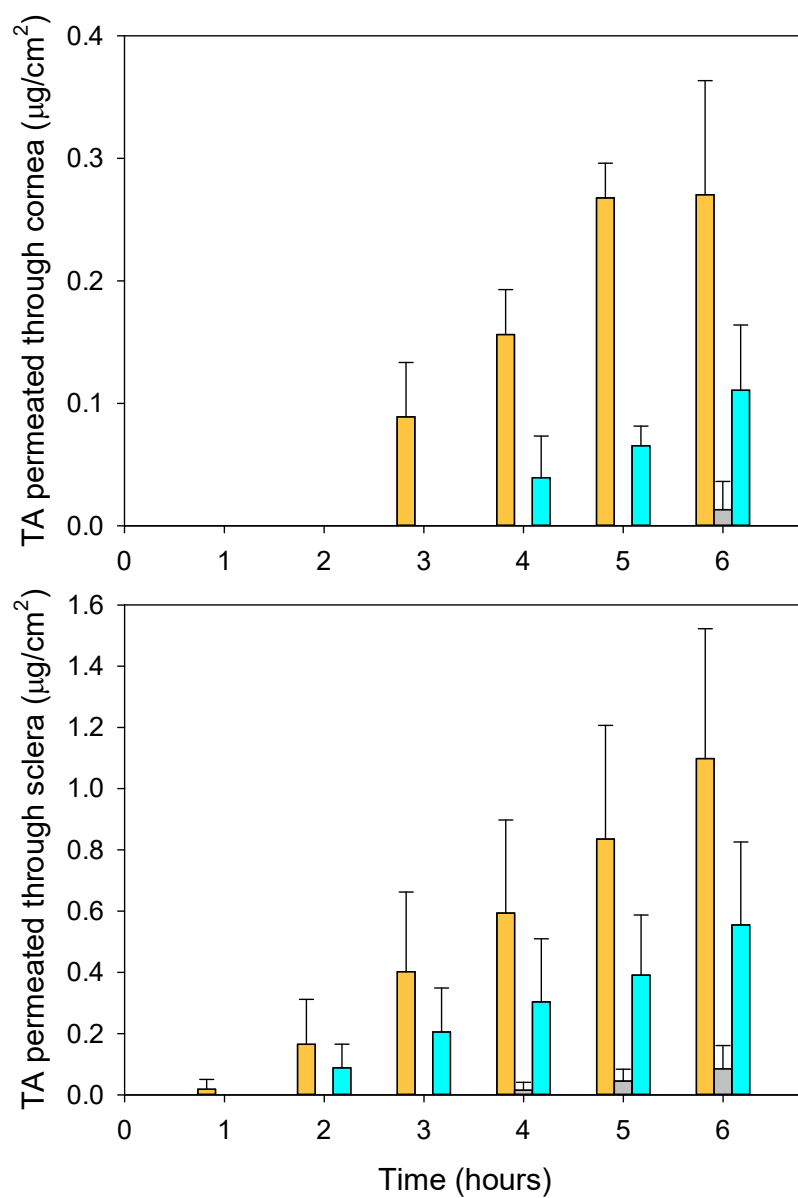


Figure 5.14. Amounts of TA permeated through cornea and sclera when delivered as TA aqueous solution (10 μg/mL; orange bars) or TA-loaded G400E200-0 (grey bars) and G400E200-C (light blue bars).

Compared to permeation studies carried out with other ocular drugs, the P values obtained for TA are in the range of those recorded for other hydrophobic molecules such as acyclovir ($4.4\text{--}7.3 \cdot 10^{-6}$ cm/s) 52,53 or lipoic acid ($4.4\text{--}12.0 \cdot 10^{-6}$ cm/s) (Alvarez-Rivera *et al.*, 2016) administered as eye drops. The prolonged lag time can be associated to accumulation inside the cornea, as observed for other drugs such as naltrexone (Alvarez-Rivera *et al.*, 2019). Indeed, compared to the amount permeated through cornea (Figure 5.14), TA accumulation inside the cornea was favored (Figure 5.15).

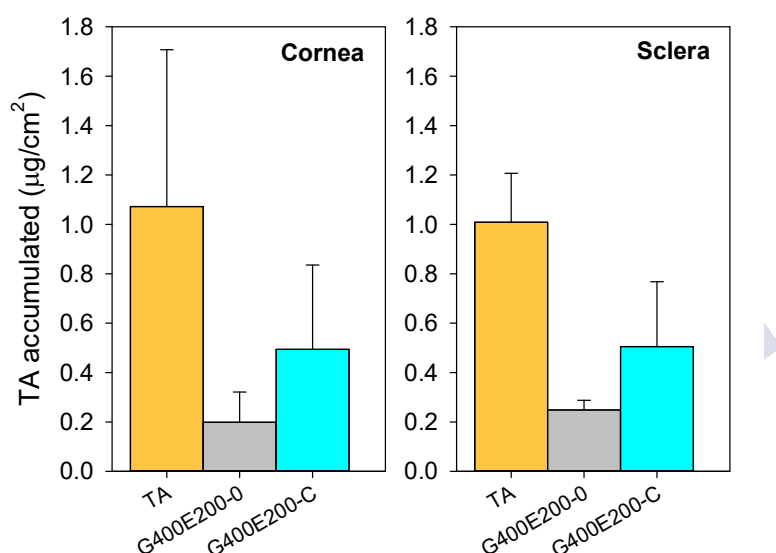


Figure 5.15. Amounts of TA accumulated inside cornea and sclera when delivered as TA aqueous solution (10 µg/mL: orange bars) or TA-loaded G400E200-0 (grey bars) and G400E200-C (light blue bars).

In the case of sclera, the amounts permeated were 3 to 4 times larger than through the cornea (**Figure 5.14**). Sclera has larger pores than cornea and thus greater permeability (*Loch et al., 2012*). Thus, no lag time was observed when TA was administered as solution. The lag time observed for the hydrogels, particularly cytosine-free G400E200-0, can be related to the low amount of TA released in the first hour compared to G400E200-C (see **Figure 5.8**). The steady state flux (J) was estimated to be 0.230 (s.d. 0.066), 0.035 (s.d. 0.010) and 0.115 (s.d. 0.038) $\mu\text{g}/(\text{cm}^2\cdot\text{h})$ for TA when administered as free in solution and when included in the G400E200-0 or G400E200-C hydrogel, respectively. Thus, P values were estimated to be $12.9\cdot 10^{-6}$ (s.d. $3.7\cdot 10^{-6}$), $5.4\cdot 10^{-6}$ (s.d. $1.7\cdot 10^{-6}$), and $11.5\cdot 10^{-6}$ (s.d. $3.8\cdot 10^{-6}$) cm/s, respectively, for TA when administered as free in solution and when included in the G400E200-0 or G400E200-C hydrogel. Once again, the TA-loaded G400E200-C hydrogel performed similarly to the TA solution in terms of permeation through and accumulation into the sclera, which means that the bioinspired hydrogels may act as reliable platforms for TA ocular delivery.

5.4. Concluding remarks

The creation of artificial receptors for drugs in CL matrix using nitrogenous bases as functional monomers was investigated here for first time. Hydrogels bearing cytosine moieties showed enhanced affinity for transferulic acid, and such an affinity was reinforced in the presence of EGPEM. Thus, compared to non-functionalized

hydrogels, the cytosine grafted networks were able to host double amount of drug and to provide sustained release for more than 8 hours. Released transferulic acid preserved its antioxidant properties and the capability to penetrate through cornea and sclera. Since cytosine-grafted hydrogels successfully passed the irritancy test, grafting of cytosine to CL appears as an useful tool to transform this medical device into a suitable platform for ocular delivery of molecules that can interact with cytosine through hydrogen bonds and π - π stacking.

5.5. References

Agudelo D., Bourassa P., Berube G., Tajmir-Riahi H.A. 2016. Review on the binding of anticancer drug doxorubicin with DNA and tRNA: Structural models and antitumor activity. *J Photochem Photobiol B.* 158:274-279

Al-Ghabeish M., Xu X., Krishnaiah Y.S., Rahman Z., Yang Y., Khan M.A. 2015. Influence of drug loading and type of ointment base on the *in vitro* performance of acyclovir ophthalmic ointment. *Int J Pharm.* 495:783-791

Ali M., Byrne M.E. 2009. Controlled release of high molecular weight hyaluronic acid from molecularly imprinted hydrogel contact lenses. *Pharm Res.* 26:714-726

Alvarez-Lorenzo C., Anguiano-Igea S., Varela-Garcia A., Vivero-Lopez M., Concheiro A. 2019. Bioinspired hydrogels for drug-eluting contact lenses. *Acta Biomater.* 84:49-62

5. Cytosine-functionalized bioinspired hydrogels for ocular delivery of
antioxidant transferulic acid

Alvarez-Rivera F., Concheiro A., Alvarez-Lorenzo C. 2018. Epalrestat-loaded silicone hydrogels as contact lenses to address diabetic-eye complications. *Eur J Pharm Biopharm.* 122:126-136

Alvarez-Rivera F., Fernandez-Villanueva D., Concheiro A., Alvarez-Lorenzo C. 2016. alpha-Lipoic acid in Soluplus® polymeric nanomicelles for ocular treatment of diabetes-associated corneal diseases. *J Pharm Sci.* 105:2855-2863

Alvarez-Rivera F., Serro A.P., Silva D., Concheiro A., Alvarez-Lorenzo C. 2019. Hydrogels for diabetic eyes: naltrexone loading, release profiles and cornea penetration. *Mater Sci Eng C Mater Biol Appl.* 105:110092

Awwad S., Mohamed Ahmed A.H.A., Sharma G., Heng J.S., Khaw P.T., Brocchini S., Lockwood A. 2017. Principles of pharmacology in the eye. *Br J Pharmacol.* 174:4205-4223

Bhamra T.S., Tighe B.J. 2017. Mechanical properties of contact lenses: the contribution of measurement techniques and clinical feedback to 50 years of materials development. *Cont Lens Anterior Eye.* 40:70-81

Bravo-Osuna I., Andres-Guerrero V., Pastoriza Abal P., Molina-Martinez I.T., Herrero-Vanrell R. 2016. Pharmaceutical microscale and nanoscale approaches for efficient treatment of ocular diseases. *Drug Deliv Transl Res.* 6:686-707

Bungau S., Abdel-Daim M.M., Tit D.M., Ghanem E., Sato S., Maruyama-Inoue M., Yamane S., Kadonosono K. 2019. Health benefits of polyphenols and carotenoids in age-related eye diseases. *Oxid Med Cell Longev.* 2019:9783429

Chen H.C., Chen Z.Y., Wang T.J., Drew V.J., Tseng C.L., Fang H.W., Lin F.H. 2017. Herbal supplement in a buffer for dry eye syndrome treatment. *Int J Mol Sci.* 18: 10.3390/ijms18081697

dos Santos J.F., Alvarez-Lorenzo C., Silva M., Balsa L., Couceiro J., Torres-Labandeira J.J., Concheiro A. 2009. Soft contact lenses functionalized with pendant cyclodextrins for controlled drug delivery. *Biomaterials.* 30:1348-1355

Engin K.N. 2009. Alpha-tocopherol: looking beyond an antioxidant. *Mol Vis.* 15:855-860

Gause S., Hsu K.H., Shafor C., Dixon P., Powell K.C., Chauhan A. 2016. Mechanistic modeling of ophthalmic drug delivery to the anterior chamber by eye drops and contact lenses. *Adv Colloid Interface Sci.* 233:139-154

Gendaszewska-Darmach E., Kucharska M. 2011. Nucleotide receptors as targets in the pharmacological enhancement of dermal wound healing. *Purinergic Signal.* 7:193-206

Gonzalez-Chomon C., Concheiro A., Alvarez-Lorenzo C. 2013. Soft contact lenses for controlled ocular delivery: 50 years in the making. *Ther Deliv.* 4:1141-1161

Gonzalez-Chomon C., Silva M., Concheiro A., Alvarez-Lorenzo C. 2016. Biomimetic contact lenses eluting olopatadine for allergic conjunctivitis. *Acta Biomater.* 41:302-311

Guzman-Aranguéz A., Gasull X., Diebold Y., Pintor J. 2014. Purinergic receptors in ocular inflammation. *Mediators Inflamm.* 2014:320906

Hou Y.Z., Yang J., Zhao G.R., Yuan Y.J. 2004. Ferulic acid inhibits vascular smooth muscle cell proliferation induced by angiotensin II. *Eur J Pharmacol.* 499:85-90

Hui A., Bajgrowicz-Cieslak M., Phan C.M., Jones L. 2017. *In vitro* release of two anti-muscarinic drugs from soft contact lenses. *Clin Ophthalmol.* 11:1657-1665

Imperiale J.C., Acosta G.B., Sosnik A. 2018. Polymer-based carriers for ophthalmic drug delivery. *J Control Release.* 285:106-141

Jantas R., Herczynska L. 2010. Preparation and characterization of the poly(2-hydroxyethyl methacrylate)-salicylic acid conjugate. *Polym Bulletin.* 64:459-469

Kadoma Y., Fujisawa S. 2008. A comparative study of the radical-scavenging activity of the phenolcarboxylic acids caffeic acid, p-coumaric acid, chlorogenic acid and ferulic acid, with or without 2-mercaptoethanol, a thiol, using the induction period method. *Molecules.* 13:2488-2499

Kojima M., Shui Y.B., Murano H., Nagata M., Hockwin O., Sasaki K., Takahashi N. 2002. Low vitamin E level as a subliminal risk factor in a rat model of prednisolone-induced cataract. *Invest Ophthalmol Vis Sci.* 43:1116-1120

Lee D., Lee N., Kwon I. 2018. Efficient loading of ophthalmic drugs with poor loadability into contact lenses using functional comonomers. *Biomater Sci.* 6:2639-2646

Loch C., Zakelj S., Kristl A., Nagel S., Guthoff R., Weitschies W., Seidlitz A. 2012. Determination of permeability coefficients of

ophthalmic drugs through different layers of porcine, rabbit and bovine eyes. *Eur J Pharm Sci.* 47:131-138

Lucas-Abellan C., Mercader-Ros M.T., Zafrilla M.P., Gabaldon J.A., Nunez-Delicado E. 2011. Comparative study of different methods to measure antioxidant activity of resveratrol in the presence of cyclodextrins. *Food Chem Toxicol.* 49:1255-1260

Mancuso C., Santangelo R. 2014. Ferulic acid: pharmacological and toxicological aspects. *Food Chem Toxicol.* 65:185-195

Mbarek A., Moussa G., Chain J.L. 2019. Pharmaceutical applications of molecular tweezers, clefts and clips. *Molecules.* 24:10.3390/molecules24091803

Nagai N., Kotani S., Mano Y., Ueno A., Ito Y., Kitaba T., Takata T., Fujii N. 2017. Ferulic acid suppresses amyloid β -production in the human lens epithelial cell stimulated with hydrogen peroxide. *Biomed Res Int.* 2017:5343010

Oza M.D., Meena R., Siddhanta A.K. 2012. Facile synthesis of fluorescent polysaccharides: Cytosine grafted agarose and κ -carrageenan. *Carbohydr Polym.* 87:1971–1979

Pan J., Cao D.L., Ren F.D., Wang J.L., Yang L. 2018. Theoretical investigation into the cooperativity effect between the intermolecular π - π and H-bonding interactions in the curcumincytosine-H₂O system. *J Mol Model.* 24:298-018-3836-z

Ribeiro A., Sandez-Macho I., Casas M., Alvarez-Perez S., Alvarez-Lorenzo C., Concheiro A. 2013. Poloxamine micellar solubilization of alpha-tocopherol for topical ocular treatment. *Colloids Surf B Biointerfaces.* 103:550-557

Ribeiro A., Sosnik A., Chiappetta D.A., Veiga F., Concheiro A., Alvarez-Lorenzo C. 2012. Single and mixed poloxamine micelles as nanocarriers for solubilization and sustained release of ethoxzolamide for topical glaucoma therapy. *J R Soc Interface*. 9: 2059-2069

Ribeiro A., Veiga F., Santos D., Torres-Labandeira J.J., Concheiro A., Alvarez-Lorenzo C. 2011. Bioinspired imprinted PHEMA-hydrogels for ocular delivery of carbonic anhydrase inhibitor drugs. *Biomacromolecules*. 12:701-709

Ribeiro A., Veiga F., Santos D., Torres-Labandeira J.J., Concheiro A., Alvarez-Lorenzo C. 2011. Receptor-based biomimetic NVP/DMA contact lenses for loading/eluting carbonic anhydrase inhibitors. *J Membr Sci*. 383:60-69

Roleira F.M.F., Tavares da Silva E.J., Pereira J.A.C., Ortuso F., Alcaro S., Pinto M.M.M. 2015. Molecular clefts of Rebek revisited: potential application as drug carriers for the antiviral acyclovir. *J Incl Phenom Macrocycl Chem*. 83:203-208

Ross A.E., Bengani L.C., Tulsan R., Maidana D.E., Salvador-Culla B., Kobashi H., Kolovou P.E., Zhai H., Taghizadeh K., Kuang L., Mehta M., Vavvas D.G., Kohane D.S., Ciolino J.B. 2019. Topical sustained drug delivery to the retina with a drug-eluting contact lens. *Biomaterials*. 217:119285

Sadeghi M., Bayat M., Cheraghi S., Yari K., Heydari R., Dehdashtian S., Shamsipur M. 2016. Binding studies of the anti-retroviral drug, efavirenz to calf thymus DNA using spectroscopic and voltammetric techniques. *Luminescence*. 31:108-117

Snelders J., Dornez E., Delcour J.A., Courtin C.M. 2013. Ferulic acid content and appearance determine the antioxidant capacity of arabinoxylanoligosaccharides. *J Agric Food Chem*. 61:10173-10182

Srinivasan M., Sudheer A.R., Menon V.P. 2007. Ferulic acid: therapeutic potential through its antioxidant property. *J Clin Biochem Nutr.* 40:92-100

Srinivasarao D.A., Lohiya G., Katti D.S. 2018. Fundamentals, challenges, and nanomedicine-based solutions for ocular diseases. *Wiley Interdiscip. Rev Nanomed Nanobiotechnol.* e1548

Tieppo A., Boggs A.C., Pourjavad P., Byrne M.E. 2014. Analysis of release kinetics of ocular therapeutics from drug releasing contact lenses: Best methods and practices to advance the field. *Cont Lens Anterior Eye.* 37:305-313

Tieppo A., White C.J., Paine A.C., Voyles M.L., McBride M.K., Byrne M.E. 2012. Sustained *in vivo* release from imprinted therapeutic contact lenses. *J Control Release.* 157:391-397

Tranoudis I., Efron N. 2004. Tensile properties of soft contact lens materials. *Cont Lens Anterior Eye.* 27:177-191

Trombino S., Cassano R., Ferrarelli T., Barone E., Picci N., Mancuso C. 2013. Trans-ferulic acid-based solid lipid nanoparticles and their antioxidant effect in rat brain microsomes. *Colloids Surf B Biointerfaces.* 109:273-279

Tsai C.Y., Woung L.C., Yen J.C., Tseng P.C., Chiou S.H., Sung Y.J., Liu K.T., Cheng Y.H. 2016. Thermosensitive chitosan-based hydrogels for sustained release of ferulic acid on corneal wound healing. *Carbohydr Polym.* 135:308-315

Ubani-Ukoma U., Gibson D., Schultz G., Silva B.O., Chauhan A. 2019. Evaluating the potential of drug eluting contact lenses for

5. Cytosine-functionalized bioinspired hydrogels for ocular delivery of antioxidant transferulic acid

treatment of bacterial keratitis using an *ex vivo* corneal model. *Int J Pharm.* 565:499-508

Volpato N.M., Santi P., Laureri C., Colombo P. 1997. Assay of acyclovir in human skin layers by high-performance liquid chromatography. *J Pharm Biomed Anal.* 16:515-520

Yang G., Zhai H.M. 2012. Synthesis and properties of glycidyl-methacrylate-grafted eucalyptus fibers. *Cellulose Chem Technol.* 46:243-248

Yellepeddi V.K., Palakurthi S. 2016. Recent advances in topical ocular drug delivery. *J Ocul Pharmacol Ther.* 32:67-82

Yoshikawa T., Umeno D., Saito K., Sugo T. 2008. High-performance collection of palladium ions in acidic media using nucleic-acid-base-immobilized porous hollow-fiber membranes. *J Membr Sci.* 307:82-87

Zdunska K., Dana A., Kolodziejczak A., Rotsztein H. 2018. Antioxidant properties of ferulic acid and its possible application. *Skin Pharmacol Physiol.* 31:332-336

Zhang K., Chen M., Drummey K.J., Talley S.J., Anderson L.J., Moore R.B., Long T.E. 2016. Ureido cytosine and cytosine-containing acrylic copolymers. *Polym Chem.* 7:6671-66



Conclusions





6. Conclusions

According to the aims of this Thesis, polymeric micelles or CLs were designed for the topical ocular delivery of antiviral drugs and antioxidant agents. Several approaches were explored, and the obtained systems characterized in detail.

The research was carried out in three steps, and the following conclusions can be drawn.

1.- Soluplus and Solutol exhibited different ability to encapsulate acyclovir even though their HLB is quite similar, which may be related to the different architecture of both copolymers. Acyclovir loaded Soluplus micelles showed homogeneous nanometric particle size and slightly negative Z-potential values, which may facilitate the penetration through cornea and sclera. Additionally, the peculiar dependence of the viscoelastic behaviour on the temperature may allow instillation as eye drops while the increase in viscosity at eye temperature should prolong the permanence on the ocular surface and

attenuate the dilution process. Although encapsulation of acyclovir in Soluplus micelles only caused a moderate increase in acyclovir apparent solubility, the micelles notably facilitated the penetration of the drug through cornea and sclera and also the accumulation in both tissues. The larger amount of acyclovir permeated through sclera compared with cornea opens the possibility of delivery the drug to the posterior eye segment.

2.- HEMA-based hydrogels functionalized with MAA were explored regarding their ability to host ACV and VACV. Although in molecular modeling both ACV and VACV showed high affinity for MAA, their different binding points may explain that MAA was only efficient in enhancing the uptake of VACV. MAA can form hydrogen bonds with the rings of both drugs, but it also interacts ionically with the amino group of the side chain of VACV. Synergism in VACV loading was observed when combining the use of MAA as functional monomer and the application of the molecular imprinting. The characterization of these hydrogels in terms of swelling, transmittance and mechanical properties were within the typical ranges of daily use contact lenses. In addition, no irritation events were recorded in the HET-CAM assay. VACV-imprinted hydrogels released the drug in a sustained manner for 10 h and favoured drug accumulation in sclera. The permeability of VACV through the sclera suggests the possibility of delivery this drug to the posterior segment. Therefore, hydrogels

containing MAA and imprinted with VACV are suitable candidates for the preparation of contact lenses that release this antiviral drug.

3.- The use of nitrogenous bases as functional monomers has been explored here for first time to create artificial receptors in CL hydrogels by mimicking the interactions of drugs with nucleotides that build up DNA and RNA. Grafting of cytosine to HEMA-based hydrogels appears as an efficient way to endow the hydrogels with affinity for antioxidant molecules, such as TA, having complementary chemical structure in terms of hydrogen bonding and π - π stacking ability. The affinity was reinforced combining cytosine with EGPEM at certain ratios, which suggests the formation of molecular clefts-like binding sites. Specifically, cytosine functionalization of networks prepared with relatively low contents in GMA (400 mM) and EGPEM (200 mM) rendered hydrogels (G400E200-C) with ~ 2.5 times higher capability to host TA compared to non-functionalized hydrogels. Such an increase in affinity also enhanced the capability of the hydrogels to sustain TA release under the most challenging, well-agitated sink conditions. Relevantly from a therapeutic point of view, G400E200-C hydrogels delivered TA preserving its powerful antioxidant capability and showing permeability coefficients through cornea and sclera as high as those recorded for TA solution, with the advantage of that the controlled release should avoid a rapid clearance from the ocular surface. From the medical device perspective, the minor changes in

HEMA hydrogel composition and subsequent functionalization with cytosine do not cause detrimental effects on the performance as CLs, which encourages further testing of the proposed strategy not only with related antioxidants but also with other therapeutic class molecules.

Taken together, the results of this Doctoral Thesis open up new possibilities for developing topical ocular drug delivery systems, both liquid and solid, that provide sustained levels of the drug in the cornea and sclera.



Patent





7. Patent

OFICINA ESPAÑOLA DE
PATENTES Y MARCAS

ESPAÑA



⑪ Número de publicación: **2 755 415**

②1 Número de solicitud: 201931063

⑤ Int. Cl.:

C08J 3/075 (2006.01)

C08F 220/06 (2008.01)

C08F 220/10 (2008.01)

C08F 222/00 (2006.01)

C08F 26/06 (2006.01)

C08F 8/30 (2006.01)

A61K 9/14 (2006.01)

G02C 7/04 (2006.01)

12

SOLICITUD DE PATENTE

A1

② Fecha de presentación:

29.11.2019

④3 Fecha de publicación de la solicitud:

22.04.2020

71 Solicitantes:

UNIVERSIDADE DE SANTIAGO DE
COMPOSTELA (100.0%)
Edificio EMPRENDIA - Campus Vida
15782 Santiago de Compostela (A Coruña) ES

72 Inventor/es:

VARELA GARCIA, Angela;
CONCHEIRO NINE, Angel y
ALVAREZ LORENZO, Carmen

(74) Agente/Representante:

TORRENTE VILASÁNCHEZ, Susana

(54) Título: HIDROGELES QUE COMPRENDEN UNA BASE NITROGENADA

⑤7 Resumen:

Resumen: La presente invención se refiere a hidrogeles acrílicos que comprenden una base nitrogenada seleccionada de entre citosina, adenina, guanina, uracilo y timina, a métodos para obtener dichos hidrogeles y a las lentes de contacto preparadas a partir de dichos hidrogeles.

ES 2 755 415 A1

ES 2 755 415 A1

DESCRIPCIÓN

Hidrogeles que comprenden una base nitrogenada

Campo de la invención

La presente invención se refiere a hidrogeles acrílicos que comprenden una base nitrogenada seleccionada de entre citosina, adenina, guanina, uracilo y timina, a métodos
5 para obtener dichos hidrogeles, así como al uso médico, especialmente oftálmico, de dichos hidrogeles.

Antecedentes de la invención

La naturaleza hidrofílica de los hidrogeles dificulta la carga eficiente de moléculas poco polares, como son la gran mayoría de los fármacos y las sustancias activas.

10 Para solucionar este problema, se han venido estudiando diferentes soluciones. Una de ellas es la incorporación del fármaco o de la sustancia activa en un vehículo de tamaño nano o micrométrico que después se incorpora en el hidrogel (como por ejemplo se describe en Y. Kapoor, A. Chauhan, Drug and surfactant transport in Cyclosporine A and Brij 98 laden p-HEMA hydrogels, J. Coll. Int. Sci. 322 (2008) 624–633). Sin embargo,
15 en la mayoría de estos estudios la carga del fármaco al hidrogel continúa siendo relativamente baja.

Así, aún es necesario el desarrollo de hidrogeles que sean capaces de captar sustancias poco polares y cederlas de forma controlada a lo largo del tiempo.

20 Descripción breve de la invención

Los autores de la presente invención han diseñado un nuevo hidrogel con capacidad para incorporar moléculas, incluidas moléculas poco polares, en particular fármacos y sustancias activas poco polares.

Los hidrogeles de la presente invención están diseñados de manera que presentan
25 microdominios en los que se incorporan moléculas, de manera más concreta se pueden incorporar fármacos y sustancias activas, que además pueden formar complejos con bases nitrogenadas que están incorporadas al hidrogel.

ES 2 755 415 A1

Los hidrogeles de la presente invención son útiles en el tratamiento de estados patológicos o fisiológicos, en la elaboración de sistemas de liberación tópica, transdérmica o transmucosal de moléculas y en la preparación de cosméticos.

Así, en un primer aspecto, la presente invención se dirige a un hidrogel en forma de red
 5 tridimensional caracterizado porque comprende cadenas metacrilicas y/o acrilicas entrecruzadas, en donde las cadenas comprenden grupos alquílicos a los que están unidas una base nitrogenada seleccionada de entre citosina, adenina, guanina, uracilo y timina.

Un segundo aspecto de la invención se dirige a un método para preparar un hidrogel como se describió en el primer aspecto de la invención, que comprende las etapas de:

- 10 a. polimerizar una mezcla que comprende i) monómeros metacrilicos o acrilicos monofuncionalizados, o sus combinaciones, ii) monómeros metacrilicos o acrilicos bifuncionalizados, y iii) monómeros metacrilicos o acrilicos que comprenden un grupo electrófilo, para formar un entramado base de red tridimensional; y
- 15 b. hacer reaccionar una base nitrogenada seleccionada de entre citosina, adenina, guanina, uracilo y timina, con el entramado base.

En otro aspecto, la presente invención se dirige a un hidrogel obtenible mediante un procedimiento tal y como se describe en el segundo aspecto de la invención.

En otro aspecto, la presente invención se refiere a una lente de contacto que comprende
 20 un hidrogel como se describió en el primer aspecto de la invención. En otro aspecto, la presente invención se refiere a un método para preparar dicha lente de contacto.

En un aspecto adicional, la presente invención se dirige a un hidrogel y a una lente de contacto, tal y como se describe en los anteriores aspectos, para su uso en medicina, preferiblemente en oftalmología. Más concretamente, dicho hidrogel o lente de contacto
 25 se emplea para tratar o prevenir la sequedad del ojo, cataratas y úlceras corneales.

En otro aspecto adicional, la presente invención se dirige al uso del hidrogel en la elaboración de sistemas de liberación tópica, transdérmica o transmucosal, y en cosmética.

Descripción de las figuras

Figura 1. Representación esquemática de la reacción entre la base nitrogenada y el grupo glicidil metacrilato en la red tridimensional de hidrogel intermedio.

Figura 2. Cantidad de TA incorporado a los hidrogeles después de 48 horas de inmersión de los mismos en una solución de TA (0,01 mg/mL) a 25°C.

Figura 3. Perfiles de cesión de TA en fluido lacrimal simulado a 35°C desde hidrogeles no funcionalizados con base nitrogenada (líneas continuas) y desde hidrogeles funcionalizados (líneas punteadas).

Figura 4. Cantidad de TA permeado a través de la córnea y esclera cuando se cede TA desde una solución acuosa (barras blancas), o desde hidrogeles sin funcionalizar (barras negras) y funcionalizados (barras grises).

Figura 5. Cantidad de TA acumulada en la córnea y en la esclera cuando se cede TA desde una solución acuosa (barras blancas), o desde hidrogeles sin funcionalizar (barras negras) y funcionalizados (barras grises).

Descripción detallada de la invención

En un aspecto, la presente invención se dirige a un hidrogel en forma de red tridimensional caracterizado porque comprende cadenas metacrílicas y/o acrílicas entrecruzadas, en donde las cadenas comprenden grupos alquílicos a los que están unidas una base nitrogenada seleccionada de entre citosina, adenina, guanina, uracilo y timina.

En la presente invención se entiende por red tridimensional un entramado polimérico que se extiende en las tres dimensiones del espacio. Esta red tridimensional se forma cuando las cadenas poliméricas que la constituyen se encuentran entrecruzadas o reticuladas por monómeros que tienen la función de agentes reticulantes (A. Yamauchi. Gels: Introduction. En: Y. Osada, K. Kajiwara. Gels Handbook, Volume 1. The Fundamentals. Academic Press, London, 2001, páginas 4-12).

En la presente invención, por cadena metacrílica o acrílica se entiende una cadena polimérica que es el resultado de la polimerización de monómeros metacrílicos o acrílicos. En la presente invención, por cadena metacrílica y acrílica se entiende una cadena polimérica que es el resultado de la polimerización de monómeros metacrílicos y acrílicos.

ES 2 755 415 A1

Por unidad metacrílica o acrílica se entiende cada unidad monomérica que constituye la cadena polimérica tras la polimerización de monómeros metacrílicos o acrílicos.

Por unidades metacrílicas o acrílicas monofuncionalizadas se entienden las unidades metacrílicas o acrílicas que son el resultado de la polimerización de monómeros que
5 contienen un único grupo metacrílico o acrílico. Por combinaciones de unidades metacrílicas o acrílicas monofuncionalizadas se entiende que se han mezclado un monómero metacrílico con otro monómero metacrílico diferente y/o con uno o más monómeros acrílicos.

Por unidades metacrílicas o acrílicas bifuncionalizadas se entienden las unidades
10 metacrílicas o acrílicas que son el resultado de la polimerización de monómeros que contienen dos o más grupos metacrílicos o acrílicos. En la presente invención, las unidades metacrílicas o acrílicas bifuncionalizadas tienen la función de agentes reticulantes.

Por unidades metacrílicas o acrílicas que comprenden un grupo electrófilo se entienden
15 las unidades metacrílicas o acrílicas que son el resultado de la polimerización de monómeros metacrílicos o acrílicos que comprenden un grupo electrófilo.

Por grupo electrófilo se entiende un átomo de carbono al que está unido un buen grupo saliente y tiene capacidad para reaccionar en una reacción de sustitución nucleófila, bimolecular o unimolecular. Así, por un monómero metacrílico o acrílico que comprende
20 un grupo electrófilo se entiende aquel que tiene un carbono al que está unido un buen grupo saliente. Hay ejemplos comerciales de dichos monómeros que son útiles para la presente invención, como por ejemplo, glicidil metacrilato, glicidil acrilato, 3-cloro-2-hidroxipropil metacrilato. Pero también se pueden preparar mediante reacciones sencillas conocidas por el experto en la materia, por ejemplo, el grupo cloro del 3-cloro-2-
25 hidroxipropil metacrilato se puede transformar en un mejor grupo saliente como por ejemplo tosilato, triflato, mesilato, fosfato, etc, y también existe bibliografía en la que se describe la preparación de estos monómeros metacrílicos o acrílicos que comprenden un grupo electrófilo y que es conocida por el experto en la materia.

En una realización preferida, las cadenas metacrílicas y/o acrílicas de los hidrogeles de la
30 invención comprenden o están formadas por unidades metacrílicas o acrílicas monofuncionalizadas, o sus combinaciones; unidades metacrílicas o acrílicas

ES 2 755 415 A1

bifuncionalizadas; y unidades metacrílicas o acrílicas que comprenden un grupo electrófilo. En una realización las cadenas no comprenden otro tipo de unidad.

En una realización preferida, los hidrogeles de la invención se caracterizan porque la proporción en peso de las unidades metacrílicas o acrílicas bifuncionalizadas está
5 preferiblemente entre el 0,1% y el 10% con respecto al peso del hidrogel. En una realización preferida, la proporción en peso de las unidades metacrílicas o acrílicas que comprenden un grupo electrófilo está preferiblemente entre el 0,1% y el 10% con respecto al peso del hidrogel.

Los hidrogeles de la presente invención poseen la capacidad de incorporar agua en
10 elevadas proporciones sin disolverse. Además, los hidrogeles de la invención presentan una elevada claridad óptica, excelente biocompatibilidad y propiedades físicas y mecánicas que hacen que los hidrogeles de la presente invención sean útiles como componentes de lentes de contacto, y en particular lentes de contacto blandas.

Los hidrogeles de la invención tienen además la capacidad de incorporar moléculas, de
15 manera preferida moléculas que presentan afinidad por la base nitrogenada que está presente en el hidrogel. Y además, los hidrogeles de la invención tienen la capacidad de controlar la cesión de dichas moléculas, de forma preferida la cesión a medios fisiológicos.

En una realización preferida, la molécula con afinidad por la base nitrogenada es un
20 antioxidante. En una realización más preferida, la molécula con afinidad por la base nitrogenada se selecciona de entre ácido trans-ferúlico, edaravona, idebenona, N-acetilcisteína, α -Lipoic acid, flavonoides, isoflavonas, rutoxidos, silibinina, baicaleína, quercetina, catequinas, polifenoles, resveratrol, curcumina, vitamina A, vitamina C, vitamina E y coenzima Q. En una realización aún más preferida el antioxidante es ácido
25 trans-ferúlico.

En una realización preferida, la invención se dirige a un hidrogel en forma de red tridimensional caracterizado porque comprende cadenas metacrílicas entrecruzadas, en donde las cadenas comprenden grupos alquílicos a los que están unidas citosinas.

En otra realización preferida, la invención se dirige a un hidrogel en forma de red
30 tridimensional caracterizado porque comprende cadenas metacrílicas entrecruzadas, en

ES 2 755 415 A1

- donde las cadenas comprenden grupos alquílicos a los que están unidas citosinas, y el hidrogel comprende además una molécula antioxidante, preferiblemente ácido trans-ferúlico. En una realización más preferida, las cadenas metacrílicas están formadas por:
- 5 i) unidades metacrílicas monofuncionalizadas procedentes de los monómeros monofuncionalizados hidroxietil metacrilato y etilenglicolfeniléter metacrilato; ii) unidades metacrílicas bifuncionalizadas procedentes del monómero bifuncionalizado etilenglicol dimetacrilato; iii) unidades metacrílicas con un grupo alquílico procedente del monómero con un grupo electrófilo glicidil metacrilato, donde el grupo alquílico está unido covalentemente a una citosina mediante un enlace amino.
 - 10 En otra realización más preferida, las cadenas metacrílicas están formadas por: i) unidades metacrílicas monofuncionalizadas procedentes de los monómeros monofuncionalizados hidroxietil metacrilato en una proporción en peso de entre 60% y 99% respecto al peso del hidrogel, preferiblemente entre 70% y 99%, más preferiblemente entre 80% y 98%, y etilenglicolfeniléter metacrilato en una proporción en peso de entre 0,1% y 10% respecto
 - 15 al peso del hidrogel; ii) unidades metacrílicas bifuncionalizadas procedentes del monómero bifuncionalizado etilenglicol dimetacrilato en una proporción en peso de entre 0,1% y 10% respecto al peso del hidrogel; iii) unidades metacrílicas con un grupo alquílico procedente del monómero con un grupo electrófilo glicidil metacrilato en una proporción en peso de entre 0,1% y 10% respecto al peso del hidrogel, donde el grupo
 - 20 alquílico está unido covalentemente a una citosina mediante un enlace amino.
- En otra realización preferida, la molécula con afinidad por la base nitrogenada presente en el hidrogel es un principio activo farmacéutico. En una realización más preferida, el principio activo farmacéutico es capaz de formar enlaces de hidrógeno o interacciones *pi-pi stacking* con la base nitrogenada presente en el hidrogel.
- 25 En un aspecto adicional, la invención se dirige a una lente de contacto que comprende el hidrogel de la invención tal y como se describe en cualquiera de sus realizaciones.
- En una realización, la lente de contacto es una lente de contacto blanda. En el contexto de la presente invención, una lente de contacto blanda es una lente de contacto que tiene un módulo de elasticidad (es decir, el módulo de Young) de menos de 2,5 MPa.
- 30 En una realización, el hidrogel o la lente de contacto posee un contenido de agua en peso respecto del peso del hidrogel o lentilla del 20 % al 80 %.

ES 2 755 415 A1

En una realización, el hidrogel o lente de contacto comprende, además, agentes activos adicionales que sirven para tratar la sequedad del ojo o algún síntoma derivado tal como la inflamación.

En una realización el agente activo adicional es un agente antiinflamatorio. Más particularmente, el agente antiinflamatorio se selecciona del grupo que consiste en ibuprofeno, cetoprofeno, flurbiprofeno, fenoprofeno, naproxeno, piroxicam, tenoxicam, isoxicam, meloxicam, indometacina, aceclofenac, diclofenac y una combinación de los mismos.

En otro aspecto la invención se dirige a un procedimiento para la preparación de los hidrogeles de la invención, que comprende las etapas de:

- a. polymerizar una mezcla que comprende i) monómeros metacrílicos o acrílicos monofuncionalizados, o sus combinaciones, ii) monómeros metacrílicos o acrílicos bifuncionalizados, y iii) monómeros metacrílicos o acrílicos que comprenden un grupo electrófilo, para formar un entramado base de red tridimensional; y
- b. hacer reaccionar una base nitrogenada seleccionada de entre citosina, adenina, guanina, uracilo y timina, con el entramado base.

A través de la polimerización de la etapa a) se van formando las cadenas metacrílicas o acrílicas, o las cadenas acrílicas y metacrílicas. El entrecruzamiento de estas cadenas según crecen se puede lograr de diversas maneras, por ejemplo a través del empleo de monómeros o agentes reticulantes que comprenden más de un grupo reactivo que reacciona con diferentes cadenas crecientes sin terminar la polimerización. En una realización preferida, el entrecruzamiento se logra a través del empleo de monómeros metacrílicos o acrílicos bifuncionalizados en la etapa a) En el contexto de la presente invención el significado de reticulación y entrecruzamiento es el mismo.

En una realización preferida, el entramado base de la red que se prepara en la etapa a) se prepara por polimerización de monómeros metacrílicos o acrílicos monofuncionalizados, o sus combinaciones, monómeros metacrílicos o acrílicos bifuncionalizados, y monómeros metacrílicos o acrílicos que comprenden un grupo electrófilo. De este modo se obtiene un entramado base, que comprende cadenas metacrílicas y/o acrílicas que comprenden o están formadas por unidades metacrílicas o acrílicas monofuncionalizadas,

ES 2 755 415 A1

o sus combinaciones, unidades metacrílicas o acrílicas bifuncionalizadas, y unidades metacrílicas o acrílicas que comprenden un grupo electrófilo.

El entramado base que se prepara en la etapa a) es en sí un hidrogel tridimensional.

Los monómeros que dan lugar a las unidades metacrílicas o acrílicas que comprenden un
5 grupo electrófilo son preferentemente glicidil metacrilato, glicidil acrilato, 3-cloro-2-hidroxipropil metacrilato.

Los monómeros que dan lugar a unidades metacrílicas o acrílicas que poseen un grupo metacrílico o acrílico en su estructura (monofuncionalizadas) son preferentemente hidroxietil metacrilato, etilenglicolfeniléter metacrilato, 1-(trimetilsiloxisilpropil)-
10 metacrilato, metilmetacrilato, N,N-dimetilacrilamida, N,N-dietilacrilamida, ácido metacrílico, ácido acrílico, aminopropil metacrilato, ciclohexil metacrilato, o fluoro-siloxano acrilato.

Los monómeros que dan lugar a unidades metacrílicas o acrílicas que poseen dos grupos metacrílicos o acrílicos en su estructura (bifuncionalizadas) son preferentemente
15 etilenglicol dimetacrilato, 1,3-Butanediol diacrilato, 1,4-Butanediol diacrilato, 1,6-Hexanediol diacrilato, Etilen glicol diacrilato, Fluorescein O,O'-diacrilato, Glicerol 1,3-diglicerolato diacrilato, Pentaeritritol diacrilato monoestearato, 1,6-Hexanediol etoxilato diacrilato, 3-Hidroxi-2,2-dimetilpropil 3-hidroxi-2,2-dimetilpropionato diacrilato, Bisfenol A etoxilato diacrilato, Di(etilen glicol) diacrilato, Neopentil glicol diacrilato,
20 Poli(etilen glicol) diacrilato, Poli(propilen glicol) diacrilato, Propilen glicol glicerolato diacrilato, Tetra(etilen glicol) diacrilato, 1,3-Butanediol dimetacrilato, 1,4-Butanediol dimetacrilato, 1,6-Hexanediol dimetacrilato, Bisfenol A dimetacrilato, Diuretano dimetacrilato, Etilen glicol dimetacrilato, Fluorescein O,O'-dimetacrilato, Glicerol dimetacrilato, Bisfenol A etoxilato dimetacrilato, Bisfenol A glicerolato dimetacrilato,
25 Di(etilen glicol) dimetacrilato, Poli(etilen glycol) dimetacrilato, Poli(propilen glicol) dimetacrilato, Tetraetilen glycol dimetacrilato, Tri(etilen glicol) dimetacrilato, Trietilen glicol dimetacrilato, Poli(lauril metacrilato-co-etilen glycol dimetacrilato), Poli(metil metacrilato-co-etilen glicol dimetacrilato).

En una realización preferida, los monómeros metacrílicos de la etapa a) son una
30 combinación de los monómeros hidroxietil metacrilato y etilenglicolfeniléter metacrilato. En una realización preferida, la mezcla de la etapa a) presenta

etileneglicolfeniléter metacrilato en una concentración de entre 50 y 1000 mM, más preferiblemente de entre 100 y 800 mM, aún más preferiblemente de entre 200 y 400 mM, y en particular de 400 mM.

En una realización, la mezcla de la etapa a) presenta glicidil metacrilato en una
5 concentración de entre 50 y 1000 mM, más preferiblemente de entre 100 y 800 mM, aún más preferiblemente de entre 200 y 600 mM, y en particular de 400 mM.

En una realización preferida, la mezcla de la etapa a) comprende hidroxietil metacrilato, etileneglicolfeniléter metacrilato, glicidil metacrilato y etilenglicol dimetacrilato. En una realización más preferida, la mezcla de la etapa a) comprende hidroxietil metacrilato en
10 una proporción en peso de entre 60% y 99% respecto al peso del hidrogel, preferiblemente entre 70% y 99%, más preferiblemente entre 80% y 98%, etileneglicolfeniléter metacrilato en una proporción en peso de entre 0,1% y 10% respecto al peso del hidrogel, glicidil metacrilato en una proporción en peso de entre 0,1% y 10% respecto al peso del hidrogel y etilenglicol dimetacrilato en una proporción en peso de entre 0,1% y 10%
15 respecto al peso del hidrogel.

En una realización preferida, la mezcla de la etapa a) consisten en monómeros metacrílicos o acrílicos monofuncionalizados, o sus combinaciones, monómeros metacrílicos o acrílicos bifuncionalizados, y monómeros metacrílicos o acrílicos que comprenden un grupo electrófilo.

20 Preferiblemente, la etapa a) se lleva a cabo en presencia de un iniciador de la polimerización, por ejemplo, el azobisisobutironitrilo (AIBN). La iniciación de la polimerización se puede realizar mediante la calefacción de la mezcla de monómeros o por exposición de esta a radiación ultravioleta-visible.

El proceso de polimerización se puede realizar en moldes de dimensiones adecuadas para
25 dotar a los hidrogeles de la forma que se requiera. Por ello, en una realización, la reacción de polimerización se lleva a cabo en un molde que dota al hidrogel de una forma de lente de contacto. En una realización preferida, el molde es un molde de vidrio, polipropileno, poletileno o politetrafluoroetileno.

En la etapa b), los grupos amino de las bases nitrogenadas, que son grupos nucleófilos,
30 reaccionan con los grupos electrófilos presentes en el entramado base del hidrogel, dando lugar a enlaces amino, mediante una reacción de sustitución nucleófila.

ES 2 755 415 A1

La base nitrogenada de la etapa b) está en disolución, preferiblemente en disolución acuosa o en una mezcla de disolución acuosa y disolvente orgánico.

En una realización adicional, el procedimiento anteriormente descrito comprende además una etapa en la que una molécula con afinidad por la base nitrogenada presente en el
5 hidrogel se incorpora al mismo en un proceso sencillo en el que dicha molécula se pone en contacto con el hidrogel obtenido en la etapa b) anteriormente descrita. Esta etapa transcurre en un medio acuoso.

En el proceso de la presente invención, se obtiene un hidrogel en el cual la base nitrogenada no ha interferido en el proceso de polimerización y entrecruzamiento, y por
10 tanto no se obtienen entramados base en los que la base nitrogenada es un eslabón estructural de las cadenas que constituyen el hidrogel.

En una realización, los hidrogeles resultantes de cualquiera de las anteriores realizaciones se lavan, y, opcionalmente, se secan.

La reacción de polimerización puede tener lugar en un molde con el diseño adecuado para
15 obtener una lente de contacto. Si la reacción de polimerización no se ha llevado a cabo en un molde que dota al hidrogel de una forma de lente de contacto, se puede preparar la lente de contacto mediante cortado por torno del hidrogel.

En otro aspecto, la presente invención se dirige a hidrogeles obtenibles mediante un procedimiento según cualquiera de las realizaciones anteriormente descritas.

20 A través del hidrogel o lente de contacto de la presente invención se administran moléculas al ojo, y más concretamente a la superficie de la parte frontal del ojo (o segmento anterior del ojo), y aún más particularmente a la córnea. Además, ventajosamente, del hidrogel o lente de contacto de la presente invención permite que dicha administración sea controlada/sostenida y no inmediata.

25 En una realización, la invención se dirige a un hidrogel de la presente invención, y más concretamente a una lente de contacto de la presente invención, para su uso en medicina. Más particularmente, el uso en medicina es un uso en oftalmología.

En una realización más concreta, la invención se dirige a un hidrogel de la presente invención, y más concretamente a una lente de contacto de la presente invención, para su
30 uso en el tratamiento o la prevención de la sequedad del ojo.

ES 2 755 415 A1

En una realización alternativa, la invención se dirige al uso de un hidrogel de la presente invención, y más concretamente de una lente de contacto de la presente invención, para la preparación de un medicamento para el tratamiento o la prevención de la sequedad del ojo.

- 5 En una realización alternativa, la invención se dirige a un método de prevención o tratamiento de la sequedad del ojo, que comprende administrar a un paciente que sufre la sequedad del ojo un hidrogel de la presente invención, y más concretamente de una lente de contacto de la presente invención.

- En una realización particular, la lente de contacto de la presente invención se emplea con
10 los fines anteriormente descritos y además para corregir la visión del usuario/paciente.

La invención se describe a continuación por medio de los siguientes ejemplos que deben considerarse meramente ilustrativos y en ningún caso limitativos del alcance de la presente invención.

15 Ejemplos

En los ejemplos que siguen fueron empleados los siguientes materiales:

- Ácido transferúlico (TA) de AlfaAesar (Kandel, Alemania). 2-Hidroxietil metacrilato (HEMA) de Merck (Darmstadt, Alemania); etilenglicol dimetacrilato 98% (EGDMA), glicidil metacrilato (GMA), elitenglicolfeniléter metacrilato (EGPEM), 2,2'-azobis(2-
20 metilpropionitrilo) (AIBN), diclorodimetilsilano, citosina, 2,2'-azobis(2- amidino- propano) dihidrocloruro (AAPH) y Trolox se compraron a Sigma-Aldrich (Steinheim, Alemania); 1,4-dioxano de Panreac (Barcelona, España); NaOH de VWR Chemicals (Leuven, Bélgica); agua purificada por ósmosis inversa (resistividad $>18\text{M}\Omega\cdot\text{cm}$, MilliQ, Millipore® España). Fluido lacrimal simulado (FLS) preparado con la siguiente
25 composición: 6,78 g/L NaCl, 2,18 g/L NaHCO_3 y 1,38 g/L KCl y 0,084 g/L $\text{CaCl}_2\cdot 2\text{H}_2\text{O}$ con pH 7,5.

Ejemplo 1. Síntesis de hidrogeles acrílicos

Los hidrogeles se prepararon a partir de las mezclas de monómeros que se resumen en la Tabla 1.

ES 2 755 415 A1

Tabla 1

Hidrogel	HEMA (mL)	EGDMA (μ L)	GMA (μ L)	EGPEM (μ L)
G0E0	8	12.1	0	0
G0E100	8	12.1	0	150
G100E0	8	12.1	110	0
G100E100	8	12.1	110	150
G0E200	8	12.1	0	300
G200E0	8	12.1	220	0
G200E200	8	12.1	220	300
G400E0	8	12.1	430	0
G400E200	8	12.1	430	300
G600E0	8	12.1	640	0
G600E200	8	12.1	640	300

Los hidrogeles se codificaron en función de la concentración de GMA, indicado como G en el código, la concentración de EGPEM, indicado como E en el código, y en el caso de que hayan sido funcionalizados con citosina (ver ejemplo 2) el código termina en C, mientras que si no está funcionalizado la terminación es cero.

Se añadieron EGDMA (8 mM), GMA (0, 100, 200, 400 o 600 mM) y EGPEM (0, 100 o 200 mM) a HEMA y las mezclas se mantuvieron en agitación magnética (300 r.p.m., a temperatura ambiente 20-23°C) durante 15 minutos. Entonces se añadió AIBN (10 mM) y se mantuvieron en agitación 15 minutos más. Finalmente, cada disolución se inyectó en un molde y se llevó a cabo la polimerización a 50°C durante 12 horas y después a 70°C durante 24 horas más.

Los hidrogeles intermedios así obtenidos se caracterizaron mediante espectrometría de IR (FTIR Varian 670-IR equipado con un PIKE GladiATR Diamond Crystal), se observaron las bandas características de los entramados poliHEMA y se evidenció la presencia de grupos glicídico a bandas de entre 900 cm^{-1} y 690 cm^{-1} .

Ejemplo 2. Funcionalización con una base nitrogenada

Cada hidrogel obtenido en el ejemplo 1 se sumergió en 100 mL de una mezcla agua:dioxano (1:1), se añadió 1,11 g de citosina, y la mezcla en un recipiente cerrado se

mantuvo en agitación oscilatoria (30 osc/min) a 80°C durante 24 horas. Este proceso se ilustra en la Figura 1.

En paralelo, otro hidrogel se sometió al mismo tratamiento, pero sin presencia de citosina. Después de la funcionalización, los hidrogeles se cortaron en discos (10 mm de diámetro) y se lavaron con agua miliQ (1L) en agitación magnética (200 r.p.m.) cambiando el medio cada 24 horas hasta ausencia de monómeros. Finalmente, los discos se secaron a 50°C durante 24 horas.

Los hidrogeles así obtenidos se caracterizaron mediante espectrometría de IR (FTIR Varian 670-IR equipado con un PIKE GladiATR Diamond Crystal), se observaron las bandas características de los entramados poliHEMA, y se evidenció la presencia de citosina al observar la banda del grupo amido a aprox. 1655 cm⁻¹.

Ejemplo 3. Propiedades de los hidrogeles

El grado de hinchamiento se testó en agua y FLS para cada hidrogel preparado en los ejemplos 1 y 2 (medidas realizadas a temperatura ambiente, 20-23°C) y se calculó del siguiente modo:

$$\text{Grado de hinchamiento (\%)} = \frac{W_t - W_0}{W_0} \cdot 100$$

Donde W₀ y W_t representan el peso del disco seco e hinchado, respectivamente.

Se observó que tanto los hidrogeles preparados en el ejemplo 1 como los hidrogeles funcionalizados con citosina preparados en el ejemplo 2, tenían un grado de hinchamiento similar, y también similar cuando se compara los resultados en agua y en FLS. El grado de hinchamiento en todos los casos se encuentra en un rango de entre 40% y 65%.

Todos los discos alcanzaron el equilibrio de hinchamiento en una hora aproximadamente.

La transmisión de la luz se midió en los discos hinchados en agua y en FLS, en un espectrofotómetro UV-Vis entre 190 y 800 nm (Agilent 8453, Alemania). Todos los discos mostraron excelentes propiedades de transmisión de la luz, con unos valores de transmitancia en el visible en un rango superior a 90%. Se observó además que los hidrogeles que incorporan citosina absorben más en el rango UV.

Todas estas propiedades hacen que los hidrogeles de la invención sean adecuados para su uso como lentes de contacto blandas, incluso los que comprenden citosinas son además adecuados para proteger al ojo de las radiaciones UV.

ES 2 755 415 A1

Ejemplo 4. Carga de moléculas con afinidad por bases nitrogenadas

Los discos de hidrogel secos se pesaron y se colocaron en 5 mL de disoluciones acuosas de TA (0,01 mg/mL) preparados con EDTA al 0,05% como estabilizante. Se mantuvieron a 25 °C bajo agitación orbital (300 rpm) durante 48 horas. La absorbancia del medio se monitorizó a 320 nm a intervalos determinados de tiempo (espectrofotómetro UV / Vis Agilent 8543, Alemania). La cantidad de TA cargado se estimó por diferencia entre la cantidad inicial y final de TA en la solución usando una curva de calibración validada previamente. Los resultados obtenidos se muestran en la tabla 2 y Figura 2.

Tabla 2

Hidrogel	Cantidad incorporada (µg/mg)
G0E0-0	0.173 (0.023)
G0E0-C	0.163 (0.009)
G0E100-C	0.226 (0.019)
G100E0-C	0.179 (0.015)
G100E100-C	0.232 (0.027)
G0E200-C	0.194 (0.003)
G200E0-C	0.272 (0.006)
G200E200-C	0.256 (0.005)
G400E0-0	0.174 (0.017)
G400E0-C	0.284 (0.007)
G400E200-0	0.199 (0.002)
G400E200-C	0.413 (0.019)
G600E0-0	0.187 (0.010)
G600E0-C	0.355 (0.009)
G600E200-0	0.193 (0.004)
G600E200-C	0.315 (0.023)

- 10 Se observó que los hidrogeles preparados en el ejemplo 1 completaron la carga en las primeras 8 horas, mientras que los hidrogeles funcionalizados con citosina obtenidos en el ejemplo 2 completaron la carga tras 24 horas. Los discos que mostraron la mayor carga fueron los procedentes de hidrogeles preparados con una concentración de GMA de 400 mM y con EGPEM en una concentración de 200 mM y funcionalizados con citosina.

Ejemplo 5. Cesión de moléculas con afinidad por bases nitrogenadas

Los discos procedentes del ejemplo 4 se enjuagaron con agua, se retiró el exceso de agua de la superficie con papel de filtro, y cada disco se dispuso en un vial con 5 mL de FLS y los viales se mantuvieron bajo agitación oscilante (300 rpm) a 35 °C. A tiempos
5 preestablecidos (0,5; 1; 2; 4; 6; 8; y 24 h) se tomaron 2,5 mL del medio de cesión, se midió la absorbancia a 320 nm (UV/VIS Agilent 8453, Alemania) y la muestra se reintegró al vial de procedencia. Para calcular la cantidad de TA cedida por cada hidrogel, a partir de las absorbancias se calculó la concentración en el medio de cesión utilizando la correspondiente recta de calibrado de TA en FLS, y a continuación se multiplicó la
10 concentración por el volumen, y los valores se refirieron al peso inicial de cada disco de hidrogel.

Los resultados se muestran en la Figura 3. Se puede observar que los hidrogeles funcionalizados con citosina proporcionaron una cesión más sostenida en el tiempo y un *burst* menos intenso en la primera hora que en el caso de la cesión con hidrogeles que no
15 incorporan citosina. Además, los hidrogeles funcionalizados con citosina ceden mayor cantidad de TA que los que no están funcionalizados, lo que es una ventaja desde un punto de vista terapéutico. Los mejores resultados se obtuvieron con hidrogeles funcionalizados con citosina que se prepararon con una concentración de GMA y EGPEM de 400 mM y 200 mM, respectivamente, y los que se prepararon con una concentración de GMA y
20 EGPEM de 600 mM y 200 mM, respectivamente.

Ejemplo 6. Estudio de actividad antioxidante

Para verificar que la actividad antioxidante de TA se mantenía después de incorporarse a los hidrogeles y de cederse, se realizó un análisis de la actividad antioxidante. Se
25 seleccionó una fuente de radicales biológicamente relevante, 2,2'-azobis (2-amidino-propano) dihidrocloruro (AAPH), para llevar a cabo el test estándar ORAC (C. Lucas-Abellan, M.T. Mercader-Ros, M.P. Zafrilla, J.A. Gabaldon and E. Nunez-Delicado, *Food Chem. Toxicol.*, 2011, **49**, 1255-1260). Este método cuantifica la capacidad de una sustancia para proteger fluoresceína de la degradación mediante radicales libres. Así, a
30 mayor capacidad antioxidante, menor descenso de la fluorescencia de la fluoresceína.

ES 2 755 415 A1

Se analizó el medio de liberación de FLS en el que se empaparon hidrogeles no cargados y cargados de TA. Los hidrogeles funcionalizados con citosina no cargados se probaron para verificar que no había sustancias de lixiviación que pudieran causar un artefacto (actividad antioxidante falsa) durante la prueba. Los resultados se expresaron como

5 capacidad antioxidante equivalente de Trolox (TEAC) para fines comparativos. Como se esperaba, los hidrogeles no cargados dieron como resultado valores cercanos a cero (o incluso negativos), lo que indica que no liberaron ninguna sustancia antioxidante. Por el contrario, el G400E200-C cargado con TA condujo a la mayor actividad antioxidante, equivalente a $53.28 \pm 2.44 \mu\text{M}$ Trolox, en comparación con su homólogo libre de citosina

10 G400E200-0 cargado con TA que tenía una actividad de $37.48 \pm 1.53 \mu\text{M}$ Trolox. Este hallazgo corrobora la utilidad de la citosina para dotar a los hidrogeles de una capacidad mejorada para albergar TA y, lo que es aún más notable, que la interacción TA-citosina no tiene ningún efecto perjudicial sobre la actividad antioxidante de TA. De hecho, la actividad antioxidante expresada como $\mu\text{molTolox} / \mu\text{molTA}$ dio valores en el rango de

15 4.8-5.0, lo cual demuestra la utilidad de los hidrogeles como vehículos de cesión de sustancias, en este caso de TA.

Ejemplo 7. Estudio de compatibilidad celular

La compatibilidad celular se evaluó en un modelo subrogado que utiliza membrana corioalantoidea de huevo de gallina fecundado (HET-CAM) (F. Alvarez-Rivera, D.

20 Fernández-Villanueva, A. Concheiro and C. Alvarez-Lorenzo, *J. Pharm. Sci.*, 2016, **105**, 2855-2863). Discos de cada hidrogel cargados con TA como se obtuvieron en el ejemplo 4 se colocaron sobre la membrana corioalantoidea. Durante 5 min se observaron los posibles cambios en la vasculatura de la membrana, registrando tiempo de lisis, hemorragia y coagulación. Como control negativo se utilizó la disolución de 0,9% NaCl

25 y como control positivo una disolución 0,1 N NaOH. Todos los discos superaron el ensayo de compatibilidad, no originando lisis, hemorragia ni coagulación.

Además, se evaluó la citocompatibilidad in vitro de los hidrogeles G0E0-0, G400E200-0 y G400E200-C en células de epitelio corneal humano (HCEC; ATCC PCS-700-010). La línea celular se cultivó en medio Keratinocyte-Serum Free (Gibco, Gran Bretaña),

30 suplementado con hidrocortisona (500 ng/mL), insulina (5 microg/mL), penicilina/streptomycin 1% y antifúngico 1%, previo al tratamiento con Fibronectin-

ES 2 755 415 A1

BSA-Bovin collgen I. Se sembraron HCEC (20.000 células/pocillo) en una placa de 48 pocillos en medio Keratinocyte-Serum Free y se cultivaron durante 24 h a 37°C (95% RH y 5% CO₂). Los discos se cargaron durante 24 horas en una solución de TA 10 µg/mL, se cortaron en cuatro piezas y luego se esterilizaron en autoclave (calor de vapor) en la misma solución, a 121°C durante 15 minutos. Luego, se colocó una pieza de disco en cada pocillo durante 24 h. También se añadió solución acuosa de TA (10 µg/mL) por triplicado (esterilización previa) y los controles negativos incluyeron células sin tratamiento. Después de 24 h en cultivo celular, se retiraron los discos y la solución del fármaco de los pocillos, y el ensayo de viabilidad celular se realizó siguiendo las instrucciones del fabricante utilizando WST-1 (Roche, Suiza). La absorbancia se leyó a 450 nm (lector de microplacas UV Bio-Rad Modelo 680, EE. UU.). La viabilidad celular (%) se calculó de la siguiente manera:

$$\text{Viabilidad celular (\%)} = \frac{\text{Abs}_{exp}}{\text{Abs}_{control\ negativo}} \times 100$$

Este estudio demostró que los hidrogeles a la concentración usada de carga (10 µg/mL, aprox. 51,5 µM) son compatibles, mostrando unos niveles de viabilidad celular superiores a 80% después de 24 horas de contacto directo.

Ejemplo 8. Estudio de permeabilidad corneal

Se recogieron en el matadero ojos de ganado bovino frescos y se transportaron sumergidos en PBS (tampón fosfato salino) con antibióticos añadidos (penicilina a 100 IU/mL y estreptomycin a 100 µg/ml) en un baño con hielo. Se aislaron la córnea con 2-3 mm de esclera circundante y la esclera y se limpiaron con PBS antes de montarlos en una célula de difusión vertical tipo Franz, separando la cámara dadora de la receptora. Las cámaras se llenaron con tampón bicarbonato pH 7,2. Las células de difusión se dispusieron en un baño termostatzado a 37 °C y se mantuvieron en agitación 30 min. Entonces, se retiró el tampón de la cámara donadora y se reemplazó por las muestras a testar: 2 mL de solución acuosa de TA (10 microL/mL), o discos G400E200-0 y G400E200-C en 2 mL de 0,9% NaCl. El área disponible para permeación era de 0,785 cm². Las cámaras se cubrieron con parafilm. A intervalos de 1 h se tomaron muestras de

ES 2 755 415 A1

1 mL de las cámaras receptoras y se reemplazó el mismo volumen con tampón, teniendo cuidado de eliminar las burbujas de las células de difusión.

Las muestras tomadas de las cámaras receptoras se filtraron a través de membranas de nailon (0,45 μ m) y se midieron con un equipo HPLC (Waters 717 Autosampler, Waters
5 600 Controller, 996 Photodiode Array Detector) acondicionado con una columna C18 (Waters Symmetry C18 5 μ m; 4,6x250 mm) y Empower 2 como software. La fase móvil consistió en metanol:acetonitrilo:tampón fosfato (20:15:65) a 1 mL/min y 35°C (tampón KH_2PO_4 0,68 g/L ajustado a pH 3-3,1 con ácido fosfórico). El volumen inyectado fue 50 μ L, y el TA fue cuantificado a 320 nm (tiempo de retención 5 min). La recta de calibrado
10 de ALA en fase acuosa se preparó en el intervalo de concentraciones comprendido entre 0,009 y 10,0 mg/mL en tampón carbonato. El contenido en TA de las muestras se calculó a partir de la curva de calibración.

Después de 6 h de ensayo, se tomó una muestra de la cámara donadora para un análisis posterior. Además, las córneas y esclera se examinaron visualmente para asegurar que no
15 habían sufrido daño durante el ensayo.

Las córneas y la esclera se mantuvieron toda la noche en 3 mL de una solución etanol:agua (50:50 v/v), se sonicaron durante 99 min a 37°C, se centrifugaron (1000 r.p.m.
5 min, 25°C), se filtró y se centrifugaron de nuevo (14000 r.p.m., 20 min, 25°C). El coeficiente de permeabilidad de TA a través de la córnea y la esclera se calculó como la
20 relación del flujo de estado estacionario y la concentración de TA en la cámara donadora.

Tanto en córnea como en esclera, los hidrogeles G400E200-C cargados con ácido trans-ferúlico dieron lugar a coeficientes de permeabilidad similar los obtenidos como la disolución de fármaco libre, lo que indica que la cesión a partir del hidrogel
funcionalizado con citosina no es un obstáculo para su penetración en córnea y en esclera,
25 a diferencia de lo que ocurre para los hidrogeles no funcionalizados (Figura 4). También se obtuvieron valores similares de cantidad de ácido trans-ferúlico acumulada en córnea y esclera (Figura 5).

ES 2 755 415 A1

REIVINDICACIONES

1. Hidrogel en forma de red tridimensional caracterizado porque comprende cadenas metacrílicas y/o acrílicas entrecruzadas, en donde las cadenas comprenden grupos alquílicos a los que están unidas una base nitrogenada seleccionada de entre citosina, adenina, guanina, uracilo y timina.
2. Hidrogel según la reivindicación 1, caracterizado porque las cadenas metacrílicas y/o acrílicas comprenden: unidades metacrílicas o acrílicas monofuncionalizadas, o combinaciones de las mismas; unidades metacrílicas o acrílicas bifuncionalizadas; y unidades metacrílicas o acrílicas que comprenden un grupo electrófilo.
3. Hidrogel según cualquiera de las reivindicaciones anteriores, caracterizado porque la proporción en peso de las unidades metacrílicas o acrílicas bifuncionalizadas está preferiblemente entre el 0,01% y el 10% en peso con respecto al peso del hidrogel.
4. Hidrogel según cualquiera de las reivindicaciones anteriores, caracterizado porque la proporción en peso de las unidades metacrílicas o acrílicas que comprenden un grupo electrófilo está entre el 0,1% y el 10% con respecto al peso del hidrogel.
5. Hidrogel según cualquiera de las reivindicaciones anteriores, donde el hidrogel comprende además una molécula con afinidad por la base nitrogenada presente en el hidrogel.
6. Hidrogel según la reivindicación 5, donde la molécula con afinidad por una base nitrogenada presente en el hidrogel es una molécula antioxidante.
7. Hidrogel según la reivindicación 5, donde la molécula con afinidad por una base nitrogenada presente en el hidrogel es un principio activo farmacéutico.
8. Método para preparar un hidrogel tal y como se ha definido en la reivindicación 1, que comprende las etapas de:
 - a. polimerizar una mezcla que comprende i) monómeros metacrílicos o acrílicos monofuncionalizados, o combinaciones de los mismos, ii) monómeros metacrílicos o acrílicos bifuncionalizados, y iii) monómeros metacrílicos o acrílicos que comprenden un grupo electrófilo, para formar un entramado base de red tridimensional; y
 - b. hacer reaccionar una base nitrogenada seleccionada de entre citosina, adenina, guanina, uracilo y timina, con el entramado base.

ES 2 755 415 A1

9. Método según la reivindicación 8, que comprende además la etapa c) poner en contacto una molécula con afinidad por la base nitrogenada con el hidrogel obtenido en la etapa b), en presencia de un medio acuoso.
10. Método según la reivindicación 8 a 9, en donde los monómeros metacrilícos o acrílicos monofuncionalizados se seleccionan del grupo que consiste en hidroxietil metacrilato, etilenglicolfeniléter metacrilato, 1-(trimetilsiloxisilpropil)-metacrilato, metilmetacrilato, N,N-dimetilacrilamida, N,N-dietilacrilamida, ácido metacrilíco, ácido acrílico, aminopropil metacrilato, ciclohexil metacrilato, y fluoro-siloxano acrilato, o combinaciones de los mismos.
11. Método según cualquiera de las reivindicaciones 8 a 9, en donde los monómeros metacrilícos o acrílicos bifuncionalizados se seleccionan del grupo que consiste en etilenglicol dimetacrilato, 1,3-Butanediol diacrilato, 1,4-Butanediol diacrilato, 1,6-Hexanediol diacrilato, Etilen glicol diacrilato, Fluorescein O,O'-diacrilato, Glicerol 1,3-díglicerolato diacrilato, Pentaeritrol diacrilato monoestearato, 1,6-Hexanediol etoxilato diacrilato, 3-Hidroxi-2,2-dimetilpropil 3-hidroxi-2,2-dimetilpropionato diacrilato, Bisfenol A etoxilato diacrilato, Di(etilen glicol) diacrilato, Neopentil glicol diacrilato, Poli(etilen glicol) diacrilato, Poli(propilen glicol) diacrilato, Propilen glicol glicerolato diacrilato, Tetra(etilen glicol) diacrilato, 1,3-Butanediol dimetacrilato, 1,4-Butanediol dimetacrilato, 1,6-Hexanediol dimetacrilato, Bisfenol A dimetacrilato, Diuretano dimetacrilato, Etilen glicol dimetacrilato, Fluorescein O,O'-dimetacrilato, Glicerol dimetacrilato, Bisfenol A etoxilato dimetacrilato, Bisfenol A glicerolato dimetacrilato, Di(etilen glicol) dimetacrilato, Poli(etilen glycol) dimetacrilato, Poli(propilen glicol) dimetacrilato, Tetraetilen glycol dimetacrilato, Tri(etilen glicol) dimetacrilato, Trietilen glicol dimetacrilato, Poli(lauril metacrilato-co-etilen glycol dimetacrilato) y Poli(metil metacrilato-co-etilen glicol dimetacrilato).
12. Método según cualquiera de las reivindicaciones 8 a 9, en donde la mezcla de la etapa a) comprende además un iniciador de la polimerización.
13. Método según cualquiera de las reivindicaciones 8 a 9, en donde la reacción de la etapa b) tiene lugar en presencia de un disolvente orgánico.
14. Hidrogel obtenible mediante un procedimiento tal y como se define en cualquiera de las reivindicaciones 8 a 13.

15. Lente de contacto que comprende un hidrogel tal y como se define en cualquiera de las reivindicaciones 1 a 7 o 14.
16. Método para preparar una lente de contacto tal y como se ha definido en la reivindicación 15, que comprende formar la lente de contacto a partir del hidrogel tal y como se define en cualquiera de las reivindicaciones 1 a 7 o 14 mediante cortado por
5 torno del hidrogel o mediante moldeo del hidrogel, o mediante una combinación de estas técnicas.
17. Hidrogel tal y como se define en cualquiera de las reivindicaciones 1 a 7 o 14, o lente de contacto tal y como se define en la reivindicación 15, para su uso en medicina,
10 preferiblemente en oftalmología.
18. Hidrogel o lente de contacto para su uso según la reivindicación 17, para su uso en el tratamiento o la prevención de la sequedad de ojo.
19. Hidrogel o lente de contacto para su uso según la reivindicación 17, para su uso en el tratamiento o la prevención de cataratas.
- 15 20. Hidrogel o lente de contacto para su uso según la reivindicación 17, para su uso en el tratamiento o la prevención de úlceras corneales.
21. Uso de un hidrogel tal y como se define en cualquiera de las reivindicaciones 1 a 7 o 14, en la elaboración de sistemas de liberación tópica, transdérmica o transmucosal.
22. Uso de un hidrogel tal y como se define en cualquiera de las reivindicaciones 1 a
20 7 o 14, en cosmética.

ES 2 755 415 A1

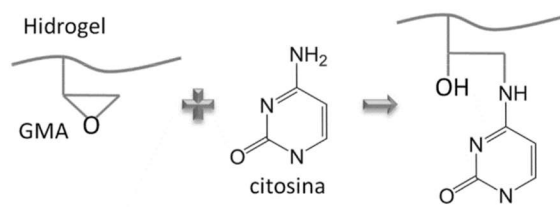


Fig. 1

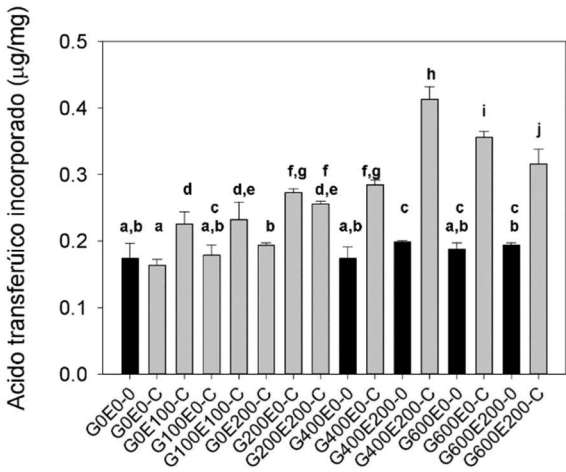


Fig. 2

ES 2 755 415 A1

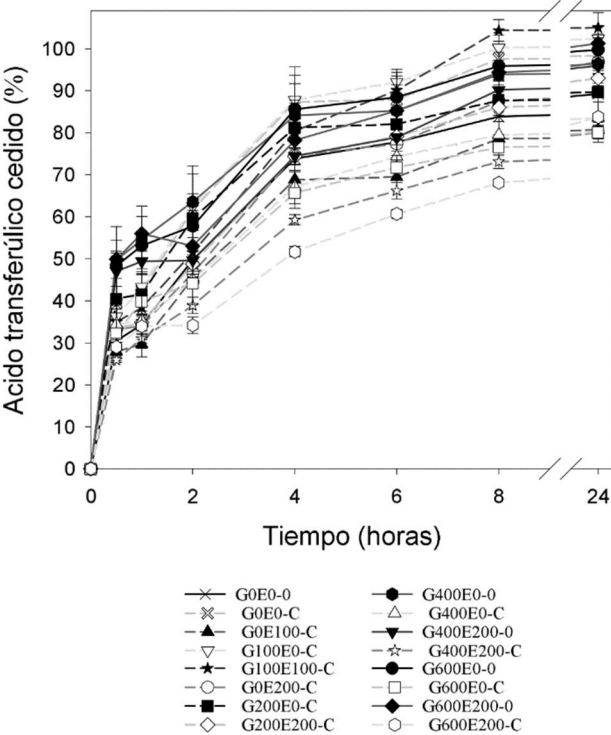


Fig. 3

ES 2 755 415 A1

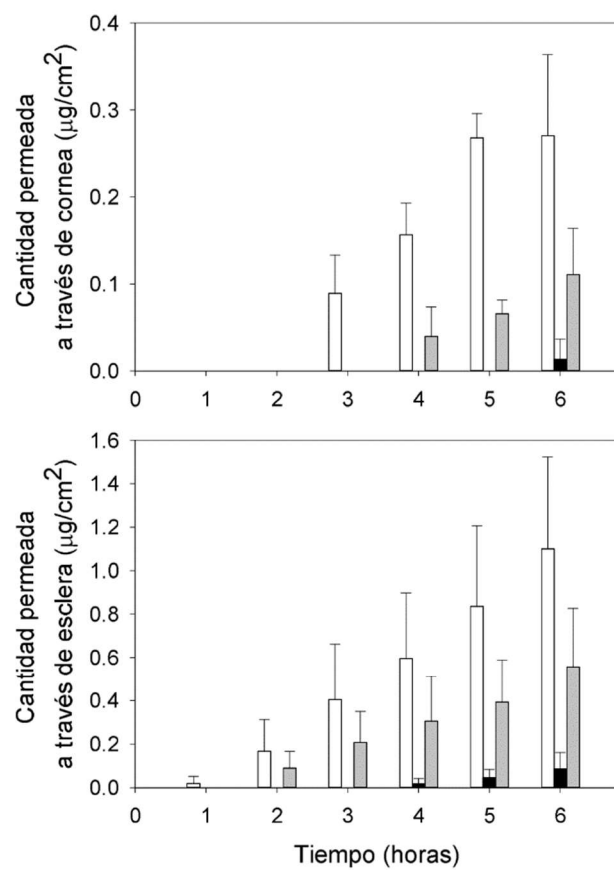


Fig. 4

ES 2 755 415 A1

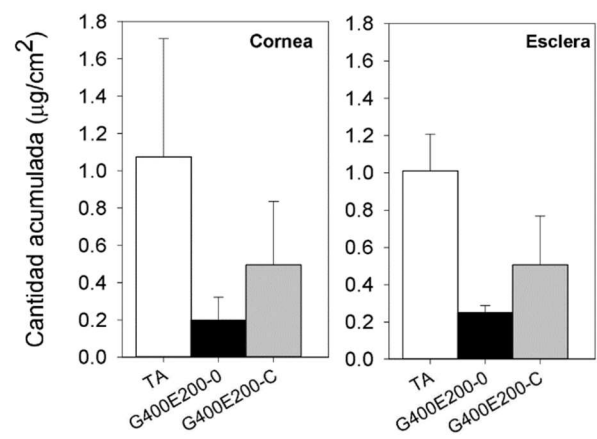


Fig. 5



OFICINA ESPAÑOLA
DE PATENTES Y MARCAS
ESPAÑA

- 21 N.º solicitud: 201931063
22 Fecha de presentación de la solicitud: 29.11.2019
32 Fecha de prioridad:

INFORME SOBRE EL ESTADO DE LA TÉCNICA

5 Int. Cl.: Ver Hoja Adicional

DOCUMENTOS RELEVANTES

Categoría	56 Documentos citados	Reivindicaciones afectadas
X	YANG, K. et ZENG, M. "Multiresponsive hydrogel based on polyacrylamide functionalized with thymine derivatives". New Journal of Chemistry 2013, Volumen 37, páginas 920-926. [Disponible en línea el 09.01.2013]. DOI: 10.1039/C3NJ41013G. ISSN: 1144-0546; 1369-9261 (en línea). Ver página 920, resumen; página 921, resultados y discusión, figura 1; página 921, columna 2, párrafo 1; página 922, columna 2, párrafo 3; página 923, figura 3.	1-7, 14, 17-22
X	MIYATA, M. et al. "Functional monomers and polymers, 115. Permeability of hidrogel membranes consisting of copolymers containing pendant nucleic acid bases". Makromolekulare Chemie 1984, Volumen 185, páginas 647-654. ISSN: 0025-116X. Ver página 647, resumen; página 648, resultados y discusión; página 649, tabla 1 y párrafo 4.	1-6, 14
A	TROMBINO, S. et al. "Synthesis and antioxidant activity evaluation of a novel cellulose hydrogel containing <i>trans</i> -ferulic acid". Carbohydrate Polymers 2009, Volumen 75, Número 1, páginas 184-188. [Disponible en línea el 29.05.2008]. DOI: 10.1016/j.carbpol.2008.05.018. ISSN: 0144-8617. Recuperado de: <https://doi.org/10.1016/j.carbpol.2008.05.018>. [Recuperado el 02.04.2020]. Ver página 184, resumen; página 185, esquema 1; página 187, apartado 5.	1-22
A	LULINSKI, P. "Molecularly imprinted polymers based drug delivery devices: a way to application in modern pharmacotherapy. A review". Materials Science and Engineering C 2017, Volumen 76, páginas 1344-1353. [Disponible en línea el 02.03.2017]. DOI: 10.1016/j.msec.2017.02.138. ISSN: 0928-4931. Recuperado de: <https://doi.org/10.1016/j.msec.2017.02.138>. [Recuperado el 03.04.2020]. Ver página 1344, resumen; páginas 1346-1347, apartado 4.1.	1-22
A	GUZMÁN-ARANGUEZ, A. et al. "Contact Lenses: Promising Devices for Ocular Drug Delivery". Journal of Ocular Pharmacology and Therapeutics 2013, Volumen 29, Número 2, páginas 189-199. [Disponible en línea el 05.12.2012]. DOI: 10.1089/jop.2012.0212. ISSN: 1080-7683. Recuperado de: <https://doi.org/10.1089/jop.2012.0212>. [Recuperado el 06.04.2020]. Ver todo el documento.	1-22
<p>Categoría de los documentos citados</p> <p>X: de particular relevancia Y: de particular relevancia combinado con otro/s de la misma categoría A: refleja el estado de la técnica</p> <p>O: referido a divulgación no escrita P: publicado entre la fecha de prioridad y la de presentación de la solicitud E: documento anterior, pero publicado después de la fecha de presentación de la solicitud</p>		
<p>El presente informe ha sido realizado</p> <p><input checked="" type="checkbox"/> para todas las reivindicaciones <input type="checkbox"/> para las reivindicaciones nº:</p>		
Fecha de realización del informe 11.04.2020	Examinador G. Esteban García	Página 1/3



OFICINA ESPAÑOLA
DE PATENTES Y MARCAS
ESPAÑA

21 N.º solicitud: 201931063

22 Fecha de presentación de la solicitud: 29.11.2019

32 Fecha de prioridad:

INFORME SOBRE EL ESTADO DE LA TECNICA

5 Int. Cl.: Ver Hoja Adicional

DOCUMENTOS RELEVANTES

Categoría	66 Documentos citados	Reivindicaciones afectadas
A	CHENG, S. et al. "Nucleobase Self-Assembly in Supramolecular Adhesives". Macromolecules 2012, Volumen 45, Número 2, páginas 805-812. [Disponible en línea el 06.01.2012]. DOI: 10.1021/ma202122r. ISSN: 0024-9297; 1520-5835 (en línea). Ver página 805, resumen; página 806, esquema 1; página 807, esquema 2.	1-22
A	YANG, H. & XI, W. "Nucleobase-Containing Polymers: Structure, Synthesis, and Applications". Polymers 2017, Volumen 9, página 666. [Disponible en línea el 01.12.2017]. DOI: 10.3390/polym9120666. ISSN: 2073-4360. Recuperado de: <https://doi.org/10.3390/polym9120666>. [Recuperado el 03.04.2020]. Ver página 1, resumen; página 6, esquema 3; página 7, figura 3; página 8, esquema 4; página 9, esquema 5; páginas 13-14, apartado 4.1.	1-22
A	US 2008/0124378 A1 (BYRNE, M.E.) 29.05.2008, Figura 2; párrafos [0003], [0021]-[0029], [0105]-[0106].	1-22
A	CN 108102117 A (UNIV CHANGCHUN TECHNOLOGY) 01.06.2018, Reivindicaciones.	1-22
<p>Categoría de los documentos citados</p> <p>X: de particular relevancia</p> <p>Y: de particular relevancia combinado con otro/s de la misma categoría</p> <p>A: refleja el estado de la técnica</p> <p>O: referido a divulgación no escrita</p> <p>P: publicado entre la fecha de prioridad y la de presentación de la solicitud</p> <p>E: documento anterior, pero publicado después de la fecha de presentación de la solicitud</p>		
<p>El presente informe ha sido realizado</p> <p><input checked="" type="checkbox"/> para todas las reivindicaciones</p> <p><input type="checkbox"/> para las reivindicaciones nº:</p>		
Fecha de realización del informe 11.04.2020	Examinador G. Esteban García	Página 2/3

INFORME DEL ESTADO DE LA TÉCNICA	Nº de solicitud: 201931063
CLASIFICACIÓN OBJETO DE LA SOLICITUD C08J3/075 (2006.01) C08F220/06 (2006.01) C08F220/10 (2006.01) C08F222/00 (2006.01) C08F26/06 (2006.01) C08F8/30 (2006.01) A61K9/14 (2006.01) G02C7/04 (2006.01) Documentación mínima buscada (sistema de clasificación seguido de los símbolos de clasificación) C08J, C08F, A61K, G02C Bases de datos electrónicas consultadas durante la búsqueda (nombre de la base de datos y, si es posible, términos de búsqueda utilizados) INVENES, EPODOC, WPI, TXTE, CAPLUS, MEDLINE, BIOSIS, XPESP, EMBASE, GOOGLE SCHOLAR, PUBMED (NCBI)	

Abbreviations





8. Abbreviations

- **AAPH** 2,2'-azobis(2-amidino-propane) dihydrochloride
- **ACV** Acyclovir
- **AFR** Africa
- **AIBN** 2,2'-azo-bis(isobutyronitrile)
- **AMD** Age-related macular degeneration
- **AMR** America
- **BAB** Hemato-aqueous barrier
- **BCOP** Bovine cornea opacity test
- **BRB** Hemato-retinal barrier
- **CAT** Catalase
- **CD** Cyclodextrins

- **CLs** Contact lenses
- **CMC** Critical micellar concentration
- **CMV** Citomegalovirus
- **CO** Corneal opacities
- **DES** Dry eye syndrome
- **DME** Macular edema
- **DR** Diabetic retinopathy
- **EDTA** Ethylenediaminetetraacetic acid
- **EGPEM** Ethylene glycol-phenyl ether methacrylate
- **EMR** Eastern Mediterranean
- **EUR** Europe
- **GMA** Glycidyl methacrylate
- **GPx** Glutathione peroxidase
- **HCEC** Human corneal epithelial cells
- **HEMA** Hydroxyethyl methacrylate

- **HET-CAM** Hen's egg test on chorio-allantoic membrane
- **HLB** Hydrophilic-lipophilic balance
- **HSV** Herpes simplex virus
- **IOP** Intraocular pressure
- **MAA** Methacrylic acid
- **MW** Molecular weight
- **ORAC** Oxygen radical antioxidant capacity
- **PBS** Phosphate buffered saline
- **PDI** Polydispersion index
- **PLGA** Poly lactic-co-glycolic acid
- **PVR** Proliferative vitreoretinopathy
- **RE** Refractive errors
- **RNS** Reactive nitrogen species
- **ROS** Reactive oxygen species
- **RT** Room temperature

- **SCL** Soft contact lenses
- **SEAR** Southeast Asia (without India)
- **SFE** Supercritical fluid assisted molecular impression
- **SLF** Simulated lacrimal fluid
- **SOD** Superoxide dismutase
- **SSI** Supercritical solvent impregnation
- **TA** Transferulic acid
- **TEAC** Trolox equivalent antioxidant capacity
- **TNF α** Tumor necrosis factor α
- **UV** Ultraviolet
- **VACV** Valacyclovir
- **VZV** Varicella-zoster virus
- **WHO** World health organization
- **WPR** Western Pacific (without China)

